NANOENCAPSULATION STRATEGIES FOR ANTIMICROBIAL

CONTROLLED RELEASE TO ENHANCE FRESH AND FRESH-CUT

PRODUCE SAFETY

A Dissertation

by

LAURA ELLEN HILL

Submitted to the Office of Graduate & Professional Studies of
Texas A&M University
in partial fulfillment of the requirements for the degree of

DOCTOR OF PHILOSOPHY

Chair of Committee,	Carmen Gomes
Committee Members,	Rosana Moreira
	Elena Castell
	Sandun Fernando
	T. Matthew Taylor
Head of Department,	Stephen Searcy

May 2014

Major Subject: Biological and Agricultural Engineering

ABSTRACT

Spice essential oils and their constituents are powerful antimicrobials against foodborne pathogens. However, their low sensory threshold and low aqueous solubility make their application to fresh produce a challenge. Encapsulation within a biocompatible material has the potential to mask sensory attributes and increase aqueous solubility of the oils, thereby improving their applicability as antimicrobials onto fresh produce. Cinnamon bark extract (CBE), *trans*-cinnamaldehyde, clove bud extract, and eugenol were encapsulated in β-cyclodextrin (BCD), poly(DL-lactide-co-glycolide) (PLGA), alginate, chitosan, and poly(N-isopropylacrylamide) (PNIPAAM) singly and in combination. All essential oil capsules were characterized for particle size and morphology, polydispersity index, entrapment efficiency, phase-solubility, and controlled release profile. Following physical and chemical characterization, the oils and their nanocapsules were analyzed for their antimicrobial activity against *Salmonella enterica* serovar Typhymirium LT2 and *Listeria spp.* using a microbroth dilution assay to determine minimum inhibitory and bactericidal concentrations at 35°C. The most efficacious antimicrobial nanocapsules during *in vitro* testing were BCD-CBE, PLGA-CBE, and chitosan-PNIPAAM-CBE, which were applied to fresh-cut romaine lettuce, along with free CBE, to determine their efficiency against *L. monocytogenes* in a food system. The chitosan-PNIPAAM-CBE yielded the greatest bacterial inhibition (P<0.05); therefore, it was subjected to a shelf-life study to determine if there were any effects of the particles on fresh-cut romaine lettuce quality over the course of storage. The

antimicrobial nanoparticles did not significantly affect (P>0.05) overall product quality, making encapsulated essential oils a viable treatment for improving food safety without negatively impacting the product's key attributes. This research project developed several natural antimicrobial delivery systems that each exhibited unique release properties and mechanisms, which improved the antimicrobial efficacy (P<0.05) of essential oils and their active compounds. This study sought to characterize and compare different nanoencapsulation systems based on their performance as controlled delivery systems for natural antimicrobials against foodborne pathogens, which has not been previously reported.

DEDICATION

       I dedicate this to my older brother, Austin, who was the first person to challenge me and push me further than I ever imagined I was capable. Also to my parents, who always picked me up when I fell, never let me give up, and loved me unconditionally through it all.

ACKNOWLEDGEMENTS

I would like to thank all of my committee members for all of their help and guidance throughout my studies. Thank you to Dr. Elena Castell for allowing me to be her teaching assistant and for being an excellent mentor in the classroom. And thank you to Dr. Rosana Moreira for her excellent and honest advice on my research as well as for my career. I would especially like to thank my advisor, Dr. Carmen Gomes, for all of the time she spent guiding me through my experiments and studies. Her advice helped me overcome countless technical hurdles and her willingness to help was always appreciated.

I would also like to thank all of my labmates in the food engineering group that provided not only help in the lab, but were also excellent company as we worked together. I would especially like to thank Alex Puerta for constantly offering great advice, Paulo Silva for his guidance, and also Kate Hills, Cassie Giacobassi, and Andre Loquercio for providing tremendous amounts of assistance with my experiments and work in the lab. I greatly appreciate the assistance of Dr. Sandun Fernando and his students for allowing me to use their lab and providing technical support. I would also like to acknowledge Dr. Matthew Taylor and the food microbiology group for welcoming me into their lab to perform extensive experiments and a special thank you to Keila Perez, to whom I owe a tremendous debt of gratitude for her years of patience, help, guidance, and cheerful attitude in the microbiology lab.

TABLE OF CONTENTS

LIST OF FIGURES

FIGURE   Page

LIST OF TABLES

xv

CHAPTER I

INTRODUCTION

Consumption of fresh and fresh-cut produce has risen over recent years due to a growing interest among consumers in eating diets that are not only low calorie and nutritious, but provide additional health benefits, such as improving cardiovascular health or protecting against certain types of cancers (Raybaudi-Massilia and others 2009). This growing trend, coupled with consumer desire for quick and ready-to-eat products has led to a steadily increasing demand for fresh and fresh-cut produce. Providing ready-to-eat products that are not only safe but of high quality will require new, more effective handling and processing procedures than those currently in place to guarantee a product is free of pathogens and spoilage microorganisms. The consequences of the increased demand for fresh and fresh-cut produce lie in a greater public impact when foodborne outbreaks associated with these products occur (Harris and others 2003).

Although there are many effective antimicrobials, many are not approved for use on ready-to-eat products, and consumers are often weary of any food additives or ingredients that are not "natural". Essential oils are extremely effective "natural" antimicrobials, and many are already classified as GRAS (Generally Recognized As Safe) (CFR 2009) substances by the FDA meaning they would not require additional approval for use on foods. Kim and others (1995) tested 11 essential oils for their antibacterial activity against five different foodborne pathogens (*Escherichia coli*, *E. coli*

O157:H7, *Salmonella* Typhimurium, *Listeria monocytogenes*, and *Vibrio vulnificus*) and found most of them to be powerful antimicrobials, but at varying concentrations. The primary challenges in using essential oils as antimicrobials on foods is that they are highly volatile, have very low aqueous solubilities, and they add intense flavors and aromas to the food product at the concentrations needed for bacterial inhibition (Kalemba and Kunicka 2003). Encapsulation of essential oils is a proposed technique to prevent transfer of sensory attributes to the food, improve their water solubility, and reduce their volatility while still delivering potent antimicrobial properties to pathogens in a controlled and targetable manner. Nanoencapsulation has been a growing technology in the pharmaceutical industry to protect active ingredients from harsh environments and improve drug delivery and uptake; it could also be an effective technology in the food industry to protect and deliver antimicrobials to food surfaces (Weiss and others 2006). Many different forms of nanoencapsulation have been used in the drug delivery industry for several years, as nanocapsules were found to have superior intracellular uptake compared to microcapsules. Nanoencapsulation is used to improve the poor cell membrane permeability of most active agents used in the pharmaceutical industry and protect the active agent from damage and degradation as it travels through the body. A variety of materials and techniques are successfully used to create nanocapsules and researchers are exploring new applications for them. Although nanoencapsulation has been used for drug delivery, it has not been widely used in the food industry. Nanoparticles are undetectable to the human eye and cannot be sensed in

the mouth (Pray and Yaktine 2009), so they will not change the texture or appearance of the food product, since this would discourage consumers from purchasing those items.

There is potential for application of nanoencapsulation for protection and delivery of nutraceuticals in food systems, flavor delivery, active packaging, and antimicrobial controlled release in foods. This research explores several types of nanoencapsulation and their potential for controlled delivery of natural antimicrobial compounds to improve the safety of fresh-cut produce. Specifically, the research contained in this dissertation sought to achieve the following objectives:

1) Examine differences in antibacterial potency of *trans*-cinnamaldehyde, eugenol, cinnamon bark extract, and clove bud extract, singularly and in combination to determine if they act synergistically when combined against both Gram-positive and -negative bacteria.

2) Synthesize beta-cyclodextrin (BCD) inclusion complexes, poly(D,L-lactide-co-glycolide) (PLGA) nanoparticles, and poly-N-isopropylacrylamide (PNIPAAM)-co-polymers with chitosan or alginate using the most effective oil listed in objective 1) (cinnamon bark extract), and characterize their physical and chemical attributes and antimicrobial activities.

3) Conduct microbial challenge study for all antimicrobial nanoparticles applied to fresh produce against *Listeria monocytogenes* for the expected shelf life of the product at refrigeration temperature (4°C) and when the product is slightly temperature abused (10°C) to mimic potential storage and shipping conditions.

4) Perform shelf-life study of fresh produce exposed to nanoparticles to determine if antimicrobial particles have an impact on produce quality attributes.

CHAPTER II

LITERATURE REVIEW

2.1 Foodborne Illness Linked to Fresh Produce

Salmonella spp. are the most common pathogen associated with foodborne outbreaks traced back to fresh and fresh-cut produce (Raybaudi-Massilia and others 2009) and can lead to severe illness, especially in young children, the elderly population and any individuals who may be immune-compromised. *Listeria monocytogenes* has been implicated as the pathogen responsible for several recent outbreaks of foodborne illness linked to contaminated fresh produce, as there is no kill-step for these types of products. Two notable *Listeria* spp. outbreaks include contaminated cut celery from SanGar Fresh Cut Produce in San Antonio, Texas in the fall of 2010 that resulted in 5 deaths due to listeriosis (USFDA 2010) and a multi-state outbreak of listeriosis in the fall of 2011 linked to whole cantaloupes that resulted in 146 people infected and 30 deaths (USFDA 2012a). There was also a recall by a California grower of several varieties of bagged lettuce due to *Listeria monocytogenes* contamination in 2012 (USFDA 2012b).   Incidence of *Listeria monocytogenes* outbreaks may be less prevalent than those related to *Salmonella* spp., but the fatality rate of listeriosis (34%) is much higher than that of salmonellosis (4.1%) making it a significant source of concern in the food industry (Jay and others 2005). There is a need in the food industry for an effective technology to inhibit the growth of foodborne pathogens on fresh produce thereby ensuring the safety of these products for human consumption.

2.2 The Mechanism of Essential Oils as Natural Antimicrobials

Several mechanisms of bacterial inhibition have been proposed and investigated for plant essential oils and their active compounds. Originally, it was postulated that the mechanism of action was purely destruction of the cytoplasmic membrane of bacterial cells, but recently additional mechanisms of inhibition have been proposed. Considering the high level of successful microbial inhibition by plant essential oils, it is likely that more than one mechanism of inhibition is taking place dependent upon what active compounds are present. Possible modes of antibacterial action include: coagulation of the cytoplasm, degradation of the cell wall, damage to the cytoplasmic membrane, damage to membrane proteins, leakage of cell contents, and depletion of the proton motive force (PMF) (Burt 2004). There are two primary classes of active compounds relevant to the plant essential oils used in this study: phenolics and aldehydes. The type of inhibition is dependent on the type of active compound present in the essential oil.

Essential oils containing a high level of phenolic compounds have generally shown the highest level of bacterial inhibition towards foodborne pathogens, but this varies with pathogen species as well (Burt 2004; Davidson and Taylor 2007; Hammer and Carson 2011). Phenolic compounds found in high concentrations in plant essential oils include eugenol, *trans*-cinnamaldehyde, thymol, and carvacrol. Eugenol (Figure 2.1) is the primary active compound in clove bud oil and thymol and carvacrol are found in high concentrations in thyme oil. Several studies have confirmed that the phenolic compounds eugenol, thymol, and carvacrol do in fact disrupt the cytoplasmic membrane via non-specific permeabilization; however, this mode of action could not be confirmed

for cinnamaldehyde (Figure 2.2) (an aromatic aldehyde compound derived from

cinnamon essential oil) (Gill and Holley 2006a).
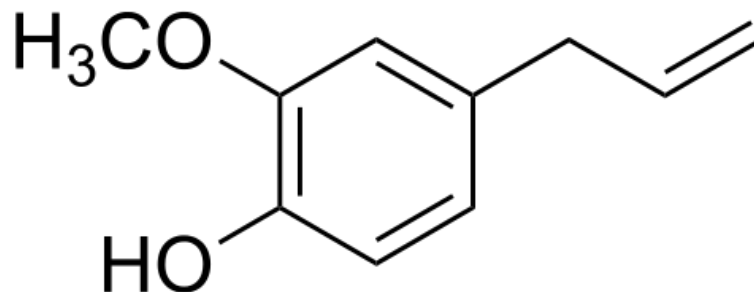
Figure 2.1. Chemical structure of eugenol, the primary active compound present in clove
extract.
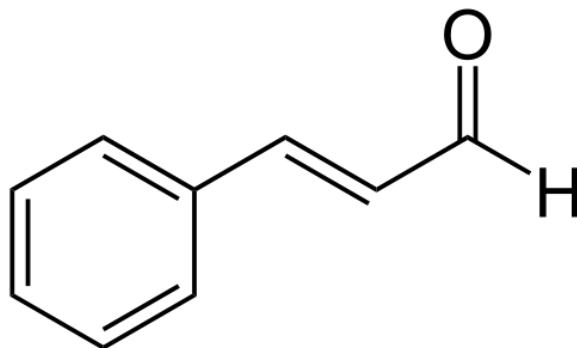
Figure 2.2. Chemical structure of *trans*-cinnamaldehyde, the primary active compound
present in cinnamon extract.

Various studies investigating the phenolic essential oil antibacterial mode of

action have indicated increased extracellular ATP along with other cellular materials and

a depleted pool of intracellular ATP in cells treated with phenolics (Helander and others

1998; Gill and Holley 2004; Gill and Holley 2006b). These results indicate disruption or

disintegration of the cytoplasmic membrane. A graphic depiction of the proposed

mechanisms of action is presented in Figure 2.3. Walsh and others (2003) measured

leakage of potassium ions of Gram-positive and Gram-negative bacteria treated with

thymol and eugenol because it is one of the earliest ways to detect microbial membrane

damage. Their measurements confirmed extensive membrane damage by these two

phenolics. This affinity for the cell membrane is due to the lipophilic nature of the

essential oils, allowing them to partition into the cell membrane. In fact, many essential

oils are more effective bacterial inhibitors at lower pHs because their hydrophobicity

increases, allowing them to more easily partition into the lipids of the cell membrane or

bind to hydrophobic regions of membrane proteins (Burt 2004). The accumulation of

compounds in the membrane leads to membrane swelling and increased membrane

fluidity (Sikkema and others 1994). Increased fluidity of the membrane allows passive

movement of intracellular material to outside the cell. It has also been suggested that

phenolics can form hydrogen bonds with membrane proteins due to their hydrophobic

nature, increasing the permeability of the membrane (Juven and others 1994). Some

studies have suggested that phenolic compounds' mode of action is concentration

dependent; at low concentrations they inhibit energy-producing enzymes and at high

concentrations they are able to denature proteins (Li and others 2011). In fact, when

eugenol was applied to *B. cereus* at sub-lethal concentrations it inhibited production of

amylase and proteases which are necessary for cell nutrient metabolism (Thoroski and

others 1989).

The mechanism of inhibition by aldehyde compounds is still relatively elusive, but several studies have sought to determine their role in bacterial inhibition. Cinnamaldehyde has been shown to be a powerful inhibitor of foodborne pathogens in countless studies (Burt 2004; Johny and others 2008; Amalaradjou and others 2009), and its activity appears to be towards other aspects of bacterial cells aside from the membrane. Helander and others (1998) showed that cinnamaldehyde was inhibitory towards pathogens at similar concentrations to thymol, but it did not increase membrane permeability or deplete intracellular ATP as thymol did. More recently, Amalaradjou and Venkitanarayanan (2011b) showed through quantitative PCR that cinnamaldehyde suppressed the expression of genes associated with biofilm formation and decreased growth of biofilms on several different types of surfaces. Brackman and others (2008) also showed evidence of bacterial gene suppression related to biofilm formation by cinnamaldehyde.

In another study, researchers showed that cinnamaldehyde binds FtsZ protein, which regulates cell division in *Bacillus cereus*, and also inhibited GTPase activity, meaning cinnamaldehyde was able to prevent cell division, leading to cell death (Domadia and others 2007). Similarly, Kwon and others (2003) found that cinnamaldehyde inhibited cell division in *B. cereus,* and they reported that although cinnamaldehyde killed the bacterial cells, they were unlysed and there was very little protein leakage meaning the cell membrane was completely intact upon cell death.

Thus far, it seems that one of cinnamaldehyde's primary modes of action is through protein binding and inhibition. This mechanism is not limited to aldehydes and

is also utilized by phenolic compounds. Gill and Holley (2006b) found that both eugenol and cinnamaldehyde inhibit ATPase activity, which is essential for energy generation in microbial cells. Eugenol and cinnamaldehyde also showed inhibition of two classes of ATPases in liver cells, with eugenol being more potent (Usta and others 2003). Not only do eugenol and cinnamaldehyde inhibit energy generation by ATP, but they are also believed to prevent glucose uptake or utilization that is vital for cell metabolism, thus killing bacteria (Gill and Holley 2004). Cinnamaldehyde and eugenol showed inhibition of amino acid decarboxylases in *Enterobacter aerogenes*, likely by binding the enzyme with the carbonyl group or hydroxyl group of the active compounds, respectively (Wendakoon and Sakaguchi 1995). Amino acid decarboxylases are responsible for the production of biogenic amines by foodborne pathogens.

Sikkema and others (1994) used model bacterial membranes to investigate the role of cyclic hydrocarbons in bacterial inhibition. These authors found that the compounds disabled the proton motive force (PMF) by dissipating the pH gradient and the electrical potential across the membrane. The activity of cyclic hydrocarbons at higher concentrations also resulted in inhibition of cytochrome c oxidase, an enzyme essential for the function of the PMF. Phenolics were able to rapidly dissipate the pH gradient of bacterial cells by increasing membrane permeability and allowing ion leakage (Lambert and others 2001).

Foodborne pathogens are much less likely to develop microbial resistance towards essential oils because they inhibit bacteria through more than one mechanism (Domadia and others 2007). This fact, along with their natural origin makes plant

essential oils a highly desirable antimicrobial for food products. Whole plant extracts,

such as cinnamon or clove extracts, frequently contain several active compounds,

making them potentially more robust bacterial inhibitors. Cinnamon and clove extracts

contain both eugenol and cinnamaldehyde, increasing the potential mechanisms of

inhibition against foodborne pathogens. Recent studies have found whole spice extracts

to be more effective bacterial inhibitors than their corresponding isolated active

compounds, likely due to synergistic effects of multiple compounds working together to

inhibit the bacteria (Valero and Salmeron 2003; Burt 2004).
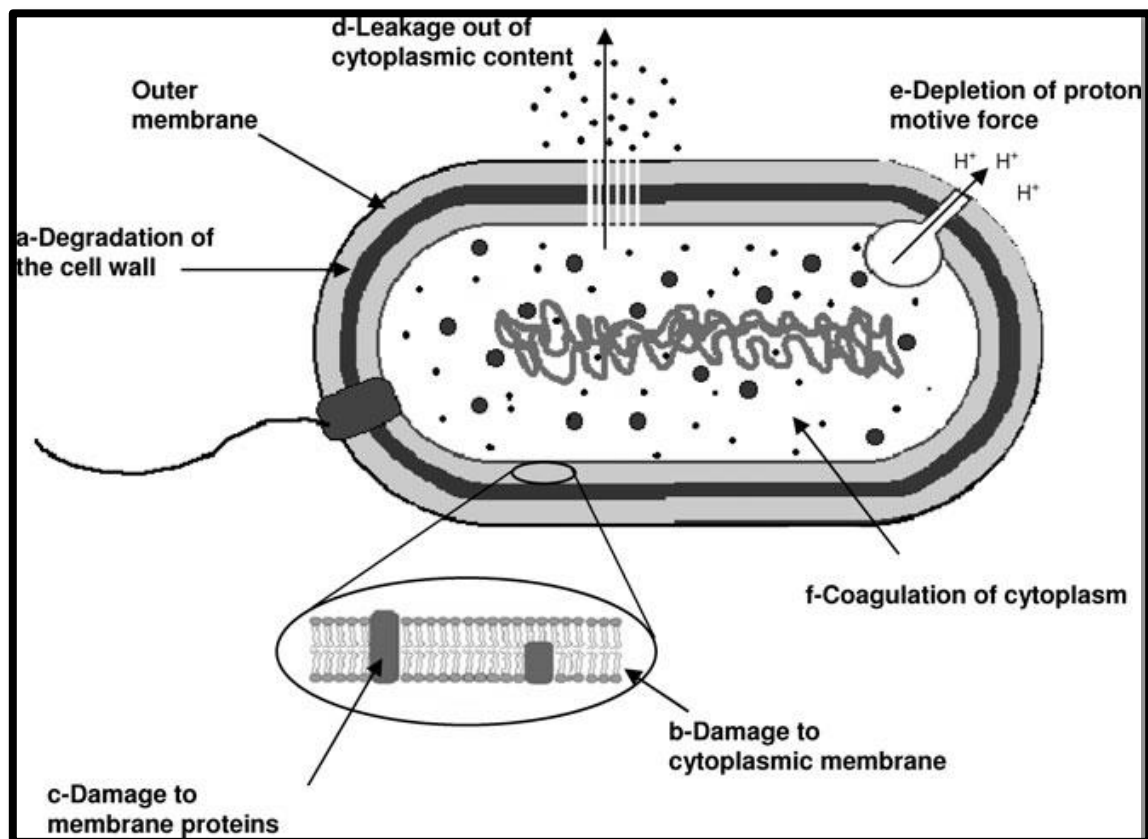
Figure 2.3. Essential oil mechanism of action on microbial cell (Raybaudi-Massilia and others 2009).

2.3 Nanoencapsulation for Controlled Release Applications

The delivery of hydrophobic antimicrobials in food products can be challenging for various reasons. Bacterial cells are usually suspended in aqueous environments in food matrices, so the low aqueous solubility of hydrophobic compounds limits contact between the cells and the antimicrobials. Once contact occurs, the hydrophobic nature of the compounds facilitates bacterial inhibition as it allows the antimicrobials to partition into the cell membrane (Burt 2004; Hammer and Carson 2011). Another challenge for antimicrobials made up of plant oils is that they have an extremely low flavor threshold, so at effective antimicrobial concentrations they can impart negative sensory effects (Kalemba and Kunicka 2003). One way to increase solubility for better pathogen contact and reduce sensory impact of these antimicrobials is through encapsulation. Biopolymers used for encapsulation of antimicrobials in food systems includes a wide range of different materials, including polysaccharides, proteins, lipids, and synthetic polymers (Kuan and others 2012).

Biodegradable polymeric nanoparticles have shown sustained, controlled release, sub-cellular particle size, compatibility with human tissues and cells, and are non-toxic (Kumari and others 2010). The most commonly used biodegradable polymers currently used for nanoencapsulation are: poly-D,L-lactide-co-glycolide (PLGA), polylactic acid (PLA), poly-ε-caprolactone (PCL), poly-alkyl-cyanoacrylates (PAC), chitosan, and gelatin (Kumari and others 2010).

2.4 Beta-Cyclodextrin

Beta-cyclodextrin (BCD) is an enzymatically modified starch molecule consisting of glucose units linked via α-1,4 glucoside bonds. It possesses a torus-shaped or truncated cone structure with a hydrophobic cavity and hydrophilic exterior (Figure 2.4). Cyclodextrins are classified by the number of glucose units linked, with the beta-cyclodextrin possessing seven glucose units. Their unique structure facilitates spontaneous entrapment of appropriately sized hydrophobic molecules, thereby forming inclusion complexes (Ponce Cevallos and others 2010). Beta-cyclodextrin is a compatible sized cyclodextrin for forming 1:1 inclusion complexes with many essential oils (Hedges and others 1995; Benita 2006). The inclusion complexes formed by BCD protect the entrapped molecules from physical or chemical degradation, increases their water solubility, and diminishes their sensory impact (Karathanos and others 2007). Carlotti and others (2007) found that cyclodextrin inclusion complexes were able to protect cinnamaldehyde from degradation due to light and heat. The formation of these inclusion complexes also improves the solubility of the hydrophobic molecule present inside the cavity, allowing better delivery of hydrophobic molecules to target sites in aqueous environments (Stella and He 2008).
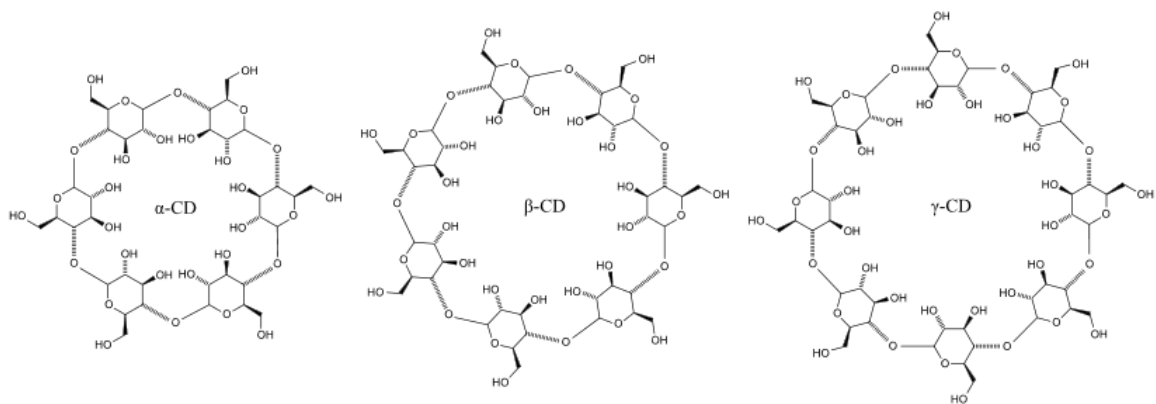
Figure 2.4. Chemical structure of alpha-, beta-, and gamma-cyclodextrin molecules.

Beta-cyclodextrin has been used extensively in the food and pharmaceutical industries and was approved as a GRAS substance in 1998 as a flavor encapsulant (Szente and Szejtli 2004; CFR 2009). Two primary methods for forming cyclodextrin inclusion complexes with essential oils are currently used: the freeze dry method and the kneading method. In freeze drying method, the cyclodextrin and guest molecule are mixed in water for enough time for the complexes to spontaneously form, and then the solution is lyophilized to remove the water. The kneading method does not use an aqueous environment to form the inclusion complexes; instead the cyclodextrin and guest molecule are mixed in the presence of a small amount of solvent and then they are dried in a desiccator. Lipophilic molecules are held within the cavity of the cyclodextrin by van der Waals forces, hydrophobic interactions, and dipole-dipole interactions (Hedges and others 1995).

In a study by Ayala-Zavala and others (2008), cinnamon and garlic extracts showed effective antifungal activity, but this activity was improved when the extracts were incorporated into BCD inclusion complexes. The authors also revealed that

cinnamon extract was a more effective microbial inhibitor than garlic extract (Ayala-Zavala and others 2008). Del Toro-Sánchez and others (2010), Ayala-Zavala and others (2008), and Gomes and others (2011a) also found improved antimicrobial activity and stability of essential oils included in cyclodextrin complexes. Del Toro-Sánchez and others (2010) showed increased inhibition of *Alternaria alternata* mold with thyme essential oil-BCD complex. Both Del Toro-Sánchez and others (2010) and Ayala-Zavala and others (2008) proposed cyclodextrins as a controlled delivery system for antimicrobial compounds that can be controlled by changing levels of relative humidity in packaging headspace. This concept could be especially beneficial in fresh-cut produce packaging as fruits and vegetables have high moisture contents that lead to higher relative humidity environments in their packaging (Astray and others 2009). Gomes and others (2011a) found that several essential oils and their active compounds (*trans-*cinnamaldehyde, eugenol, and garlic extract) were more effective bacterial inhibitors against *Salmonella* and *Listeria* species when the active compounds were protected by beta-cyclodextrin inclusion complexes.

The enhanced activity of BCD-essential oil inclusion complexes is due to improved aqueous solubility and stability of the essential oils. The lipophilic nature of essential oils and their constituents allows them to interfere with the cytoplasmic membrane that protects pathogens. However, because most fresh produce has a high water content the essential oils have a low solubility and need a more soluble carrier to have sufficient contact with the pathogens present in the aqueous environment (Kalemba and Kunicka 2003). Increased aqueous solubility of hydrophobic guest molecules is

shown in several studies exploring essential oil inclusion complexes with cyclodextrins (Carlotti and others 2007; Karathanos and others 2007; Mourtzinos and others 2007; Gomes and others 2011a). The changes in solubility were evident through thermodynamic stability experiments. These results showed the increased solubility of the hydrophobic compounds after their incorporation in the cyclodextrin inclusion complexes (Tang and others 2002; Karathanos and others 2007). Improved antimicrobial activity of the BCD-essential oil complexes can lessen the sensory impact of the essential oils by lowering the effective dosage of the essential oils.

2.5 Poly-D,L-Lactide-co-Glycolide (PLGA)

PLGA is a synthetic polymer that has been extensively used for drug delivery applications with great success because it undergoes hydrolysis in the body to produce lactic acid and glycolic acid which are easily metabolized (Kumari and others 2010) (Figure 2.5). PLGA nanoparticles can be prepared by several different methods including: emulsification-diffusion, solvent emulsion-evaporation, interfacial deposition, and nanoprecipitation. The molecular weight of the encapsulated material and the ratio of lactide to glycolide in the polymer affects the release characteristics of the PLGA nanoparticles, so a desired release profile can be designed (Kumari and others 2010). PLGA has been approved by the US Food and Drug Administration (USFDA) for human use, so it can potentially be used for encapsulation in the food industry (Anderson and Shive 1997). Active ingredients are released from PLGA nanoparticles at a sustained rate via diffusion through the capsule and degradation of the polymer nanoparticle (Panyam and Labhasetwar 2003). In a recent study PLGA was used to

16

encapsulate α-tocopherol, which is an important bioactive compound that has been linked to the prevention and treatment of chronic diseases associated with aging (Zigoneanu and others 2008). The PLGA nanocapsules were able to protect α-tocopherol from degradation caused by contact with oxygen, light, heat, alkali, trace minerals, and hydroperoxides during storage and then provide a steady controlled release in aqueous media (Zigoneanu and others 2008).
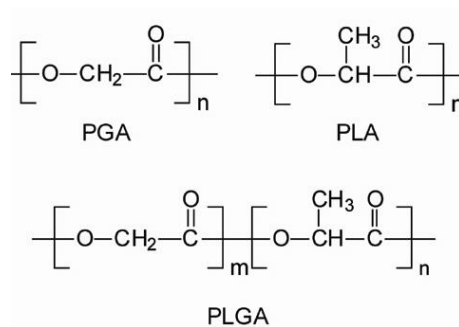
Figure 2.5. Schematic of Poly (D,L-lactide-co-glycolide) (PLGA) and its components, Polyglycolic acid (PGA) and Polylactic acid (PLA).

A study conducted by Donsì and others (2011) used PLGA to encapsulate essential oils to combat spoilage microorganisms in fruit juices. These PLGA nanocapsules were able to inhibit or inactivate the microorganisms at concentrations low enough to prevent any negative sensory impact to the juice products. The inhibitory activity of benzoic and vanillic acids against *Listeria monocytogenes, Escherichia coli* O157:H7, and *Salmonella* Typhimurium was also enhanced by encapsulation in PLGA (Ravichandran and others 2011). These PLGA nanoparticles were tested in microbial growth media broth as well as raw and cooked chicken meats. The nanoencapsulation

protected the hydrophobic phenolic acids from environmental degradation and aided their delivery to the aqueous sites of pathogens (Ravichandran and others 2011). Carvacrol, the primary active compound in oregano extract, was encapsulated in PLGA and used to weaken microbial biofilm formation (Iannitelli and others 2011). The authors also proposed that PLGA nanocapsules could have the ability to deliver antimicrobial compounds deep within the biofilms, as they were able to penetrate the film's mucus membranes (Iannitelli and others 2011). Gomes and others (2011b) showed that PLGA encapsulated essential oils are more effective inhibitors of both Gram-positive and Gram-negative pathogens than free essential oils at similar concentrations. The authors used eugenol and *trans*-cinnamaldehyde, which were also explored for this dissertation research.

2.6 Stimuli-Responsive Polymers

Researchers are now creating nanocapsules that only release their active contents in response to specific environmental conditions to improve the potency of the active material. The two methods for targeted nanocapsule delivery are by using stimuli-responsive materials to form nanocapsules or by created surface-labeled nanocapsules that can bind specific target sites. Stimuli-responsive nanocapsules are designed to begin releasing their contents only when subjected to specific environmental conditions such as: pH, temperature, light, magnetic fields, ion concentration, or a combination of any of these stimuli (Zha and others 2011). These nanocapsules have improved activity because they are not releasing their contents until they will have the greatest impact. The ability to control when and where nanocapsules are releasing their contents can improve

the efficacy of the active agent because it is localized to the specific area of interest. For

drug delivery, this means improved bioavailability at the target tissue and for

antimicrobials it means increased contact with microorganisms.

One of the most frequently studied temperature responsive nanoencapsulant

materials is poly(N-isopropylacrylamide) (PNIPAAM) (Figure 2.6). PNIPAAM exhibits

inverse aqueous solubility at a lower critical solution temperature (LCST) between 30-

35°C, meaning that above this temperature it is insoluble in water and contracts,

squeezing out any entrapped compounds (Schild 1992). The LCST can be adjusted by

using different synthesis techniques or by co-polymerization with other monomers.

Temperature controlled nanocapsules are more suitable for applications in the food

industry than for drug delivery because the human body is essentially one constant

temperature in all tissues. It would be difficult to target a particular site within the body

using temperature only-responsive nanocapsules. Nanocapsules with temperature active

properties could be used for antimicrobial encapsulation in food systems so that when

foods are stored at abusive temperatures (Doyle and Beuchat 2007), a release response

could be triggered from the nanocapsule in response to the environmental conditions.

While the response temperature for PNIPAAM would be highly abusive for the storage

of fresh produce, this polymer can be used as a model for future studies of stimuli-

responsive nanocapsules.
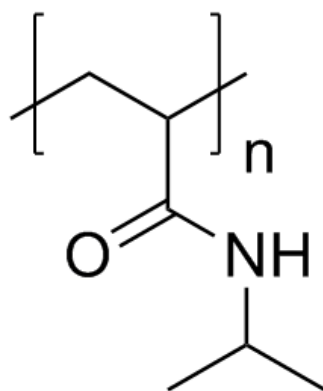
Figure 2.6. N-isopropylacrylamide (NIPAAM) monomer unit chemical structure.

Co-polymerization of PNIPAAM with pH-responsive materials, such as chitosan or alginate, will increase the range of applications for these nanocapsules and allow for more specific controlled release. Dual stimuli-responsive nanocapsules can be engineered to respond to each stimulus separately or to respond only when both stimuli exist in the external environment (Zha and others 2011). The way that dual stimuli-responsive nanocapsules function is determined by the manner in which they are manufactured.

Chitosan is a natural cationic biopolymer derived from chitin, which is found in the shells of crustaceans and insects (Kumari and others 2010) (Figure 2.7). Chuang and others (2010) produced PNIPAAM-co-chitosan nanocapsules for drug delivery of hydrophilic active compounds. The authors monitored the release of doxycycline hyclate loaded nanocapsules in four different temperature and pH environments: pH=2.0 at 25°C or 37°C and pH=7.0 at 25°C or 37°C. At 25°C, the PNIPAAM is swollen due to its hydrophilicity below the LCST, but at 37°C it becomes hydrophobic and contracts. Similarly, the chitosan in the nanocapsules swells at pH 2.0 due to its cationic nature and

shrinks at pH 7.0. As a consequence of the behavior of these two polymers, drug release was greatest at pH 2.0 and 37°C because the PNIPAAM shrinks and squeezes out the drug, while the chitosan expands and allows the encapsulated material to diffuse out of the particle more readily (Chuang and others 2010). This type of particle could be an excellent delivery vehicle for antimicrobials in food products because bacteria grow rapidly at 37°C and most bacteria ferment carbohydrates to produce acid, which would lower the pH of the food products. However, produce is unlikely to be stored at this temperature, with the exception of extreme abuse by end consumers and at the point of human consumption.
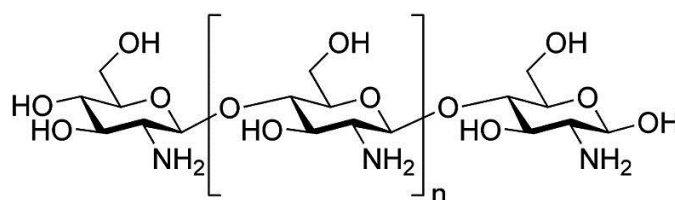
Figure 2.7. Chemical structure of chitosan, a biopolymer extracted from chitin.

Another study prepared PNIPAAM-co-alginate polymers by two different methods to demonstrate the impact of preparation conditions on the stimuli response of the co-polymers (Ju and others 2001). Alginate (Figure 2.8) exhibits the reverse behavior to pH that chitosan displays; it becomes more hydrophilic as the pH increases because it is an anionic polymer. It is a biocompatible polysaccharide extracted from the brown algae Phaeophyceae (de Moura and others 2009). Alginate contributes good

biocompatibility, hydrophilicity, biodegradeability, and porosity to a PNIPAAM co-

polymer. The co-polymers were formed by grafting the alginate onto the PNIPAAM or

by physical assembly using the interpenetrating polymer network (IPN). The grafted co-

polymers showed a much more rapid response than those formed using the IPN, but the

pH and temperature at which they responded were similar. PNIPAAM grafted with

alginate formed by Kim and others (2002) also showed the same rapid response behavior

to temperature and pH. A rapid response is desirable for these nanocapsules so that

release can begin to take place immediately when the environmental conditions are

suitable.
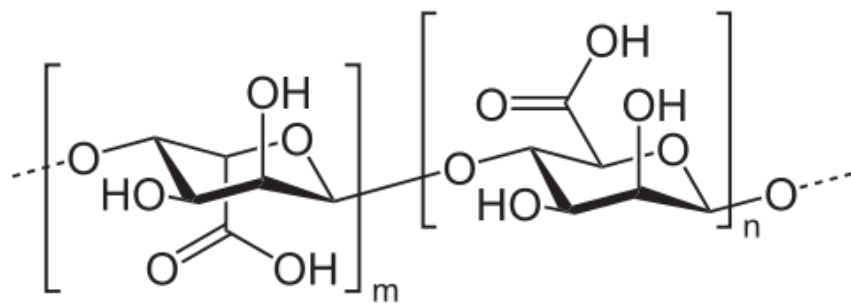
Figure 2.8. Chemical structure of alginate, a polysaccharide extracted from brown algae.

        PNIPAAM nanoparticles can be formed by two primary methods: physical

assembly and grafting co-polymerization. Physical assembly uses the interpenetrating

polymer network (IPN) technology to form the polymer mixture where hydrophilic and

hydrophobic polymer networks are physically interconnected, but no chemical bonds are

formed. This allows all the polymers included to retain all of their individual properties

(Yu and others 2006; Klouda and Mikos 2008). Graft co-polymerization allows for more rapid swelling/deswelling behavior, which indicates a more rapid response to pH/temperature stimuli (Ju and others 2001; Kim and others 2002). The nanoparticles themselves can be created by self-assembly in a heated solution so that polymer micelles form, in order to minimize unfavorable hydrophobic interactions, and then the micelles can be crosslinked to reinforce the particle structure.

An alternate method of forming co-polymer particles is described by Ju and others (2001) to form semi-IPN co-polymer. This method employs the IPN to form co-polymers between PNIPAAM-NH$_2$ (amino semi-telechelic PNIPAAM) and alginate by forming amide bonds between carboxyl group in alginate gel and amino group in the PNIPAAM. Antimicrobial loading of these hydrogels can be accomplished by the emulsion evaporation method, similar to that described by Astete and Sabliov (2006).

A food product subjected to these conditions, treated with antimicrobials encapsulated in the aforementioned nanocapsules, would trigger release of the antimicrobial to inactivate the bacteria as it begins to proliferate and improve the safety of the food. A rapid response is desirable for these nanocapsules so that release can begin to take place immediately when the environmental conditions are suitable. Nanoencapsulation is a rapidly growing area of research, but thus far has been heavily focused on drug delivery applications. There are countless potential uses for nanocapsules in different industries, including the food industry, but extensive research must be done before this technology can be widely applied in other industries. There are numerous potential encapsulation materials for hydrophobic essential oil antimicrobials.

The biggest gap in the research of encapsulated antimicrobials is comparing different encapsulation systems for release and efficacy towards foodborne pathogens in food and beverage products. Extensive research has been conducted on free essential oils as antimicrobials, but their use is not practical for most food products due to their negative sensory impact at effective concentrations, low aqueous solubility, and high volatility. Encapsulation of essential oils can delay their release and intensify their impact against pathogens by preventing their volatilization and improving their delivery (Weiss and others 2006).

2.7 Summary

There are numerous potential encapsulation materials for hydrophobic essential oil antimicrobials, even beyond those studied here. The biggest gap in knowledge of encapsulated antimicrobials is testing different encapsulation systems for release and efficacy towards foodborne pathogens in food and beverage products. Flavor encapsulation is widely published for food applications, but the encapsulation properties needed for flavor release are in opposition to what is proposed for antimicrobial release. Flavor encapsulation benefits from a burst release in the mouth, but this type of release for essential oil antimicrobials would be undesirable. One of the goals of antimicrobial encapsulation is to mask sensory qualities of the potent essential oils on food products. Release from lipid and synthetic polymer-based antimicrobial capsules has had some publications recently, but not extensively. These types of capsules as well as polysaccharide and protein-based capsules need further experimentation on release

properties, capsule characteristics and stability, antimicrobial efficacy *in vitro* and

incorporated into food and beverage products.

CHAPTER III

CHARACTERIZATION OF BETA-CYCLODEXTRIN INCLUSION COMPLEXES CONTAINING ESSENTIAL OILS (*TRANS-CINNAMALDEHYDE*, EUGENOL, CINNAMON BARK, AND CLOVE BUD EXTRACTS) FOR ANTIMICROBIAL DELIVERY APPLICATIONS*

3.1 Overview

This study aimed to elucidate the physico-chemical characteristics of EO-BCD inclusion complexes and their resulting antimicrobial activity. Cinnamon bark extract, *trans*-cinnamaldehyde, clove bud extract, eugenol, and a 2:1 (*trans*-cinnamaldehyde:eugenol) mixture were microencapsulated by the freezedrying method. EO-BCD complexes were characterized for particle size, morphology, polydispersity index, entrapment efficiency, and phase solubility. All particles showed a spherical shape, smooth surface, no significant differences in size distribution and strong tendency to agglomerate. The entrapment efficiencies ranged from 41.7 to 84.7%, where pure compounds were higher (P < 0.05) than extracts. The oils and their BCD complexes were analyzed for their antimicrobial activity against *Salmonella enterica* serovar Typhimurium LT2 and *Listeria innocua*. All antimicrobials effectively inhibited bacterial growth within the concentration range tested, except free eugenol. The EO-BCD complexes were able to inhibit both bacterial strains at lower active compound concentrations than free oils, likely due to their increased water solubility that led to increased contact between pathogens and essential oils. The cinnamon bark and clove

bud extract BCD complexes were the most powerful antimicrobials, despite showing the lowest entrapment efficiencies amongst the oils. Results suggest that the application of these antimicrobial complexes in food systems may be effective at inhibiting pathogens.

3.2 Introduction

The Centers for Disease Control and Prevention (CDC) have estimated that up to 48 million illnesses, 128,000 hospitalizations, and 3,000 deaths each year in the United States are caused by foodborne pathogens (Centers for Disease Control and Prevention (CDC) 2011a; Centers for Disease Control and Prevention (CDC) 2011b; Centers for Disease Control and Prevention (CDC) 2012). Symptoms of the illnesses caused by these pathogens may range from mild gastroenteritis to life-threatening neurological, hepatic, or renal syndromes. *Salmonella* and *Listeria monocytogenes* are two of the major pathogens that cause foodborne illnesses. *Salmonella* are the most common bacterial pathogens associated with foodborne outbreaks around 1.2 million cases of salmonellosis occur in the United States annually. Infection often leads to diarrhea, fever, and abdominal cramps and can lead to severe illness in young children, the elderly population and anyone who is immune-compromised (Centers for Disease Control and Prevention (CDC) 2011a; Centers for Disease Control and Prevention (CDC) 2012). *L. monocytogenes* has been attributed to foodborne pathogen outbreaks on a variety of food products (ready-to-eat meat, poultry products, and vegetables) and can cause serious health problems including still births, premature delivery, meningitis, and septicemia (Swaminathan and others 2007). There is a need in the food industry for effective

technologies to inactivate foodborne pathogens on food products and ensure their safety for consumers.

Essential oils (EOs) have been shown to be powerful natural antimicrobials against a variety of foodborne pathogens (Kim and others 1995). Their "natural" reputation makes them highly desirable for use in food products, as consumers have become weary of chemical or synthetic additives in their foods in recent history. Many have already been granted Generally Recognized as Safe (GRAS) status by the FDA in 21 CFR (Code of Federal Regulation) part 172.515 (CFR 2009), meaning they can be used in food products without further approval. Different EOs exhibit varying inhibitory effects on microbial pathogens. Cinnamon extract, *trans*-cinnamaldehyde, clove extract, and eugenol have been found to be some of the most effective antimicrobials against foodborne pathogens and it has been reported that spice extracts are more powerful inhibitors than purified compounds (Valero and Salmeron 2003; Gomes and others 2011a). The challenges with using these antimicrobials on food products are: (i) they have an extremely low flavor threshold and can drastically change the sensory properties of the food and (ii) they are highly insoluble in water due to their lipophilic nature and may have limited contact with pathogens in high moisture content foods (Kalemba and Kunicka 2003).

One way to avoid or lessen these effects is through an encapsulation process, a technique designed to improve aqueous solubility and potentially enhance delivery of antimicrobials. Cyclodextrins are enzymatically modified starch that have the ability to form inclusion complexes with hydrophobic molecules such as essential oils

(Mourtzinos and others 2008). Cyclodextrins can not only mask the flavor of essential oils to be used as antimicrobials but can also protect against oxidation or heat damage, allowing the essential oils to remain effective as antimicrobial agents under a wide variety of environmental conditions and for longer time periods (Hedges and others 1995; Qi and Hedges 1995). The type of cyclodextrin (α-, β-, γ-) indicates its size and therefore the size of the hydrophobic molecule that the cyclodextrin can entrap in its inner cavity (Karathanos and others 2007). The interaction between BCD (host) and active compounds (guests) may involve total inclusion or association with the hydrophobic or hydrophilic part of the molecule (Szente and Szejtli 2004). Beta-cyclodextrin is GRAS, appropriately sized cyclodextrin for forming 1:1 inclusion complexes with *trans*-cinnamaldehyde, eugenol, cinnamon bark extract, and clove bud extract molecules (USFDA 2001; Benita 2006). Once oils are within the inclusion complexes, their sensory impact on food products can be reduced and their water solubility increased, providing sufficient contact with pathogens to inhibit their growth, making foods safer for human consumption. Considering the requirements of natural antimicrobial application effectiveness and convenience in food systems, the goal of this study was to determine the physico-chemical characteristics of various EO-BCD inclusion complexes and their resulting antimicrobial activity against foodborne pathogens.

3.3 Materials & Methods

3.3.1 Materials

All extracts and essential oils were of food-grade quality and were purchased from Sigma Aldrich Co. (St. Louis, MO, U.S.A.). The *trans*-cinnamaldehyde (93%), eugenol (99%), clove bud and cinnamon bark extracts (100%) were used in this study. Beta-cyclodextrin (BCD) hydrate was purchased from Alfa Aesar (Ward Hill, MA, U.S.A.), and tryptic soy agar (TSA), tryptic soy broth (TSB), peptone, modified Oxford's medium (MOX), and tryptose phosphate broth (TPB) for bacterial growth and enumeration were purchased from Becton, Dickinson and Co. (Franklin Lakes, NJ, U.S.A.). HPLC-grade acetonitrile was purchased from Mallinckrodt Chemical (Hazelwood, MO, U.S.A.). All other reagents were analytical grade.

3.3.2 Preparation of beta-Cyclodextrin Inclusion Complexes

The inclusion complexes were prepared via the freeze-drying method (Karathanos and others 2007). BCD and EOs were mixed in an aqueous solution in a 1:1 molecular ratio at concentrations of 16 mM each. The mixture was magnetically stirred in a sealed container for 24 h at room temperature (25°C) to allow for complex formation and prevent loss of volatiles to the atmosphere. After mixing, the solution was frozen and lyophilized at -50°C and 1.09 Pa in a Labconco Freeze Dryer-5 (Kansas City, MO) for approximately 48 h or until all moisture had been sublimated. The lyophilized powders were stored in sealed containers inside a desiccator at -20°C until use. Inclusion complexes containing *trans*-cinnamaldehyde, eugenol, 2:1 *trans*-cinnamaldehyde:eugenol, cinnamon bark extract, and clove bud extract were prepared.

Calculations for mixing the 1:1 molecular aqueous solutions for the cinnamon bark and clove bud extract inclusion complexes were based upon the concentrations of active compound present (*trans*-cinnamaldehyde and eugenol, respectively). The concentration of each active compound in the spice extracts was measured spectrophotometrically at 280 nm (Shimadzu UV-1601 spectrophotometer, Columbia, MA).

3.3.3 Particle Characterization

Oxidative Differential Scanning Calorimetry (DSC)

Oxidative DSC was used to study complex formation between EOs and BCD. Analysis was performed using a Pyris 6 Perkin Elmer instrument (Pyris 5.0 Software, Boston, MA) with a scanning rate of 90°C/min from 25 to 120°C, maintained at 120°C for 1 min to ensure even sample heating, then heated to 400°C at a rate of 10°C/min under an oxygen atmosphere (ultra-pure air) (Mourtzinos and others 2007). The instrument was calibrated using zinc and indium metals before sample testing. Samples of free EOs or the BCD complexes containing the same quantity of EO (~2.0 mg) were weighed to the nearest 0.1 mg into 20 μL aluminum pans and sealed with one hole in their lids.

Particle Size Analysis and Morphology

A Delsa™ Nano C Particle Analyzer (Beckman Coulter, Brea, CA) was used to measure the average size and polydispersity indices (PDI) for each type of BCD inclusion complex particle. The particles were suspended in distilled water at a 4:1 ratio for measurement in 1 cm path length plastic cuvettes at scattering angle of 165°, with a pinhole set to 20 μm, and a refractive index of 1.3328 for 120 continuous accumulation

times. PDI is a measure of the uniformity of particle sizes present in the suspension. A value close to zero (<0.10) indicates little variability in size (monodisperse), whereas values > 0.10 indicate polydisperse systems (Zigoneanu and others 2008). The advantage of a monodisperse system is related to its ability to deliver a consistent amount of compound, as compared to a mixture of polydisperse particles, of different loading capacities (Astete and Sabliov 2006).

Aqueous suspensions of inclusion complex particles were examined using a JEOL 1200 EX Transmission Electron Microscope (TEM) (JEOL USA Inc., Peabody, MA) at the Microscopy Imaging Center of Texas A&M University (College Station, TX). Aqueous suspensions of particles were placed on 400 mesh copper grids and stained with a 2.0% uranyl acetate aqueous stain (EMS, Hatfield, PA) to provide contrast under magnification. Excess liquid on the mesh was removed with filter paper and the grid was allowed to dry before viewing under 50,000 times magnification. Observations were performed at 100 kV.

Entrapment Efficiency (EE)

The amount of active compound (eugenol and *trans*-cinnamaldehyde) entrapped in the inclusion complex particles was determined spectrophotometrically at 280 nm. For each type of inclusion complex, 5 mg of sample was dissolved in 5 mL of 95% (w/v) acetonitrile and left for 24 h after being well mixed to allow enough time for all entrapped active compound to be in solution. Before measurement, the solutions were centrifuged at 3200 x g for 15 min to remove any BCD from the solution, leaving only the active compound. The EE was calculated (Gomes and others 2011a):

$$EE = \frac{amount\ of\ active\ compound\ entrapped}{initial\ active\ compound\ amount} \times 100 \qquad [3.1]$$

where "amount of active compound entrapped" is the amount of compound present in the inclusion complex particles and "initial active compound amount" indicates the amount of active compound initially used to manufacture the inclusion complex particles.

Phase Solubility Determination

Phase solubility experiments were performed for each type of inclusion complex as described by Higuchi and Connors (1965). An excess of EO was added to 10 mL aqueous solutions of BCD ranging in concentration from 0 to 10 mmol/L and placed at 25, 35, and 45°C in a laboratory shaker (VWR 18L Shaking Water Bath, Radnor, PA) for 24 h at 200 rpm. The quantity of EO remaining in solution after 24 h was measured spectrophotometrically at 280 nm. All samples were filtered through 0.45-µm hydrophilic PTFE filters (IC Millex-LH, Millipore, Billerica, MA) prior to measurement to remove any insoluble material, so that only solubilized EO was measured. Calculations for cinnamon bark and clove bud extracts were based on molecular weights of *trans*-cinnamaldehyde and eugenol, respectively. The stability constants, K_c (L/mol), were calculated:

$$K_c = \frac{slope}{intercept \cdot (1 - slope)} \qquad [3.2]$$

The experimental data from the phase solubility can be used to estimate thermodynamic properties of the complex formation using the integrated form of the Van't Hoff Eq. (3.3) and the experimentally determined K_c values.

33

$$\ln K_c = -\frac{\Delta H}{RT} + \frac{\Delta S}{R} \qquad\qquad [3.3]$$

where ΔH is the enthalpy change for the reaction, R is the gas constant, T is the absolute

temperature, ΔS is the change in entropy for the reaction. Van't Hoff plots for complex

formation showed linear relationships between K_c and the inverse of temperature. The

Gibbs free energy (ΔG) can be calculated using the aforementioned parameters and Eq.

(3.4) at standard pressure and temperature.

$$\Delta G = \Delta H - T . \Delta S \qquad\qquad [3.4]$$

3.3.4 Minimum Inhibitory and Bactericidal Concentration

<u>Bacterial Cultures</u>

Salmonella enterica serovar Typhimurium LT2 and *Listeria innocua* were

obtained from Texas A&M University Food Microbiology Laboratory (College Station,

TX). These strains were chosen as representative of Gram-negative and Gram-positive

bacteria, respectively. The *S.* Typhimurium and *L. innocua* were resuscitated in TSB and

TPB, respectively, by identical duplicate transfers and incubated aerobically for 24 h at

35°C. The bacterial cultures were maintained on TSA slants at 4°C. The organisms'

identities were confirmed using Enterotube[®] II (Becton, Dickinson and Co., Franklin

Lakes, NJ) for *S.* Typhimurium and RAPID' *Listeria* spp. Agar (Bio-Rad, Hercules, CA)

for *L. innocua* according to manufacturer instructions.

Antimicrobial Activity

Minimum inhibitory concentrations (MICs) for the inclusion particles and the
pure essential oils were determined using a broth dilution assay (Brandt and others
2010). Growth curves were first performed at 35°C on each strain to correlate plate
counts with optical density values at 630 nm (OD630) using an EL_{800} absorbance
microplate reader (BioTek® Instruments, Inc., Winooski, VT). *Salmonella*
Typhimurium and *L. innocua* cultures were incubated 20-22 h and then prepared by
serial dilution in double-strength TSB (2x TSB) and TPB (2x TPB), respectively, for an
initial inoculum of approximately 5.0 $\log_{10}$ CFU/mL in each sample well. Initial inocula
were enumerated via spread plating on TSA (*Salmonella* spp.) or MOX (*Listeria* spp.)
and incubated for 24 h at 35°C. Aliquots of 100-µL of all antimicrobial solutions and
solvent blanks were spread plated to ensure sterility.

The MIC experiments were conducted in 96 well microtiter plates (sterilized
300-µl capacity – MicroWell, NUNC, Thermo-Fisher Scientific, Waltham, MA). The
antimicrobial inclusion complexes were added to the microtiter plates as aqueous
suspensions, while the EOs were added as aqueous microemulsions containing 1.0%
ethanol and 0.01% Tween 20 (w/w). The concentration of inclusion complex added to
the test wells ranged from 1,000-10,000 µg/mL, while the concentration of EOs ranged
from 100-1,000 µg/mL for *S.* Typhimurium and 200-2,000 µg/mL for *L. innocua*.

Equivalent volumes (100-µL) of antimicrobial solution and bacterial inoculum in
2x broth were loaded into each test well. Negative controls were prepared with
antimicrobial solutions and sterile 2x broth to account for baseline OD630 readings.

Positive controls were also prepared containing inoculum and sterile distilled water, Tween 20, and ethanol at test concentrations (combined and singly) to ensure solvents and additives had no effect on OD630. Once plates were prepared, they were covered with a mylar plate sealer (Thermo-Fisher Scientific) and OD630 of the wells was read (0 h). The microtiter plates were incubated (24 h at 35°C) and then another OD630 reading was taken. Any antimicrobial test wells that showed ≤0.05 change in OD630 after 24 h of incubation were considered "inhibited" by the antimicrobial (after appropriate baseline adjustments). The MIC was determined by the lowest concentration of antimicrobial that inhibited growth for all test replicates (Brandt and others 2010).

All wells that showed inhibition of the test organism were then tested for bactericidal capability by spreading 100 µL from each well showing inhibition onto TSA or MOX plates and incubating for 24 h at 35°C. If no colonies were observed on the plate surfaces following incubation, the treatment concentration was considered bactericidal. The lowest concentration of antimicrobial demonstrating bactericidal activity across all replicates was considered the MBC.

3.3.5 Statistical Analysis

For all analyses, determinations were made in triplicate as independent experiments. Data analysis was performed using JMP v. 9 software (SAS Institute, Cary, NC) for size, PDI of inclusion complexes, entrapment efficiency, partition coefficient, and MIC. Differences between variables were tested for significance by one-way analysis of variance (ANOVA). Significantly different means ($P<0.05$) were separated

by the Tukey's Honestly Significant Differences (HSD) test. Linear regression and analysis of covariance with 95 % confidence interval were used when appropriate.

3.4 Results and Discussion

3.4.1 Particle Characterization

Oxidative Differential Scanning Calorimetry

The formation of inclusion complexes for each EO was confirmed by oxidative DSC. Since the Eos used in this study are liquid at room temperature, their inclusion complexes can be confirmed using DSC indirectly by comparing the thermal stability of the free compound with the encapsulated form (Karathanos and others 2007; Gomes and others 2011a).The thermal oxidation stability of free EOs was compared to their BCD encapsulated form. Figure 3.1 depicts exothermic peaks at approximately 265°C and 260°C which can be interpreted as resulting from the hydrolysis or oxidation of *trans*-cinnamaldehyde and eugenol (Karathanos and others 2007). Similar exothermic peaks were observed in previous studies (Seo and others 2010; Gomes and others 2011a).These peaks are not detected in the thermogram of the equivalent BCD inclusion complex, indicating active compounds were protected within the cavity of the BCD. Endothermic peaks detected at approximately 100°C were attributed to water evaporation for all samples and the exothermic peaks around 300°C for the BCD samples due to melting and thermal decomposition of the BCD itself (Hedges and others 1995). Figure 3.2 shows similar results for the extracts and their BCD inclusion complex particles, meaning all were successfully encapsulated by the BCD.
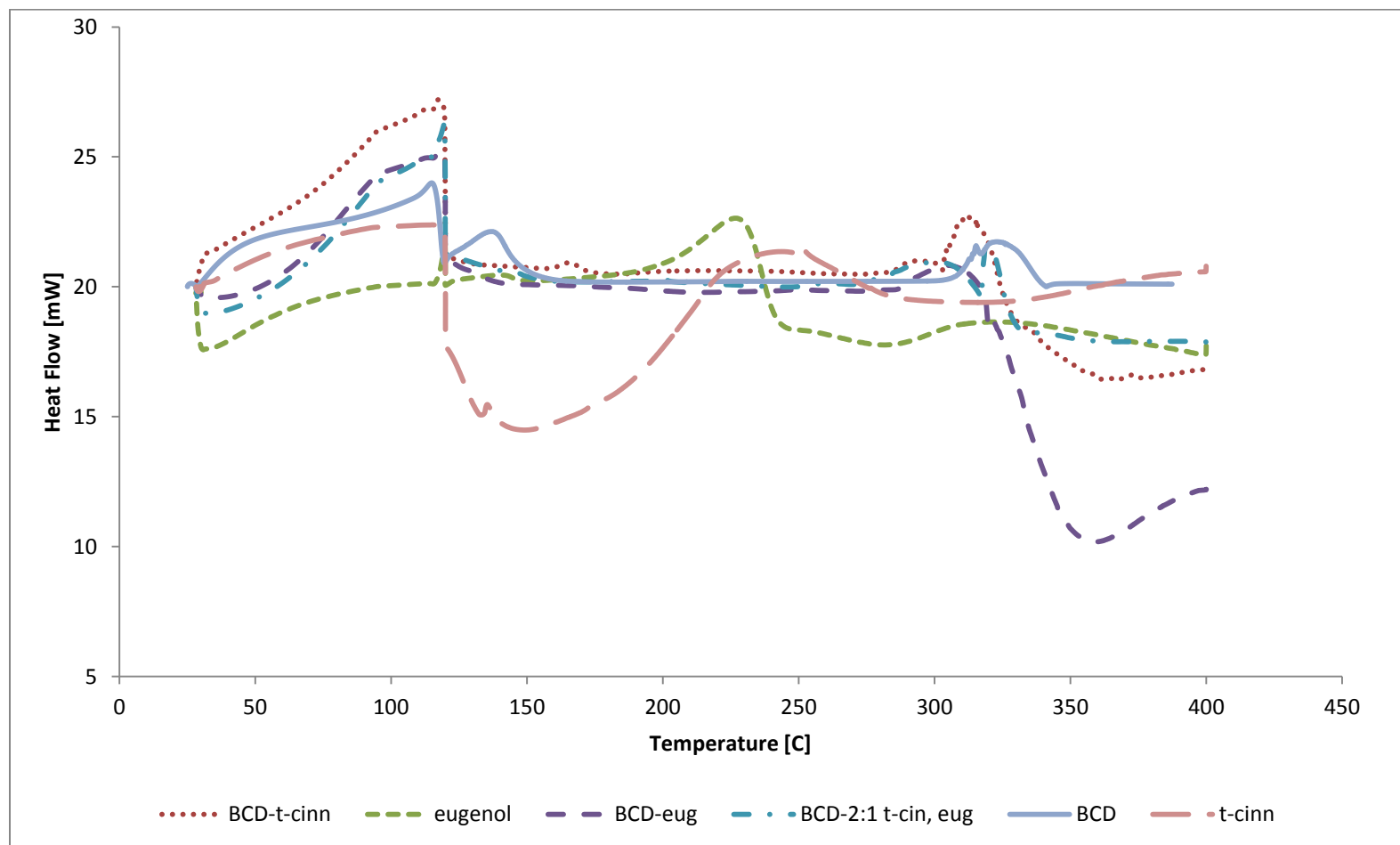
Figure 3.1. Oxidative differential scanning calorimetry (DSC) thermogram of *trans*-cinnamaldehyde (t-cinn), eugenol (eug), their respective BCD complexes and a BCD complex containing a 2:1 mixture of *trans*-cinnamaldehyde and eugenol.
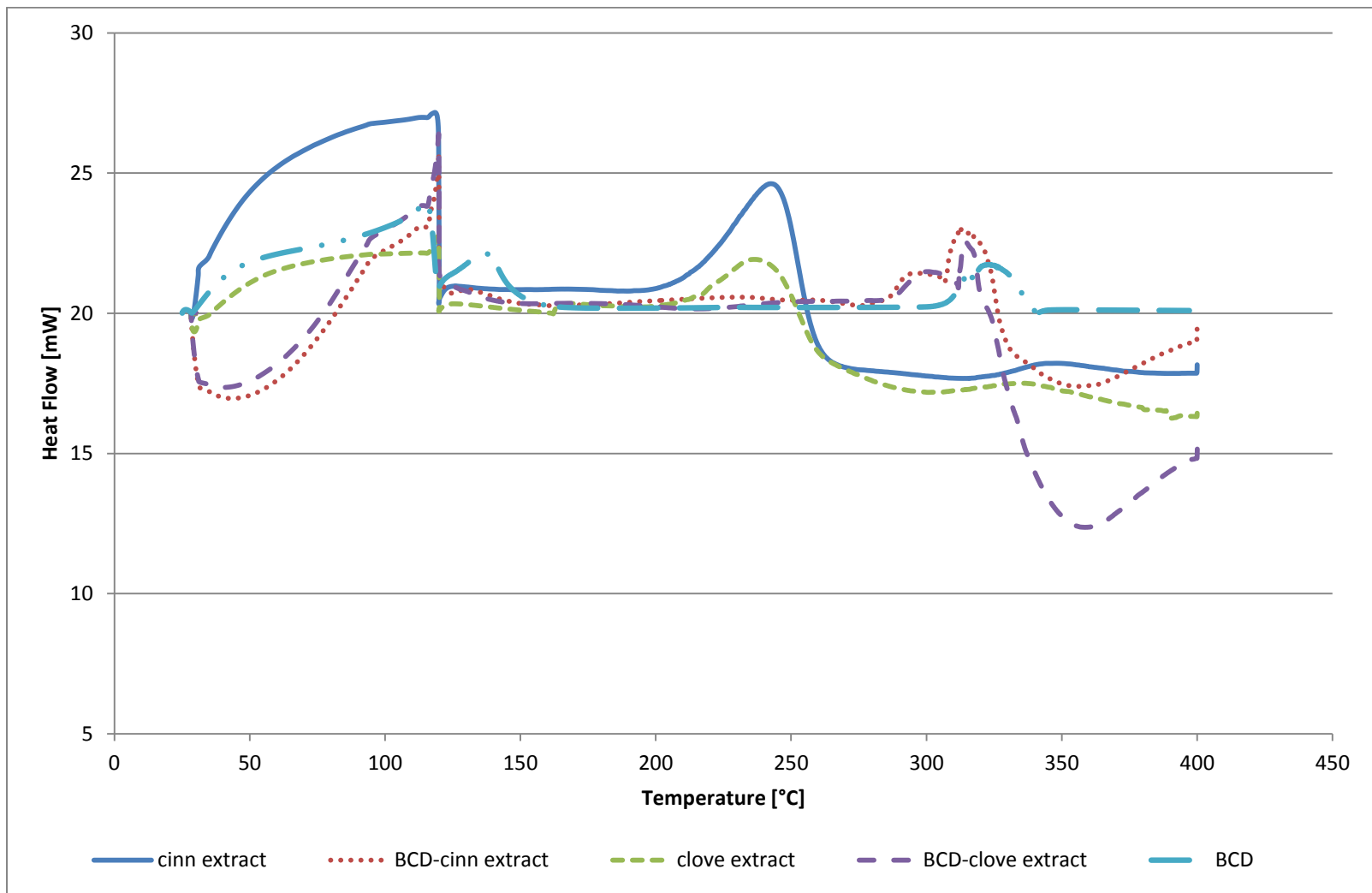
Figure 3.2. Oxidative differential scanning calorimetry (DSC) thermogram of cinnamon (cinn extract), clove extract, and their respective BCD complexes.

<u>Particle Size Analysis</u>

The average inclusion complex diameters and PDIs are listed in Table 3.1. There were no significant differences (P>0.05) in the average diameters of the inclusion complexes, though PDI for *trans*-cinnamaldehyde inclusion complexes was significantly higher than all other particles except the clove extract complexes. Variability in PDI could be due to the tendency of the BCD inclusion complex particles to agglomerate. The strong tendency for agglomeration is a consequence of the self-assembly of BCD in water (Seo and others 2010) due to the lack of significant net charge on the inclusion complex particles, which means there are no repulsive forces to prevent particle agglomeration. Cyclodextrins and their complexes can form large water soluble aggregates in aqueous solutions and these aggregates are able to solubilize lipophilic drugs (Loftsson and others 2004; Choi and others 2009a). The *trans*-cinnamaldehyde particles may have experienced a less uniform pattern of agglomeration than the other particles, producing greater variation in particle size though it did not affect its antimicrobial capacity. Agglomeration will not occur uniformly, potentially creating more variability in particle size. Agglomeration is also the reason the average particle size is larger than anticipated. The size of the inclusion complex particles was similar to that found by Choi and others (2009b) for BCD inclusion complexes with fish oil.

Table 3.1. Polydispersity Index (PDI) and average diameter of each of the beta-cyclodextrin inclusion complexes.

Entrapped Compound	Polydispersity Index	Particle Diameter [μm]
trans-cinnamaldehyde	0.56 [a] (0.14)	2.006 [a] (0.544)
Eugenol	0.00 [b] (0.00)	0.860 [a] (0.007)
2:1, *t*-cinnamaldehyde:eugenol	0.024 [b] (0.05)	1.229 [a] (0.753)
cinnamon bark extract	0.00 [b] (0.00)	1.390 [a] (0.319)
clove bud extract	0.27 [ab] (0.21)	1.398 [a] (0.567)

*Values given are averages of three replicates; standard deviations are displayed in parentheses. Average values with differing superscript letters (within columns) indicate significantly different values ($p<0.05$).

Particle Morphology

TEM images (Figure 3.3) show the size and morphology of the BCD complex particles (*trans*-cinnamaldehyde/eugenol and *trans*-cinnamaldehyde BCD complexes are shown as examples). The images reveal evidence of agglomeration where large particles appear to be attracting smaller particles. Smaller clusters of particles were identified at

the beginning stages of particle agglomeration. Similar results were observed by Seo and others (2010) with BCD-eugenol complex forming large aggregates suggesting that their irregular form was a consequence of the self-assembly of BCD in water. All particles showed a spherical shape and smooth surfaces with a broad size distribution and a strong tendency to form clusters. Chun and others (2012) observed a time-dependent aggregation of BCD-eugenol complexs becoming larger and more aggregated with time of shaking (time for complex formation). Choi and others (2009b) reported similar discrepancies in size when measuring BCD inclusion complexes by light diffraction and TEM. The reason has to do with the preparation of samples for TEM which charges the particles on the grid in order to set and adhere the sample, causing the agglomerated particles to separate into smaller particles in the TEM images (Choi and others 2009a; Choi and others 2009b).
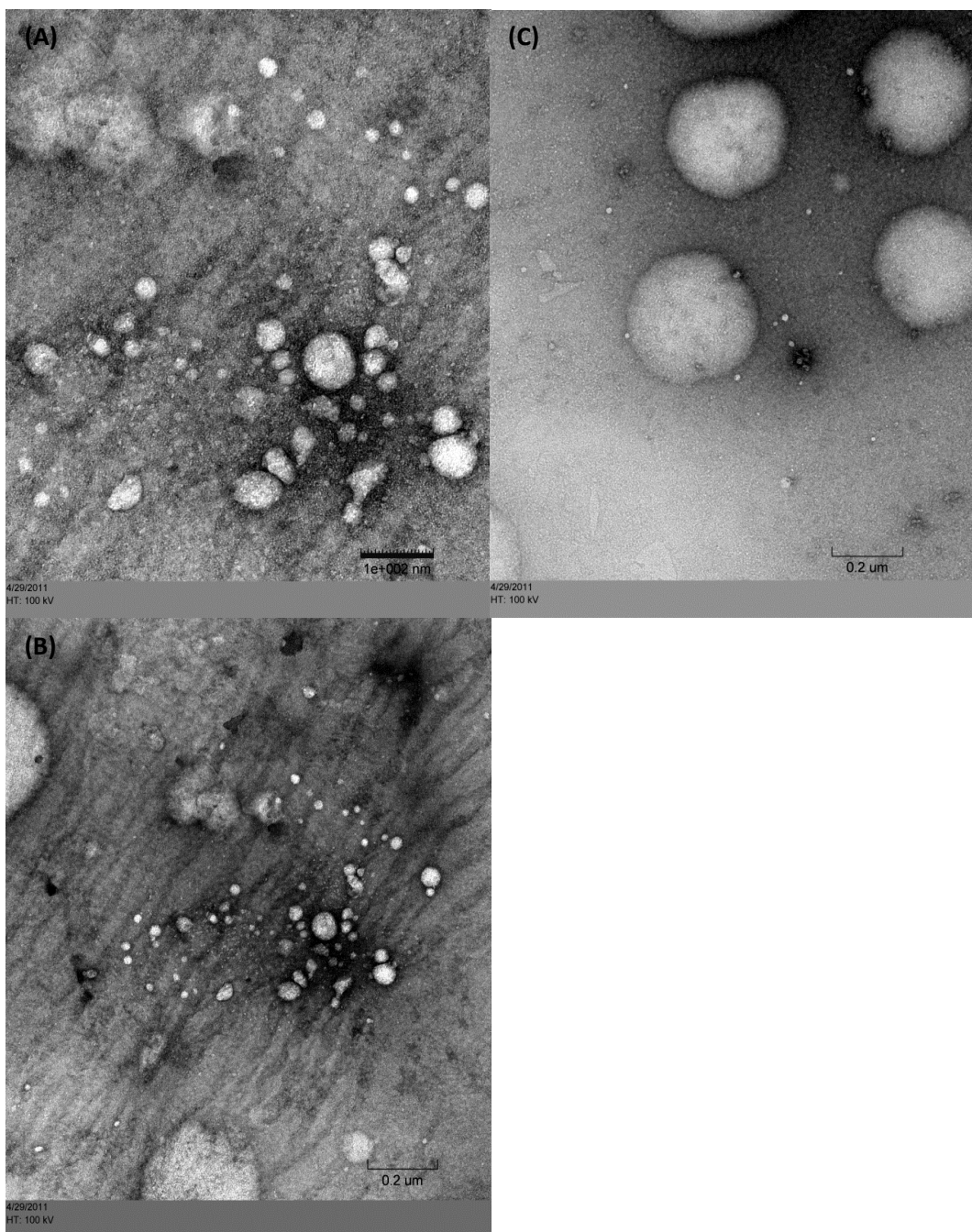
Figure 3.3. Transmission electron microscope (TEM) images of beta-cyclodextrin inclusion complexes. Images are representative of samples and depict particles containing a 2:1 mixture of *trans*-cinnamaldehyde:eugenol at 100,000 times magnification (a), 50,000 times magnification (b), and *trans*-cinnamaldehyde at 50,000 times magnification (c).

<u>Entrapment Efficiency</u>

The entrapment efficiencies were calculated using Equation 1 and are listed in
Table 3.2. The BCD entrapped the EOs very effectively, with the exception of cinnamon
bark extract. This difference in entrapment efficiency has resulted from the presence of
other constituents in the cinnamon extract with higher affinities for BCD than *trans*-
cinnamaldehyde, such as eugenol or benzoic acid (Davidson and Taylor 2007). Different
molecules have different equilibria in solution that drive them to form inclusion
complexes or remain in solution (Hedges and others 1995).

Table 3.2. Entrapment efficiency (EE) values determined for each type of beta-
cyclodextrin inclusion complex using spectrophotometer at 280 nm.

Entrapped Molecules	EE [%][*]
trans-cinnamaldehyde	84.70 [a] (0.02)
eugenol	90.15 [a] (0.06)
2:1, *t*-cinnamaldehyde:eugenol	82.00 [a] (0.09)
cinnamon bark extract[**]	41.72 [b] (0.02)
clove bud extract[**]	77.74 [a] (0.13)

[*]Values given are averages of three replicate samples; standard deviations are displayed
in parentheses. Entrapment efficiency values with differing superscript letters indicate
significantly different values ($p < 0.05$). [**] EEs of extracts were based on their primary
active compound (*trans*-cinnamaldehyde and eugenol for cinnamon bark and clove bud,
respectively).

Choi and others (2009b) measured an entrapment efficiency of 90.9% for
eugenol in BCD inclusion complexes prepared by the freeze drying method, similar to

that reported in this study (Table 3.2). Carlotti and others (2007) achieved approximately 60% entrapment efficiency for *trans*-cinnamaldehyde in gamma-cyclodextrins, which have a larger inner cavity diameter than BCD. Entrapment efficiency of the active compounds for the extracts should be lower than for the purified molecules since there are other compounds competing for inclusion reactions with the BCD. Similar observation was reported by Ayala-Zavala and others (2008) with entrapment efficiencies ranging from 39.94 to 78.18% which was inversely proportional to the weight ratio of cinnamon leaf oil to BCD. The concentration of active compound in the spice extracts was measured and the values were 73.89% (w/w) of *trans*-cinnamaldehyde and 92.80% (w/w) of eugenol for cinnamon bark and clove bud extracts, respectively.

Phase Solubility

All phase solubility constants (K_c) for the EOs and BCD at three different temperatures and their thermodynamic properties are listed in Table 3.3. Differences in K_c constants as well as thermodynamic properties for the different essential oils are due to differences in equilibria between the free and complexed states of the essential oils (Higuchi and Connors 1965). The rate of release depends upon the relative affinities of the original guest for the cavity of the cyclodextrin and the relative guest concentration (Hedges and others 1995). The phase solubility diagrams of *trans*-cinnamaldehyde and eugenol with BCD are presented in Figure 3.4. The plots showed linear trends with slopes less than one for all oils, indicating A_L-type diagrams (type A indicates a complexation reaction where EO solubility increases as the BCD concentration

45

increases, subscript L refers to a 1:1 molecular ratio formation of soluble complexes) (Higuchi and Connors 1965), as anticipated during preparation. Figure 3.4 also shows that water solubility of EOs increases with increasing temperature, as the y-intercepts increase with temperature. The water solubility for *trans*-cinnamaldehyde proved to be higher than for eugenol as was anticipated. Solubility for eugenol (4.6-15.0 mmol/L) is lower than *trans*-cinnamaldehyde (13.0-15.0 mmol/L), but both can exhibit a small overlapping range of aqueous solubility values (Yalkowsky and He 2003). Decreasing K_c values with increasing temperatures were expected for exothermic processes. Similar temperature effect on the stability constants were observed by Tommasini and others (2004) and by Rekharsky and Inoue (1998); K_c values for the same temperature vary greatly among studies (Tommasini and others 2004; Karathanos and others 2007) and differ by orders of magnitude, demonstrating to be a function of the compound or extract used and their interaction with the host (Ayala-Zavala and others 2008).

Table 3.3. Phase solubility coefficients (Kc) as well as the slope and intercept values used to determine them for complex formation between BCD and essential oils and the thermodynamic properties of complex formation reactions at specified temperatures.

Essential Oil	Temperature (°C)	Intercept	Slope	Kc (M^{-1})	^{1}R^2	ΔH (J/mol)	ΔS (J/mol·K)	ΔG (J/mol·K)
t-cinnamaldehyde	25	7.50	0.16	26.64[a]	0.84	-17661.40	-3.18	-16714.90
	35	10.74	0.17	19.06[b]	0.87	-	-	-
	45	11.64	0.18	18.41[c]	0.86	-	-	-
Eugenol	25	9.82	0.63	174.58[d]	0.93	-7622.44	-17.52	-2402.94
	35	12.01	0.67	168.44[e]	0.86	-	-	-
	45	14.12	0.67	143.67[f]	0.93	-	-	-
cinnamon bark extract	25	10.97	0.16	18.16[g]	0.93	-20665.30	-45.37	-7143.68
	35	11.68	0.13	13.19[h]	0.9	-	-	-
	45	13.79	0.13	10.76[i]	0.88	-	-	-
clove bud extract	25	10.42	0.64	169.91[j]	0.88	-43007.50	-100.50	-13043.70
	35	11.57	0.62	143.98[k]	0.97	-	-	-
	45	13.60	0.43	56.53[l]	0.88	-	-	-

[a,b] Means within a column which are not followed by a common superscript letter are significantly different (P < 0.05).
[1] Coefficient of determination of the linear relationship between BCD concentration vs. EO concentration.
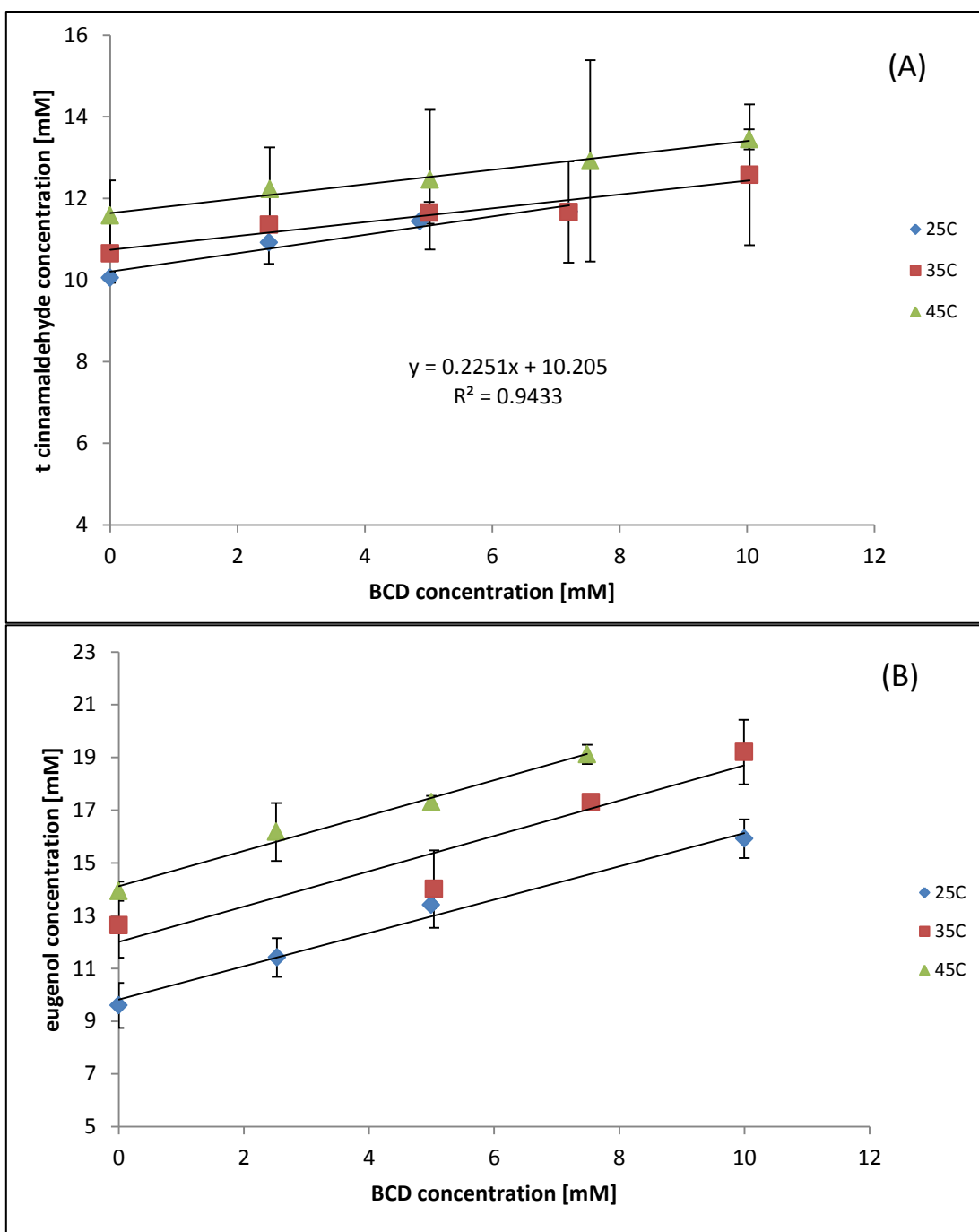
Figure 3.4. Phase solubility of (a) *trans*-cinnamaldehyde and BCD (b) eugenol and BCD in water at 25, 35, and 45°C.

For the thermodynamic properties (Table 3.3), the negative enthalpy values confirm that complex formation is an exothermic reaction and their relatively small magnitudes (<100 kJ/mol) are typical of lower energy reactions. The complex formation is driven by hydrophobic interactions caused by the replacement of water molecules with the essential oils in the cavity of the BCD, increased van der Waals interactions, and hydrogen bond formation (Mourtzinos and others 2008). The negative entropy values reflect an increase in order in the system caused by complex formation, which reduces translational and rotational degrees of freedom in comparison to free molecules. These thermodynamic results provide more evidence that inclusion complex molecules were in fact created. EOs with higher aqueous solubilities are more likely to favor the free oil state than the inclusion complex, which explains why eugenol and clove extract have higher K_c values. The negative Gibbs free energies values indicate that inclusion complex formation is a spontaneous process (Karathanos and others 2007). Similar observations were reported on previous studies (Tommasini and others 2004; Mourtzinos and others 2008); however, the thermodynamic properties values differ greatly (orders of magnitude) which can be explained by specific guest-host interactions (Rekharsky and Inoue 1998; Ayala-Zavala and others 2008; Ayala-Zavala and others 2008).

3.4.2 Minimum Inhibitory and Bactericidal Concentration

Antimicrobial Activity

The MICs and MBCs of the EOs and their BCD inclusion complexes for *S. Typhimurium* and *L. innocua* are provided in Tables 3.4 and 3.5, respectively. The MIC

49

values for eugenol and clove bud extract, and eugenol BCD complex were higher than all other EOs (P<0.05). It is possible this resulted from eugenol's lower aqueous solubility that would prevent maximum contact with the pathogens in solution. It could also be due to the different steric conformation of the guest molecules; *trans*-cinnamaldehyde may protrude more from the cavity of the BCD, allowing it to act upon the pathogens without being fully released from the inclusion complex (Hedges and others 1995). Wang and others (2011) found that eugenol BCD complexes were able to inhibit *Escherichia coli* growth, but were ineffective against *Salmonella paratyphi* B and *Staphylococcus aureus*, suggesting eugenol is a selective antimicrobial. The BCD complexes improved water solubility of the compounds and improved EOs' antimicrobial efficacy at lower concentrations of active compound. The MIC value for BCD encapsulated cinnamon bark extract for both pathogens was 166 µg/mL, this is an improvement of 59% in inhibition (P<0.05) over free cinnamon bark extract. The MIC for free cinnamon bark extract was 400 µg/mL for *S.* Typhimurium and 500 µg/mL for *L. innocua*. Antimicrobial MIC values for *L. innocua* were higher (P<0.05) than *S.* Typhimurium for the free EOs, but were identical for the BCD entrapped essential oils with the exception of eugenol. *L. innocua* is usually more resistant to antimicrobials because it is Gram-positive and its cell membrane is more difficult for the antimicrobial to disrupt (Walsh and others 2003). The BCD seems to enhance the antimicrobial capabilities of the essential oils in several ways, but the primary sites of antimicrobial action of EOs are at the membrane and inside the cytoplasm of bacteria and BCD may

have enhanced essential oil access to these regions by increasing EO aqueous solubility

(Wang and others 2011).

Table 3.4. Minimum inhibitory and bactericidal concentration (MIC, MBC) against
Salmonella Typhimurium LT2 for both free essential oil and beta-
cyclodextrin encapsulated compounds. Values based on the actual
concentrations of essential oils present on the BCD inclusion complexes.

Antimicrobial Compound	MIC[a] [µg/mL]	MBC[a] [µg/mL]
trans-cinnamaldehyde	400	>1000[b]
Eugenol	>1000	>1000
2:1 *trans*-cinnamaldehyde:eugenol	500	>1000
cinnamon bark extract	400	1000
clove bud extract	>1000	>1000
trans-cinnamaldehyde BCD inclusion complexes	479	>957
eugenol BCD inclusion complexes	693	>1155
2:1 *trans*-cinnamaldehyde:eugenol BCD inclusion complexes	487	>974
cinnamon bark extract BCD inclusion complexes	166	>665
clove bud extract BCD inclusion complexes	281	>1125

[a] Values are the lowest concentration of unencapsulated or BCD-encapsulated essential
oil for which a ≤0.05 OD630 change was observed after 24 h incubation at 35°C in
tryptic soy broth.

[b] Values preceded by a higher than (>) means that tested concentrations were not
sufficient to determine the MIC or MBC values.

Table 3.5. Minimum inhibitory and bactericidal concentration (MIC, MBC) against
Listeria innocua for both free essential oil and beta-cyclodextrin encapsulated
compounds. Values based on the actual concentrations of essential oils
present on the BCD inclusion complexes

Antimicrobial Compound	MIC[a] [μg/mL]	MBC[a] [μg/mL]
trans-cinnamaldehyde	500	2000
eugenol	2000	>2000[b]
2:1 *trans*-cinnamaldehyde:eugenol	800	2000
cinnamon bark extract	500	2000
clove bud extract	2000	>2000
trans-cinnamaldehyde BCD inclusion complexes	479	>957
eugenol BCD inclusion complexes	1155	>1155
2:1 *trans*-cinnamaldehyde:eugenol BCD inclusion complexes	584	>974
cinnamon bark extract BCD inclusion complexes	166	>665
clove bud extract BCD inclusion complexes	281	>1125

[a] Values are the lowest concentration of unencapsulated or BCD-encapsulated essential
oil for which a ≤0.05 OD630 change was observed after 24 h incubation at 35°C in
tryptic soy broth.
[b] Values preceded by a higher than (>) means that tested concentrations were not
sufficient to determine the MIC or MBC values.

Tested extract BCD inclusion complexes were more effective inhibitors (P<0.05)
of pathogen growth than the purified compounds and their inclusion complexes (Table
3.4, 3.5). Friedman and others (2004) reported that although purified compounds tended
to be more effective immediately, while plant extracts exhibited prolonged effects on
pathogen growth. These authors noted that in order for the purified compounds to be
effective they needed to be thoroughly suspended in the solution before the pathogens
were added, so they could lose effectiveness as they volatilized into the atmosphere or
coalesced in solution. There could also be some synergistic activity occurring among the

compounds present in the extracts to increase their antimicrobial potency (Burt 2004). Ayala-Zavala and others (2008) studied antifungal activity of BCD complexes (cinnamon leaf and garlic oils) and these essential oil BCD complexes showed good antifungal activity at low concentrations, with similar amounts of active compound as the free one, by delaying *Aternaria alternata* growth. Bactericidal effects were not observed for the majority of concentrations tested, though MBCs were observed for cinnamon bark extract at 1000 µg/mL and 2000 µg/mL for *S.* Typhimurium and *L. innocua*, respectively. MBC values for *trans*-cinnamaldehyde and the combined *trans*-cinnamaldehyde:eugenol oils were identified only for *L. innocua* (2000 µg/mL). All compounds tested are believed to possess bactericidal activity, but at higher concentrations than those tested in this study (Johny and others 2010).

3.5 Conclusions

This study aimed to elucidate the physico-chemical characteristics of EO-BCD inclusion complexes and their resulting antimicrobial activity. Inclusion complex formation with EOs was successfully obtained as shown by DSC and phase solubility analysis. Moreover, inclusion complexes increased EOs water solubility and protected them from oxidation. The cinnamon bark and clove bud extract BCD inclusion complexes were the most effective antimicrobial systems against representative Gram-positive and -negative microorganisms (MIC of 166 and 281 µg/ml, respectively), despite a lower entrapment efficiency (42% and 78%, respectively) than other EO inclusion complexes. The benefits of BCD encapsulation extend beyond masking sensory attributes of antimicrobial compounds. Encapsulation can also enhance the

53

mechanism of antimicrobial action and decrease the concentration of antimicrobial

compound needed for inhibition through increased EO delivery to the membranes of

microorganisms in aqueous environments possibly due to their increased aqueous

solubility (Kc values). The results indicate that such EO inclusion complexes could be

useful antimicrobial delivery systems with a broad spectrum of application in food

systems where Gram-positive and –negative bacteria could present a risk.

CHAPTER IV

ANTIMICROBIAL EFFICACY OF POLY (DL-LACTIDE-CO-GLYCOLIDE) (PLGA) NANOPARTICLES WITH ENTRAPPED CINNAMON BARK EXTRACT AGAINST *LISTERIA MONOCYTOGENES* AND *SALMONELLA TYPHIMURIUM**

4.1 Overview

Nanoencapsulation of active compounds using poly-(D,L-lactide-co-glycolide) (PLGA) is commonly used in the pharmaceutical industry for drug delivery and may have important applications in the food industry. Control of growth of foodborne bacteria with the goals of reducing the number of foodborne illness outbreaks, assuring consumers a safer food supply remains a priority in the food industry. Natural antimicrobials are an excellent way to eliminate pathogens without introducing chemical preservatives that consumers may find undesirable. Cinnamon bark extract (CBE) is an effective pathogen inhibitor isolated from cinnamon spice. PLGA nanoparticles containing CBE were produced using an emulsion-solvent evaporation method and characterized for size, polydispersity, morphology, entrapment efficiency, *in vitro* release and pathogen inhibition. PLGA with two different ratios of lactide to glycolide (65:35 and 50:50) were used to determine how polymer composition affected nanoparticle characteristics and antimicrobial potency. The size of the nanoparticles ranged from 144.77 to 166.65 nm and the entrapment efficiencies of CBE in 65:35

PLGA and 50:50 PLGA were 38.90% and 47.60%, respectively. The *in vitro* release

profile at 35°C showed an initial burst effect for both types of PLGA followed by a more

gradual release of CBE from the polymer matrix. Both types of PLGA nanoparticles

loaded with CBE were effective inhibitors of *Salmonella enterica* serovar Typhimurium

and *Listeria monocytogenes* after 24 and 72 hours at concentrations ranging from 224.42

to 549.23 µg/mL. The PLGA encapsulation improved delivery of hydrophobic

antimicrobial to the pathogens in aqueous media.

4.2 Introduction

Foodborne pathogens have become an increasingly relevant health and safety

concern in the food industry. This study focuses on two particular pathogens of interest

to the food industry: *Salmonella enterica* serovar Typhimurium and *Listeria*

monocytogenes. *Salmonella* has been indicated in several recent outbreaks of foodborne

disease; it has been identified as the most common pathogen associated with foodborne

outbreaks (Raybaudi-Massilia and others 2009) and has a fatality rate of about 4.1% (Jay

and others 2005). Outbreaks associated with *Listeria monocytogenes* are much less

frequent; however, the fatality rate associated with infection is approximately 34% (Jay

and others 2005), making it a pathogen of great concern to public health.

Antimicrobials are a useful technology to eliminate foodborne pathogens, but

many consumers are becoming increasingly weary of synthetic additives or ingredients

in food products. Spice essential oils have proved to be powerful inhibitors of foodborne

pathogens (Kim and others 1995; Gomes and others 2011b). They are a desirable

alternative to using synthetic antimicrobials in food products because they are natural

materials extracted from spices already used in the food industry. Cinnamon bark extract (CBE) has been approved as a GRAS material for food use based on 21 CFR (Code of Federal Regulation) part 172.515 (CFR 2009). CBE contains multiple active compounds that inhibit microorganisms through different mechanisms (Valero and Salmeron 2003; Burt 2004). The challenges with applying essential oils to food products are that they produce strong odors and flavors (high volatility) at concentrations necessary for pathogen inhibition and they are highly hydrophobic, which can limit their contact with pathogens in aqueous environments (Kalemba and Kunicka 2003). Nanoencapsulation is one way to mask sensory attributes and improve delivery and distribution throughout aqueous environments. Nanocapsules are not visible to the human eye and should not be sensed in the mouth, so they will not impact the texture or appearance of food products or make them less appealing to consumers (Pray and Yaktine 2009). Poly-D,L-lactide-co-glycolide (PLGA) is a biocompatible polymer widely used in the pharmaceutical industry to protect active ingredients from harsh environments and improve their delivery and uptake; this type of nanoencapsulation could be a useful technology in the food industry for controlled delivery of antimicrobials (Weiss and others 2006). PLGA can be used to encapsulate hydrophobic active materials through a relatively simple process, so its application to the food industry should be relatively straightforward.

The objectives of this study were to: (1) synthesize and characterize biodegradable PLGA nanoparticles with different lactide:glycolide ratios containing CBE (natural antimicrobial extract); (2) assess nanoparticles' antimicrobial efficiency against foodborne pathogens (*Listeria monocytogenes* and *Salmonella* Typhimurium).

4.3 Materials & Methods

4.3.1 Materials

Poly-D,L-lactide-co-glycolide (65:35 and 50:50), poly(vinyl alcohol) (87%, M_W 30 to 70 kDa) and CBE (99%) were purchased from Sigma Aldrich Co. (St. Louis, MO, U.S.A.). Dichloromethane was purchased from CTL Scientific Supply Corp. (Deer Park, NY, U.S.A.). D(+)-Trehalose was purchased from EMD Chemicals (Philadelphia, PA, U.S.A.). Nanopure water was purchased from Macron Chemicals (Charlotte, NC, U.S.A.). All other reagents were of analytical grade.

4.3.2 Nanoparticle Synthesis

Nanoparticles were formed using the emulsion evaporation method similar to the method outlined by Gomes and others (2011b). First, the organic phase was created by dissolving 50 mg of poly-D,L-lactide-co-glycolide (PLGA) into 2 mL dichloromethane along with 16% (w/w) CBE relative to PLGA. The organic phase was added drop-wise to 20 mL of aqueous 0.5% (w/w) polyvinyl alcohol (PVA) solution in nanopure water. This mixture was emulsified for 2 minutes at 9500 rpm using an Ultra-Turrax T25 basic Ika (Works, Inc., Wilmington, NC). The emulsion was sonicated in an ice bath for 30 minutes at 70 W (Cole Parmer sonicator 8890, Vernon Hill, IL), before removing the dichloromethane using a rotoevaporator (Buchi R-210 Rotavapor, Buchi Co., New Castle, DE) for 20 minutes under vacuum (0.97 psi). Unloaded (control) particles were generated by the same method with the absence of CBE in the organic phase. Once synthesized, the nanoparticles were purified by ultrafiltration to remove excess PVA and non-encapsulated CBE. A Millipore-Labscale^{TM} TFF system fitted with a 50 kDa

molecular weight cutoff Pellicon XL-Millipore (Millipore Co., Kankakee, IL) was used. The nanoparticles were ultrafiltered with 200 mL of water and 50 mL of the retentate was collected. Inlet pressure was 25 psi and outlet pressure in the system was 5 to 10 psi. After ultrafiltration, nanoparticles were kept at -20°C overnight then lyophilized at -50°C and 1.45 x 10^{-4} psi vacuum for 24 hours in a Labconco Freeze Dry-5 unit (Labconco, Kansas City, MO). D(+)-trehalose was added to the nanoparticle solution prior to freezing to act as a cryoprotectant at a 1:1 ratio relative to the PLGA. Dried particles were collected and stored in a dessicator at -20°C until needed for analysis.

4.3.3 Particle Size Analysis and Morphology

Aqueous suspensions of nanoparticles were analyzed for size distribution and polydispersity index (PDI) using a Delsa™ Nano C Particle Analyzer (Beckman Coulter, Brea, CA). Nanoparticles were dispersed in distilled water at a concentration of 10 mg/mL and sonicated for 15 minutes before analysis using 1 cm path length plastic cuvettes at scattering angle of 165°, with a pinhole set to 20 μm, and a refractive index of 1.3328 for 120 continuous accumulation times.

Aqueous suspensions of nanoparticles were examined using a FEI Morgagni Transmission Electron Microscope (TEM) (FEI Company, Hillsboro, OR) at the School of Veterinary Medicine and Biomedical Sciences of Texas A&M University (College Station, TX). Aqueous suspensions of particles were placed on 300 mesh copper grids and stained with a 2% (w/v) uranyl acetate aqueous stain (Electron Microscopy Sciences, Hatfield, PA) to provide contrast under magnification. Excess liquid on the

mesh was removed with filter paper and the grid was allowed to dry before viewing

under 50,000 to 100,000 times magnification. Observations were performed at 80 kV.

4.3.4 Entrapment Efficiency

Nanoparticles were dispersed in 95% (w/v) acetonitrile and well mixed, then left

in solution for 72 hours with periodic mixing to allow time for all CBE to be in solution.

The solutions were passed through 0.2 µm nylon membrane syringe filters (VWR

International, Radnor, PA) to remove all PLGA and PVA. The amount of CBE was then

measured spectrophotometrically (Shimadzu UV-1601 spectrophotometer, Columbia,

MA) at 280 nm in a 1 cm path length quartz cuvette. The entrapment efficiency was

calculated according to Equation (4.1) (Gomes and others 2011):

$$EE\% = \frac{amount\ of\ active\ compound\ entrapped}{initial\ active\ compound\ amount} x100 \qquad [4.1]$$

4.3.5 Controlled Release

Controlled release experiments were conducted to observe the rate of release of

CBE from the PLGA nanoparticles similar to those reported by Zigoneanu and others

(2008). Nanoparticles were suspended in water and then added to the release medium to

achieve a 1.0 mg/mL concentration of particles (sink conditions). The release medium

consisted of phosphate buffered saline (PBS, 0.15M, pH 7.4) and after addition of the

nanoparticles, the PBS was divided into 1.0 mL aliquots in eppendorf tubes. The tubes

were placed in a shaking water bath (VWR International, Radnor, PA) set at 100 rpm

and 35°C, from which samples were removed and analyzed for CBE content at

predetermined time points up to 72 h. Samples were filtered using 0.2 μm nylon membrane syringe filters prior to spectrophotometric analysis at 280 nm.

In this work we are proposing a modified empirical equation to describe the release of CBE from PLGA-nanoparticles (Ritger and Peppas 1987b):

$$\frac{M(t)}{M_o} = b_1 * \exp(-k_1 t) + b_2 * \exp(-k_2 t) \qquad [4.2]$$

where M(t) is the nanoparticles' antimicrobial content at time t, and M$_o$ the initial antimicrobial content, b_1, b_2, k_1, and k_2 are constants. The values k_1, and k_2 are defined as the antimicrobial release rate constants. This model can be seen as a generalized form of the solution of the Fickian model when employing only the first two terms of Eq. 4.3 for 1-dimensional radial antimicrobial content in a sphere of radius r, under perfect sink initial and boundary conditions, with constant diffusion coefficient D (Crank 1975).

$$\frac{M(t)}{M_o} = \frac{6}{\pi^2} \sum_{n=1}^{\infty} \frac{1}{n^2} \exp\left(-\frac{Dn^2\pi^2 t}{r^2}\right) \qquad [4.3]$$

4.3.6 Minimum Inhibitory and Bactericidal Concentration

<u>Bacterial Cultures</u>

S. enterica serovar Typhimurium LT2 and *L. monocytogenes* strain Scott A were obtained from Texas A&M University Food Microbiology Laboratory (College Station, TX). Both pathogens were chosen for their importance to the food industry and are representatives of Gram-negative and Gram-positive bacteria, respectively. *S. Typhimurium* and *L. monocytogenes* were resuscitated in tryptic soy broth (TSB) and

tryptose phosphate broth (TPB) (Becton, Dickinson and Co., Sparks, MD), respectively, by two identical consecutive transfers and incubating for 24 hours aerobically at 35°C. The bacterial cultures were maintained on TSA slants stored at 4°C for no more than 3 months. Transfers from slants were conducted similarly to the resuscitation method to prepare microorganisms for analysis.

<u>Antimicrobial Activity</u>

Minimum inhibitory concentrations (MICs) for PLGA nanoparticles were determined using a broth dilution assay (Brandt and others 2010). Growth curves were first performed at 35°C on each strain to correlate plate counts with optical density values at 630 nm (OD630) using an Epoch microplate spectrophotometer (BioTek® Instruments, Inc., Winooski, VT). Bacterial cultures were incubated 20-22 h and then prepared by serial dilution in double-strength TSB (2x TSB) or TPB (2x TPB), as appropriate, for an initial inoculum of approximately 3.0 $\log_{10}$ CFU/mL in each sample well. Initial inocula were enumerated via spread plating on TSA and incubated for 24 h at 35°C. Aliquots of 100-µL of all antimicrobial solutions and solvent blanks were spread plated to ensure sterility.

The MIC experiments were conducted in 96 well microtiter plates (sterilized 300 µl capacity – MicroWell, NUNC, Thermo-Fisher Scientific, Waltham, MA). The nanoparticles were added to the microtiter plates as aqueous suspensions of concentrations ranging from 5,000 to 30,000 µg/mL for both pathogens. Free CBE ranging from 100 to 2000 µg/mL were also tested for MIC values against both pathogens. Equivalent volumes (100 µL) of antimicrobial nanoparticle solution and

bacterial inoculum in 2x broth were loaded into each test well. Negative controls were prepared with nanoparticle solutions and sterile 2x broth to account for baseline OD630 readings. Positive controls were also prepared containing inoculum and sterile distilled water or control nanoparticles to ensure nanoparticle materials (PLGA, PVA, and so on) had no inhibitory effect on bacterial growth. Once plates were prepared, they were covered with a mylar plate sealer (Thermo Fisher Scientific), shaken gently, and OD630 of the wells was read (0 h). The microtiter plates were incubated (24 h at 35°C) and shaken gently before OD630 readings were taken at 24 h, 48 h, and 72 h to observe bacterial growth and inhibition over the course of several days. Antimicrobial test wells that showed ≤0.05 change in OD630 after 24 h, 48 h, and 72 h of incubation were considered "inhibited" by the antimicrobial (after appropriate baseline adjustments) for that time period. The MIC for each incubation length was determined by the lowest concentration of antimicrobial that inhibited growth for all test replicates (Brandt and others 2010).

All wells that showed inhibition of the test microorganism after 24 h or 72 h were then tested for bactericidal capability by spreading 100 μL from each well showing inhibition onto TSA plates and incubating for 24 h at 35°C. Two identical sets of 96-well plates were prepared for each replicate so that 100 μL could be taken from inhibited wells at 24 h without impacting measurements at 48 and 72 h. If no colonies were observed on the plate surfaces following incubation, the treatment concentration was considered bactericidal. The lowest concentration of nanoparticles demonstrating bactericidal activity across all replicates was considered the MBC.

4.3.7 Statistical Analysis

For all analyses, determinations were made in triplicate as independent experiments. All statistical analyses were performed using JMP v. 9 Software (SAS Institute, Cary, NC). Differences between variables were tested for significance using one-way analysis of variance (ANOVA) and significantly different means ($P<0.05$) were separated using Tukey's Honestly Significant Differences (HSD) test. Controlled release data were fit to model data using JMP software and the non-linear modeling procedure to determine rate constants, k_1 and k_2. The model parameters were analyzed for goodness of fit using the non-linear procedure to determine coefficients of determination (R^2).

4.4 Results & Discussion

4.4.1 Particle Size Analysis and Morphology

Nanoparticles formed from the 50:50 PLGA (PLGA50) and 65:35 PLGA (PLGA65) were very similar in size. For the same polymer composition; however, the unloaded PLGA65 and CBE loaded PLGA65 particles were significantly smaller ($P<0.05$) than the PLGA50 particles (Table 4.1). The unloaded particles tended to be slightly smaller in diameter than those with entrapped CBE, similar to results found in other studies and attributed to the increased viscosity of the organic phase. This makes it more difficult to disperse the phases during the emulsification process and leads to larger particles (Mainardes and Evangelista 2005). Their sizes ranged from 144.77 nm for the unloaded PLGA65 to 166.65 nm for the PLGA50 CBE (Table 4.1). The higher amount of lactide present in the PLGA65, which is more hydrophobic than the glycolide component of the polymer, could explain the smaller size of the particles because they

are less likely to aggregate (Astete and Sabliov 2006). A small particle size is desirable

because nanoparticles are not visible to the human eye and cannot be detected in the

mouth, so they will not adversely affect texture or appearance of food products where

antimicrobial particles may be applied (Pray and Yaktine 2009).

Table 4.1. Average particle diameter, polydispersity index, and entrapment efficiency of
unloaded poly-D,L-lactide-co-glycolide (PLGA) and loaded with cinnamon
bark extract (CBE).

Nanoparticle	Polydispersity Index	Average Diameter [nm]	Entrapment Efficiency
PLGA50 CBE	0.26[a] (0.01)	166.65[a] (6.98)	47.60[a] (3.16)
Unloaded PLGA50	0.24[a] (0.01)	162.11[ab] (0.64)	--
PLGA65 CBE	0.18[b] (0.01)	152.29[bc] (4.27)	38.90[a] (6.67)
Unloaded PLGA65	0.24[a] (0.01)	144.77[c] (1.25)	--

Two types of PLGA were used with lactide:glycolide ratios of 65:35 (PLGA65) and
50:50 (PLGA50). Determinations are an average of 3 replicates and different superscript
letters within a column represent significantly different values ($P<0.05$). Values in
parentheses are standard deviations.

Polydispersity index values were all found to be close to 0.2, indicating slightly

polydisperse systems for all nanoparticles manufactured, consisting of a heterogeneous

mixture of particle sizes. The PDI is a measure of the uniformity of particle sizes present

in a suspension, where a value less than 0.10 indicates a homogeneous, monodisperse

system and increasing values (>0.10) indicate an increasingly heterogeneous size

distribution (Zigoneanu and others 2008). Particle size impacts active compound release,

meaning that monodisperse suspensions of particles deliver a more consistent amount of compound (Astete and Sabliov 2006).

The TEM images (Figure 4.1) also showed a variety of particle sizes present, which explains the PDI values determined in the size analysis. The shape and appearance of the PLGA particles were very similar regardless of type of PLGA, whether or not there was CBE entrapped within the particle. Nanoparticles were all spherical with a darker perimeter on the edge of the spheres similar to PLGA nanoparticles seen in other studies (Gomes and others 2011b). This dark "corona" is attributed to the PVA which forms connections between its hydrophobic regions and the PLGA chains to form a matrix, while the hydrophilic regions of PVA are exposed to the water phase (Zigoneanu and others 2008).
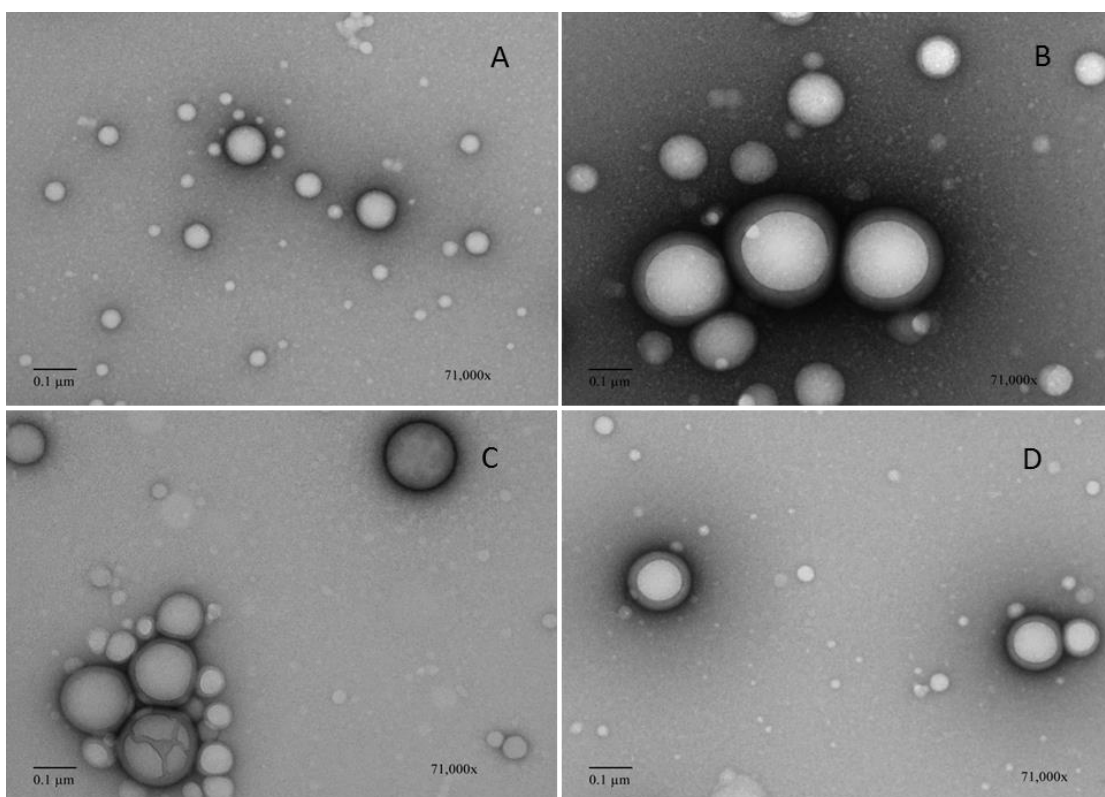
Figure 4.1. Transmission Electron Microscope images of (A) Unloaded PLGA50 (B) PLGA50 CBE (C) Unloaded PLGA65 (D) PLGA65 CBE mounted on 300 mesh copper grids with carbon film and stained with 2% uranyl acetate. Images were taken at 71,000x magnification.

4.4.2 Entrapment Efficiency

The entrapment efficiencies for the CBE in both the PLGA65 and PLGA50 were similar ($P<0.05$) to other studies that used PLGA to encapsulate hydrophobic compounds and are related to the solubility of the entrapped material in water which is the main drawback in forming smaller size nanospheres and improving the drug entrapment efficiency (Song and others 1997; Astete and Sabliov 2006). Decreasing particle size also tends to correspond with lower entrapment efficiencies (Mainardes and

Evangelista 2005; Wischke and Schwendeman 2008). The PLGA50 entrapment efficiency was 47.60% while it was only 38.90% for the PLGA65; even though these values were not significantly different (Table 4.1). The total amount of CBE present within the particle would be 0.07 mg CBE/mg PLGA65 or PLGA50. Entrapment efficiency values vary greatly from study to study depending on entrapped material, polymer molecular weight and lactide:glycolide ratio (Panyam and Labhasetwar 2003; Panyam and others 2004; Wischke and Schwendeman 2008). These low entrapment efficiency values did not hinder the antimicrobial effect of the nanoparticles.

4.4.3 Controlled Release

The temperature used for the controlled release study was chosen as an ideal case for microbial growth and the worst-case scenario for food safety. At the lower temperatures typically used for storage, the release rates will likely be slower. These lower release rates will also be met with lower microbial loads, as microorganisms cannot proliferate as easily at cooler temperatures. The release of CBE from the PLGA nanoparticles showed an initial burst effect for the first hour, but then leveled off to a steady plateau quickly thereafter (Figure 4.2). The release of the CBE from the nanoparticle is governed by several factors, including capsule wall thickness, affinity of the CBE for the PLGA50 or PLGA65, diffusion of active compound through the polymer matrix, polymeric erosion, PLGA swelling, and degradation (Blanco and Alonso 1997; Zigoneanu and others 2008). The burst effect can be explained by the fast release of CBE found close to or attached to the surface of the nanoparticles (Zigoneanu and others 2008). Eventually the release rate slows as the active compound must travel a

longer distance between polymer chains from further within the nanocapsule's matrix (Gomes and others 2011b). PLGA degradation is generally slow, so CBE release is more dependent on diffusion constants, PLGA swelling, and surface or bulk PLGA erosion (Mu and Feng 2003). The PLGA50 had a slower initial release than the PLGA65 but then exhibited a rapid burst of greater magnitude than the PLGA65 burst after 45 minutes in the release media. The PLGA65 is more hydrophobic, due to a higher lactide component present and this greater hydrophobicity may have made it more difficult for the lipophilic CBE to diffuse through the polymer capsule initially, resulting in a smaller initial burst effect and slower more sustained release (Wischke and Schwendeman 2008; Gomes and others 2011b). A constant steady release after the burst effect from the PLGA65 is attributable to diffusion of CBE found deeper within the polymer matrix, which was more easily incorporated deeper within the PLGA65 due to the higher affinity of CBE for the more hydrophobic nature of this polymer (Zigoneanu and others 2008).

The lower lactide content and lower molecular weight of PLGA50 means it is more hydrophilic so it exhibits a more rapid water uptake and begins to degrade more quickly via hydrolytic cleavage of ester groups (Cohen and others 1991). The faster degradation of the polymer matrix will lead to a more rapid release of the entrapped material through pores created in the nanoparticle surface. Hydrolytic degradation of the PLGA nanoparticles will produce acidic by-products (Wischke and Schwendeman 2008) that could improve the inhibitory effect of the nanoparticles. Previous studies have shown that as PLGA molecular weight increases, the initial burst during release decreases in magnitude (Cohen and others 1991). The PLGA65 demonstrated a smaller burst followed by a more gradual release over the course of the current experiment. The majority of the CBE was released from both the PLGA50 and PLGA65 within approximately 24 hours, and there were no significant changes in the amount released after 12 hours which was similar to the release profile of phenolics isolated from essential oils encapsulated in PLGA measured by Iannitelli and others (2011). The modified 2-term Fickian model (Eq. 4.2) fit well to the experimental release data for both types of PLGA as it did in a previous study (Gomes and others 2011b) (Table 4.2).
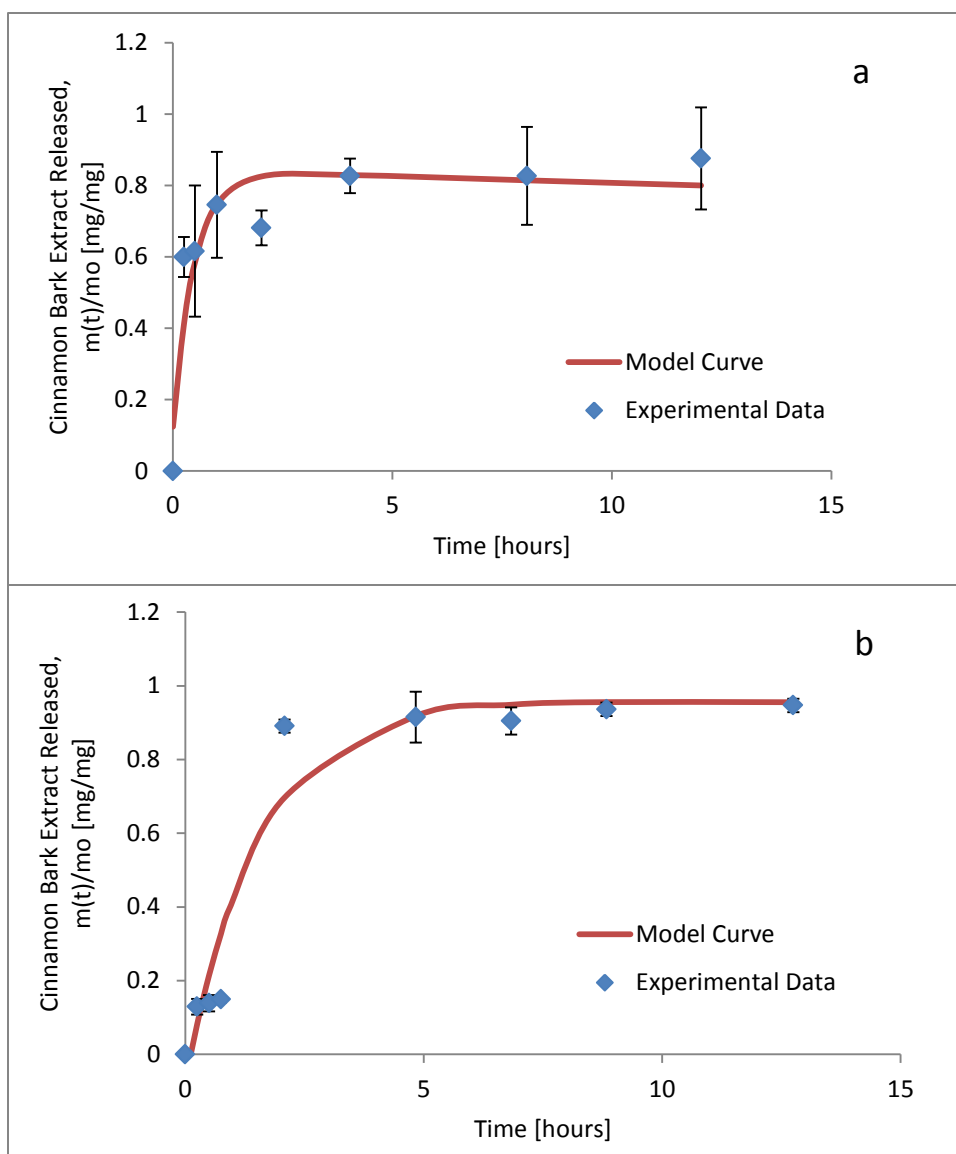
Figure 4.2. Cinnamon bark extract release kinetic from a) PLGA (65:35) nanoparticles and b) PLGA (50:50) nanoparticles at 35°C in phosphate buffered saline (0.15M, pH 7.4). Symbols are means of three replicate measurements via spectrophotometer at 280 nm and the solid line is the values modeled by the modified Fickian diffusion release equation [4.2].

71

Table 4.2. Release rate constants and coefficients of determination (R^2) from cinnamon
bark extract release from PLGA65 and PLGA50 at 35°C fit to equation [4.2].

Nanoparticle	k_1 [1/h]	k_2 [1/h]	R^2
PLGA65 CBE	5.69×10^{-4}	1.25×10^{-6}	0.91
PLGA50 CBE	1.81×10^{-4}	2.47×10^{-7}	0.95

4.4.4 Minimum Inhibitory and Bactericidal Concentration

The MIC of CBE encapsulated in PLGA65 was lower ($P<0.05$) than the MIC of

free CBE for both *S.* Typhimurium (400 µg/mL) and *L. monocytogenes* (500 µg/mL)

(Table 4.3). However, the MIC for CBE encapsulated in PLGA50 (549.23 µg/mL) was

slightly higher than the MIC values for free CBE. This could be attributed to the more

gradual ($P<0.05$) initial burst effect in the CBE release exhibited by the PLGA65. A

more consistent release of antimicrobial after the initial burst allowed more inhibitory

activity over a longer period of time, allowing less recovery time for pathogens damaged

during the initial burst of antimicrobial. Both nanoparticles inhibited the bacteria after 24

and 72h in the liquid media, however none of the concentrations tested were found to be

completely bactericidal. The MIC values were slightly higher for *L. monocytogenes* than

for *S.* Typhimurium. Gram-positive microorganisms are less susceptible to inhibition by

essential oils because their cell membranes are more difficult for essential oils to access

(Walsh and others 2003). The MIC values found for PLGA encapsulated CBE were also

lower ($P<0.05$) than those found for PLGA encapsulated *trans*-cinnamaldehyde as

previously reported by our group (Gomes and others 2011b). The nanoparticles were not

visible to the naked eye in solution (transparent solution) at the concentrations needed

for antimicrobial activity and likely would not affect food appearance or texture.

However, sensory testing would be necessary to confirm these assertions.

Table 4.3. MIC and MBC values for *Salmonella enterica* serovar Typhimurium LT2 and *Listeria monocytogenes* Scott A found through microbroth dilution assay after incubation for 24 and 72h at 35°C. Bacterial turbidity measurements were taken at 630 nm. MICs and MBCs were identified as the lowest concentration of antimicrobial producing $\leq$0.05 OD630 change after 24 h or 72 h at 35°C and the lowest concentration for which a 3.0 $\log_{10}$ CFU/ml inactivation in cells was determined by plating, respectively.

Microorganism	Antimicrobial	Time Elapsed [h]	MIC [µg/mL]	MBC [µg/mL]
Salmonella	PLGA65 CBE	24	224.42	>448.85
		72	299.23	>448.86
	Unloaded PLGA65	24	>30,000	>30,000
	PLGA50 CBE	24	549.23	>549.23
		72	549.23	>549.23
	Unloaded PLGA50	24	>30,000	>30,000
	Free CBE	24	400.00	1000
Listeria	PLGA65 CBE	24	299.23	>448.85
		72	448.85	>448.86
	Unloaded PLGA65	24	>30,000	>30,000
	PLGA50 CBE	24	549.23	>549.23
		72	549.23	>549.23
	Unloaded PLGA50	24	>30,000	>30,000
	Free CBE	24	400.00	1000

The primary active compound found in CBE is *trans*-cinnamaldehyde, but other researchers have found that spice extracts can be more effective antimicrobials than

purified compounds due to the presence of several active compounds that work to inhibit

microorganisms via different mechanisms (Valero and Salmeron 2003; Burt 2004;

Davidson and Taylor 2007). CBE contains *trans*-cinnamaldehyde (an aromatic

aldehyde), eugenol (a phenolic), and benzoic acid (a phenolic acid). These different

classes of compounds inhibit pathogens through different mechanisms (damage to

cytoplasmic membrane, cell wall degradation, damage or inhibition of cell proteins,

leakage of cell contents, interference with proton motive force, and gene suppression),

making CBE a more powerful and effective pathogen inhibitor (Burt 2004; Davidson

and Taylor 2007; Amalaradjou and Venkitanarayanan 2011a).

The hydrophobic nature of these compounds presents both a challenge and an

advantage for microbial inhibition. It is more difficult to deliver these compounds to

microbial cells in aqueous media; however, when they are encapsulated in PLGA they

can be more effectively distributed throughout the aqueous media and delivered to the

microbial cells (Ravichandran and others 2011). Once the essential oils are delivered to

the sites of microbial cells, their hydrophobic nature gives them a higher affinity for the

cell membrane which allows them to more easily partition into the cell membrane (Burt

2004; Ravichandran and others 2011). Without the PLGA encapsulation, CBE

constituents may not come in contact with the pathogens, but instead coalesce in the

solution to limit unfavorable hydrophobic-hydrophilic interactions or lose their potency

over time due to interactions with media components or volatilization (Lapidot and

others 2002). In fact, not only does it aid delivery and distribution, as PLGA begins to

degrade and produce acid by-products, it lowers the media pH, increasing the

hydrophobic nature of the CBE and allowing it to more readily partition into the lipids of the cell membrane or bind to hydrophobic regions of membrane proteins (Burt 2004).

Other studies using PLGA encapsulation have also found lower MIC values compared with free compounds (Mohammadi and others 2010; Gomes and others 2011b). Ravichandran and others (2011) found that encapsulated phenolic compounds in PLGA produced higher log reductions of both *L. monocytogenes* and *S*. Typhimurium than their un-encapsulated counter parts. Furthermore, there is the possibility of combining these two delivery systems with different release mechanisms to enhance their antimicrobial activity, the antimicrobial delivery systems can be manufactured to release the encapsulated antimicrobial payload over a period of time, maintaining selective pressure on contaminating microbes for significantly longer compared to the non-encapsulated antimicrobial.

4.5 Conclusions

Biodegradable PLGA with different lactide to glycolide ratio were used to prepare antimicrobial loaded nanoparticles containing CBE by the emulsion evaporation method. There were significant differences in size, entrapment efficiency, controlled release profile, and MIC for the two different types of PLGA but both successfully inhibited bacterial growth over the course of 24 and 72 h. The MIC value was lower for PLGA65 against both *Salmonella* and *Listeria* despite having a lower (P<0.05) entrapment efficiency than the PLGA50. This was likely due to the slower, more gradual release of CBE from the PLGA65 in comparison to the PLGA50 release. Both types of nanoencapsulation could be successfully used to deliver natural antimicrobials to

pathogens in food products, as they both decreased ($P<0.05$) the concentration of CBE needed for pathogen inhibition. The nanoencapsulation will protect the spice extract, reduce its sensory impact and improve its efficacy as a foodborne pathogen inhibitor.

CHAPTER V

OPTIMIZATION OF A SYNTHESIS PROCEDURE FOR THERMALLY-RESPONSIVE POLY-N-ISOPROPYLACRYLAMIDE NANOPARTICLES FOR THE ENTRAPMENT OF HYDROPHOBIC SPICE EXTRACTS

5.1 Overview

Cinnamon bark extract (CBE) is a hydrophobic natural spice extract that is a potent antimicrobial compound against foodborne pathogens. The goal of this study was to determine the best method to produce temperature-responsive poly-N-isopropylacrylamide (PNIPAAM) nanocapsules for the entrapment of CBE. PNIPAAM is a hydrogel that becomes hydrophobic at a lower critical solution temperature (LCST). It has the potential to provide a temperature-dependent release system for natural antimicrobial compounds in food systems, improving the antimicrobial effects. A top-down procedure using crosslinked PNIPAAM was compared to a bottom-up procedure using NIPAAM monomer. Both processes relied on self-assembly of the molecules into micelles around the CBE at 40°C. Processing conditions were compared within the procedures, including homogenization time of the polymer, hydration time prior to homogenization, lyophilization, and the effect of particle ultrafiltration. The nanoparticles were examined for size, morphology, entrapment efficiency, thermal stability, LCST, and controlled release. Upon heating above the LCST, the diameter of the particles decreased (P<0.05) due to contraction of the polymers. The synthesis methods affected particle size, with the bottom-up procedure resulting in smaller

77

(P<0.05) diameters than the top-down procedure. Particle size also increased (P<0.05) slightly when the particles were homogenized for less time and when they were lyophilized after synthesis. The entrapment efficiency of CBE in the PNIPAAM capsules was lower (P<0.05) for the bottom-up procedure and within the top-down procedures the entrapment efficiency decreased (P<0.05) as homogenization time was increased. The controlled release profile of CBE from nanoparticles was dependent on the release media temperature. A faster, burst release was observed at 40°C and a slower, more sustained release was observed at lower temperatures. The top-down procedure is more advantageous for food industry applications due to the higher loading capacity of the particles, and the more thorough purification procedures available to eliminate solvents.

5.2 Introduction

Poly(N-isopropylacrylamide) (PNIPAAM) is a temperature-responsive polymer with a lower critical solution temperature (LCST) that ranges from 30-35°C (Schild 1992). PNIPAAM possesses both hydrophilic and hydrophobic groups in the polymer chain that result in its unique LCST behavior (Gran 2011). At temperatures below the LCST, hydrogen-bonding interactions between water and the hydrophilic groups of the polymer lead to a swollen hydrogel state. Once temperatures are increased above the LCST, there is a weakening of the polymer-water hydrogen bonds and a strengthening of polymer to polymer interactions among the hydrophobic groups (Pelton 2000). When this polymer contraction occurs, it forces out some of the active material entrapped within the polymer matrix, creating a burst release at the transition temperature (Sershen

78

and others 2000). The temperature range for PNIPAAM's LCST is similar to the optimal temperature range for microbial growth for several foodborne pathogens of interest. This temperature-responsive polymer could provide the ability entrap antimicrobial material within PNIPAAM particles and then trigger its release when foods are stored at temperatures ideal for microbial growth. A temperature-triggered release of antimicrobial could reduce the incidence of foodborne pathogen related illnesses that occur as a result of improper food handling or storage.

PNIPAAM is one of the most commonly studied temperature-responsive polymers for drug delivery applications, but there are many different methods described to form PNIPAAM nanoparticles, primarily a top-down procedure and bottom-up procedure (Neradovic and others 2004; Fan and others 2008; Chuang and others 2010). Currently, there is no consensus on the best method to synthesize PNIPAAM nanoparticles for controlled release applications, and no studies have compared the characteristics and performance of nanoparticles synthesized via different processes. This study sought to determine the best nanoparticle synthesis method and optimize the nanoparticle production for antimicrobial controlled release applications and to determine what stages of the synthesis procedure had an important impact on the final nanoparticles.

Essential oils are naturally occurring antimicrobial compounds extracted from herbs and spices (Kalemba and Kunicka 2003). Spice essential oils have shown enhanced antimicrobial activity compared to their corresponding isolated active compounds due to the presence of several different active compounds working

79

synergistically to inhibit microorganisms (Valero and Salmeron 2003; Davidson and Taylor 2007). Cinnamon bark extract (CBE) contains three active compounds that inhibit bacterial growth through different mechanisms of action (Burt 2004). The primary active compound present in CBE is *trans*-cinnamaldehyde, which is a powerful phenolic compound on its own, but it also contains eugenol and benzoic acid which contribute additional antimicrobial activity (Burt 2004; Davidson and Taylor 2007; Amalaradjou and Venkitanarayanan 2011b). CBE has been found to effectively inhibit various foodborne pathogens, but its low aqueous solubility and high volatility make its delivery to microbial cell sites in aqueous media challenging (Hill and others 2013a); (Valero and Salmeron 2003; Ayala-Zavala and others 2008). The goal of this study was to develop an effective method to synthesize PNIPAAM nanoparticles with entrapped CBE to improve its delivery to foodborne pathogens and control its release with temperature stimuli.

5.3 Materials & Methods

5.3.1 Materials

N-isopropylacrylamide (NIPAAM) was purchased from TCI America (Portland, OR, U.S.A.). Poly(vinyl alcohol) (PVA) (87%, M_w 30-70 kDa), N,N-methylene-bisacrylamide (MBA), glutaraldehyde (25%), and cinnamon bark extract (CBE) (99%) were purchased from Sigma Aldrich Co. (St. Louis, MO, U.S.A.). N,N,N',N'-Tetramethyl-ethylenediamine (TEMED) was purchased from Alfa Aesar (Ward Hill, MA, U.S.A.). Ammonium Persulfate was purchased from BDH Chemicals (London, England). All other reagents were of analytical grade.

5.3.2 Particle Synthesis

Bottom-Up Synthesis

    The bottom-up method (Figure 5.1) used to synthesize particles was similar to the methods outlined by (Wadajkar and others 2009) with slight modifications. This method employs a free radical polymerization reaction to form PNIPAAM nanoparticles. Briefly, 1.54 g of NIPAAM monomer was dissolved in 90 mL of a 0.5% (w/v) aqueous PVA solution. Once the monomer is dissolved, 26.2 mg of MBA along with cinnamon bark extract (16% w/w, relative to NIPAAM) was added to the reaction flask and stirred continuously with a magnetic stirrer for 30 minutes. Meanwhile, the initiator solution is prepared by dissolving 62.40 mg of APS into 10 mL of 0.5% (w/v) aqueous PVA solution. Once the initial solution has mixed for 30 minutes, the initiator solution is added and shaken for 4 hours at 70°C in a shaking water bath (VWR International, Radnor, PA) set at 150 rpm.

    After synthesis, the nanoparticles were purified by ultrafiltration to remove excess PVA, NIPAAM monomer, and non-encapsulated CBE. A Millipore-Labscale^{TM} TFF system fitted with a 50 kDa molecular weight cutoff Pellicon XL-Millipore (Millipore Co., Kankakee, IL) was used. The nanoparticles were ultrafiltered with 300 mL of water and 100 mL of the retentate was collected. Inlet pressure was 25 psi and outlet pressure in the system was approximately 5-10 psi. After ultrafiltration, nanoparticles were kept at -20°C overnight then lyophilized at -50°C and 1.45×10^{-4} psi vacuum for 24 hours in a Labconco Freeze Dry-5 unit (Labconco, Kansas City, MO).

Unloaded (control) particles were synthesized through the same procedure without the addition of CBE into the reaction flask. Dried nanoparticles were stored at -20°C until they were needed for analysis.

Top-Down Synthesis

The top-down synthesis method (Figure 5.1) utilizes the IPN method outlined by Zhang and others (2004b) and Zhang and others (2004a) with minor adjustments to develop nanoparticles. NIPAAM monomer is dissolved in distilled water to obtain a concentration of 6.7% (w/w) and then 2.0% (w/w, relative to NIPAAM) MBA is added. Free radical polymerization was carried out in a glass flask at room temperature for 3 hours, using 1.0% (w/w) APS and TEMED as redox initiators. After polymerization, the crosslinked hydrogel was immersed in fresh distilled water at room temperature for 48 hours to allow all unused reactants to leach out of the gel. The water was replaced with fresh water every several hours. The final hydrogel was cut into small pieces and dried in a vacuum oven (Squared Lab Line Instruments, Melrose Park, Ill., U.S.A.) at room temperature and a pressure ≤ 13.3 kPa until all moisture was removed (approximately 24 hours).

To form nanoparticles, 1.5 mg/mL of dried PNIPAAM was suspended in 150 mL of 0.5% (w/v) aqueous PVA solution with 16% (w/w) cinnamon bark extract or without CBE (for control particles) and allowed to hydrate overnight. Following polymer hydration, the solution was homogenized using an Ultra-Turrax T25 basic Ika (Works, Inc., Wilmington, NC) at 9500 rpm for either 7 minutes or 10 minutes to break the

polymer into smaller particles. Two different homogenization times were tested to determine if a longer homogenization time would significantly decrease the final nanoparticle diameter, as synthesis in the absence of homogenization yielded extremely large agglomerations of polymer (Zhang and others 2007; Chuang and others 2009). Once the solutions were homogenized, they were placed in a shaking water bath (VWR International, Radnor, PA) at 40°C and 150 rpm for 24 hours to allow self-assembly into micelles. The micelles were then crosslinked with glutaraldehyde (2:1 molar ratio of glutaraldehyde to monomers) to stabilize the particles. The finished particles were then purified via ultrafiltration similarly to the bottom-up procedure to remove excess reactants, and lyophilized at -50°C and 1.45×10^{-4} psi vacuum for 24 hours in a Labconco Freeze Dry-5 unit (Labconco, Kansas City, MO). Dried nanoparticles were stored at -20°C until they were needed for analysis.
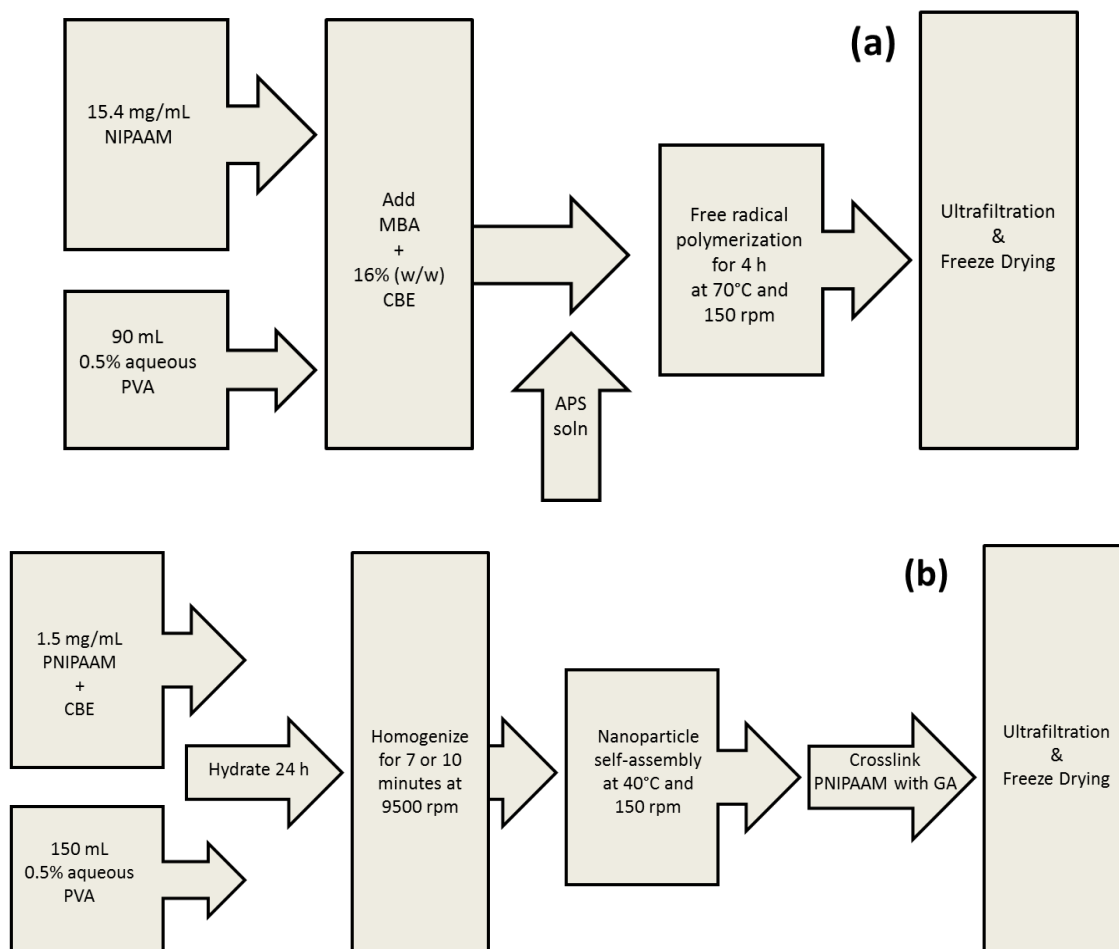
Figure 5.1. Schematic diagram of (a) bottom-up PNIPAAM nanoparticle synthesis by free radical polymerization and (b) top-down PNIPAAM nanoparticle synthesis method by self-assembly.

5.3.3 Particle Characterization

Particle Size and Morphology

Aqueous suspensions of each nanoparticle were analyzed for size distribution and polydispersity index (PDI) using a Delsa™ Nano C Particle Analyzer (Beckman Coulter, Brea, CA). Nanoparticles were dissolved in distilled water at a concentration of 30 mg/mL and sonicated at 70 W (Cole Parmer sonicator 8890, Vernon Hill, IL) for 15

84

minutes before analysis using 1 cm path length plastic cuvettes at scattering angle of 165°, with a pinhole set to 50 μm, and a refractive index of 1.3328 for 120 continuous accumulation times. As well as comparing the different types of nanoparticles, the 10min top-down nanoparticles were also measured for particle size at different stages of synthesis (i.e.; before freeze drying and before ultrafiltration) to elucidate the impact of each step on the particle size.

Nanoparticles were suspended in distilled water and examined using a FEI Morgagni Transmission Electron Microscope (TEM) (FEI Company, Hillsboro, OR) at the School of Veterinary Medicine and Biomedical Sciences of Texas A&M University (College Station, TX). Aqueous suspensions of particles were placed on 300 mesh copper grids and stained with a 2% (w/v) uranyl acetate aqueous stain (Electron Microscopy Sciences, Hatfield, PA) to provide contrast under magnification. Excess liquid on the mesh was removed with filter paper and the grid was allowed to dry before viewing under 4,400-71,000 times magnification. Observations were performed at 80 kV.

Entrapment Efficiency (EE) and Drug Loading (DL)

The entrapment efficiency and drug loading of CBE were measured indirectly by determining the amount of CBE that was present in the permeate collected during ultrafiltration. It was assumed that any CBE left in the retentate portion of the nanoparticle suspension was entrapped within particles. The amount of CBE present in the permeate was measured spectrophotometrically at 280 nm (Shimadzu UV-1601 spectrophotometer, Columbia, MA) in a 1 cm path length quartz cuvette. The EE and DL

were calculated according to Equation (5.1) and (5.2), respectively (Gomes and others 2011b; Iannitelli and others 2011):

$$EE = \frac{amount\,of\ active\,compound\,entrapped}{initial\ active\,compound\,amount} x100 \qquad [5.1]$$

$$DL = \frac{amount\,of\ active\,compound\,entrapped}{amount\,of\ particles\,produced} x100 \qquad [5.2]$$

Cloud Point and Lower Critical Solution Temperature (LCST)

The LCST behavior of the PNIPAAM hydrogel was determined using differential scanning calorimetry in a Pyris 6 Perkin Elmer instrument (Pyris 5.0 Software, Boston, MA). Hydrogel samples were submerged in water and allowed to swell to equilibrium before DSC measurements were taken. Approximately 10 mg of swollen PNIPAAM was placed into 20 µL aluminum pans and sealed with one hole in their lids and scanned from 25°C to 50°C at a rate of 3°C per minute under nitrogen atmosphere (Zhang and others 2004b).

The cloud point method (Kim and others 2005b) was used to find the thermal transition temperature of the hydrated nanoparticles. A 0.1% wt/wt aqueous solution of particles was prepared for each type of nanoparticle and 200 µL of each particle suspension was placed into 3 wells of a 96-well plate. Turbidity measurements were measured at 450 nm using a 96-well plate reader equipped with temperature control (VERSAmax Tunable Microplate Reader, Molecular Devices, Sunnyvale, CA). The cloud point was defined as the inflection point on a plot of absorbance versus temperature for each nanoparticle suspension as the temperature was increased from

86

25°C to 50°C at a rate of 2°C every 10 minutes. The cloud point of the crosslinked

PNIPAAM hydrogel produced for the top-down method was also measured to ensure the

cloud point method and DSC method produced comparable results.

<u>Controlled Release</u>

Controlled release experiments were conducted at 25°C, 35°C, and 45°C to

determine the rate of CBE release below, above, or near the LCST of the nanoparticles.

Nanoparticles were suspended in the release medium to achieve a 1.0 mg/mL

concentration of particles (sink conditions). The release medium consisted of 10 mL of

phosphate buffered saline (PBS, 0.15M, pH 7.4) placed in 15 mL conical tubes. The

tubes were placed in a shaking water bath (VWR International, Radnor, PA) set at 100

rpm and the desired temperature, from which 1 mL samples were removed and analyzed

for CBE content at predetermined time points up to 5 days. Additional PBS was not

added after sample removal, so that the same sink conditions were maintained

throughout the experiment. Samples were centrifuged at 23506g for 15 minutes to

separate any encapsulate material prior to spectrophotometric analysis of the supernatant

at 280 nm.

The controlled release could best be described by a semi-empirical equation

formulated by Korsmeyer and others (1986) (Equation 5.3) that accounts for Fickian

diffusion and transport due to swelling effects (termed "non-Fickian Type II transport"):

$$\frac{M_t}{M_\infty} = kt^n \qquad\qquad [5.3]$$

where M_t/M_∞ is the percent of antimicrobial released at time t (s), k is a rate constant (1/s), and n is the diffusional exponent (unit less). The release mechanism from swelling particles deviates from the traditional Fickian model since the release is not governed by diffusion of the antimicrobial alone, but also the polymer behavior upon swelling (Arifin and others 2006).

5.3.4 Minimum Inhibitory and Bactericidal Concentration (MIC and MBC)

Bacterial Cultures

Salmonella enterica serovar Typhimurium LT2 and *Listeria monocytogenes* strain Scott A were obtained from Texas A&M University Food Microbiology Laboratory (College Station, TX). Each pathogen was chosen as a representative of Gram-negative and Gram-positive bacteria, respectively. *S.* Typhimurium and *L. monocytogenes* were resuscitated in tryptic soy broth (TSB) and tryptose phosphate broth (TPB) (Becton, Dickinson and Co., Sparks, MD), respectively, by two identical consecutive transfers and incubated for 24 hours aerobically at 35°C. The bacterial cultures were maintained on Tryptic Soy Agar (TSA) slants stored at 4°C for no more than 3 months. Transfers from slants were conducted similarly to the resuscitation method to prepare microorganisms for analysis.

Antimicrobial Activity

Minimum inhibitory concentrations (MICs) for the PNIPAAM nanoparticles were determined using a broth dilution assay (Brandt and others 2010). Growth curves were first performed at 35°C on each strain to correlate plate counts with optical density values at 630 nm (OD630) using an Epoch microplate spectrophotometer (BioTek®

88

Instruments, Inc., Winooski, VT). Bacterial cultures were incubated 20-22 h and then prepared by serial dilution in double-strength TSB (2x TSB) or TPB (2x TPB), as appropriate, for an initial inoculum of approximately 3.0 $\log_{10}$ CFU/mL in each sample well with the appropriate amount of nutrient media present upon dilution. Initial inocula were enumerated via spread plating on TSA or Modified Oxford Agar (MOX) and incubated for 24 h at 35°C. Aliquots of 100-µL of all antimicrobial solutions and solvent blanks were spread plated at the time of the experiment to ensure their sterility.

The MIC experiments were conducted in 96 well microtiter plates (sterilized 300 µl capacity – MicroWell, NUNC, Thermo-Fisher Scientific, Waltham, MA). The nanoparticles were added to the microtiter plates as aqueous suspensions in concentrations ranging from 5,000-25,000 µg/mL for both pathogens. Equivalent volumes (100 µL) of antimicrobial nanoparticle solution and bacterial inoculum in 2x broth were loaded into each test well. Negative controls were prepared with nanoparticle solutions and sterile 2x broth to account for baseline OD630 readings. Positive controls were also prepared containing inoculum and sterile distilled water or control nanoparticles to ensure nanoparticle encapsulate materials had no inhibitory effect on bacterial growth. Once plates were prepared, they were covered with a mylar plate sealer (Thermo Fisher Scientific), shaken gently, and OD630 of the wells was read (0 h). The microtiter plates were incubated (24 h at 35°C) and shaken gently before OD630 readings were taken at 24 h to observe bacterial growth and inhibition over the course of the typical bacterial growth cycle. Antimicrobial test wells that showed ≤0.05 change in OD630 after 24 h of incubation were considered "inhibited" by the antimicrobial (after

89

appropriate baseline adjustments) for that time period. The MIC for each nanoparticle and pathogen was determined by the lowest concentration of antimicrobial that inhibited growth for all test replicates (Brandt and others 2010).

All wells that showed inhibition of the test microorganism after 24 h were then tested for bactericidal activity by spreading 100 µL from each well showing inhibition onto TSA plates and incubating for 24 h at 35°C. If no colonies were observed on the plate surfaces following incubation, the treatment concentration was considered bactericidal. The lowest concentration of nanoparticles demonstrating bactericidal activity across all replicates was considered the MBC.

5.3.5 Statistical Analysis

This experiment was based on a completely randomized design with equal replications. All determinations were made in triplicate as independent experiments. All statistical analyses were performed using JMP v. 9 Software (SAS Institute, Cary, NC). Differences between variables were tested for significance using one-way analysis of variance (ANOVA) and significantly different means ($p<0.05$) were separated using Tukey's Honestly Significant Differences (HSD) test. Controlled release data were fit to model data using JMP software and the non-linear modeling procedure to determine rate constants (k) and diffusional coefficients (n). The model constants were analyzed for goodness of fit using the non-linear procedure to determine coefficients of determination (R^2).

5.4 Results and Discussion

5.4.1 Particle Characterization

<u>Particle Size & Morphology</u>

       The nanoparticles produced (monomer (bottom up), 7min and 10min (top-down) were measured for particle size with and without CBE entrapped at 25°C and 50°C to determine their average diameter and polydispersity distribution (PDI) in water (Table 5.1 and Figure 5.2). The average diameter of all particles and their controls were smaller (P<0.05) when heated above the LCST because the polymer contracts at the transition temperature and becomes hydrophobic (Schild 1992). The monomer control particles (bottom-up process) showed the most dramatic decrease in diameter when heated above the LCST (466.76 nm compared to 134.25 nm), likely because the monomer nanoparticles were made up of smaller molecules and therefore able to collapse into a more compact particle without the presence of the CBE to prevent complete collapse. The nanoparticles ranged in diameter from 344.40 nm to 466.76 nm at room temperature, with the 7min control being the smallest (P<0.05) and the monomer control being the largest (P<0.05) particles. Once heated to 40°C, the particle diameters ranged from 134.25 nm for the monomer control to 331.75 nm for the 7min CBE. The top-down particles (7 and 10min) both had higher (P<0.05) entrapment efficiencies, so this is likely the reason their diameters were larger (P<0.05) after the particles collapsed at the LCST. The amount of time the PNIPAAM solution was homogenized did significantly impact the final particle size, with the longer homogenization time resulting in smaller (P<0.05) particles.
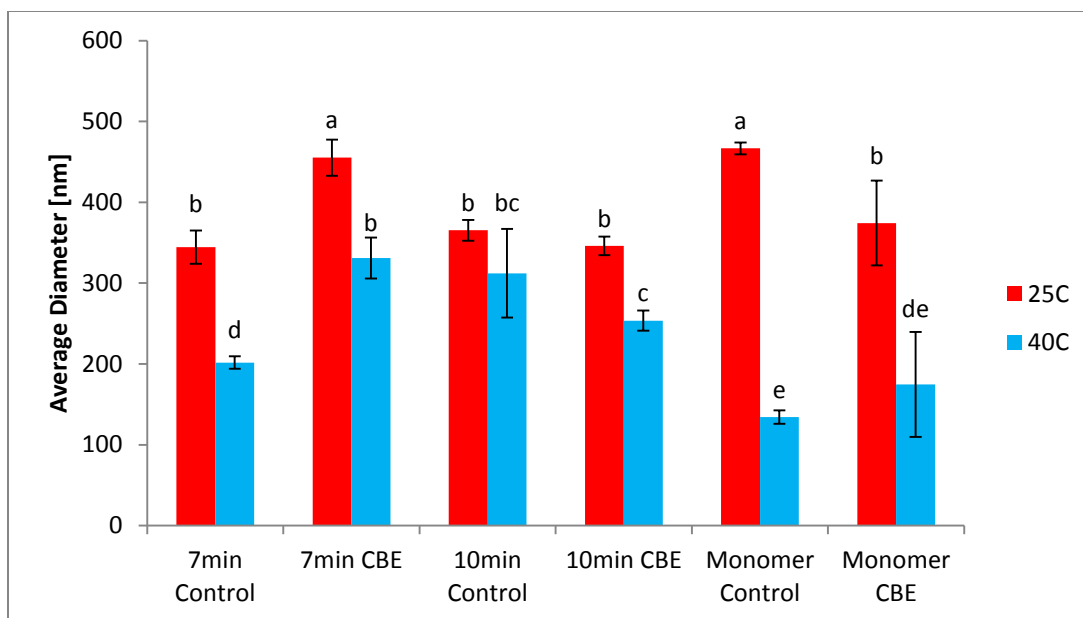
Figure 5.2 Average diameter of PNIPAAM nanoparticles and their controls suspended in water, synthesized through different methods at 25°C and 40°C. Monomer are nanoparticles produced by the bottom-up process and 7min and 10min are nanoparticles produced by the top-down process with different homogenization times. Average diameter columns that display different letters above their error bars represent significantly different values across all treatments ($P<0.05$). Values given are averages of three replicates ± standard deviations.

Table 5.1 Polydispersity (PDI) values of PNIPAAM control (unloaded) and CBE loaded nanoparticles made by the top-down (7 and 10 min) and bottom-up (Monomer) processes at temperatures of 25°C and 40°C.

Nanoparticle	PDI	
	25°C	**40°C**
7min Control	$_w0.32^a\pm0.02$	$_w0.32^a\pm0.01$
7min CBE	$_w0.31^a\pm0.003$	$_w0.23^a\pm0.11$
10min Control	$_w0.29^a\pm0.02$	$_w0.19^a\pm0.07$
10min CBE	$_w0.30^a\pm0.03$	$_w0.26^a\pm0.07$
Monomer Control	$_w1.21^a\pm0.90$	$_w0.38^a\pm0.09$
Monomer CBE	$_w0.25^a\pm0.02$	$_w0.19^a\pm0.07$

[a]Different superscript letters within a column represent significantly different values ($P<0.05$). [w]Means within a row, of the same parameter, that are not preceded by a common subscript letter are significantly different ($p<0.05$). Values given are averages of three replicates ± standard deviations.

Not only were the particle diameters of all the different nanoparticles measured, but also the 10min top-down control (unloaded) particles were analyzed at different stages of the synthesis process. Figure 5.3 shows the average particle size without freeze drying, without ultrafiltration, and when all stages of the synthesis process have been completed. The freeze drying process seems to have the biggest impact on particle size, as the particles are significantly smaller ($P<0.05$) when they are not lyophilized. This phenomenon is not surprising, as it has been found to occur in other studies of nanoparticle synthesis and addition of cryoprotectants such as trehalose, is sometimes recommended to minimize this effect (Astete and others 2007; Gomes and others 2011b). The ultrafiltration step had little impact on the average particle diameter

(P>0.05), which was expected, as the goal is to remove smaller molecular weight

components from the particle suspension.
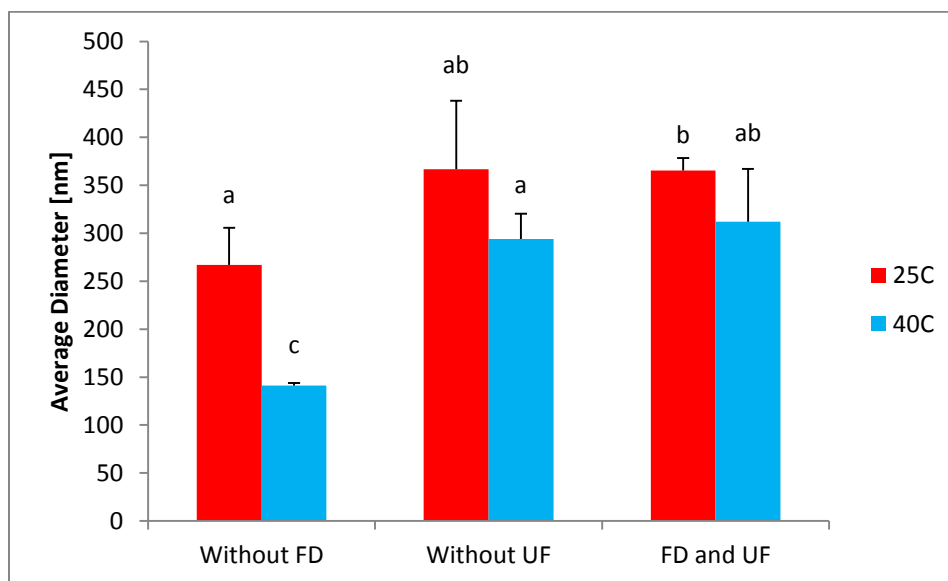
Figure 5.3 Comparison of average particle diameter for top-down, 10min homogenized
     PNIPAAM nanoparticles at various stages of the synthesis process below and
     above the LCST. FD = Freeze drying; UF = Ultrafiltration. Average diameter
     columns that display different letters above their error bars represent
     significantly different values across all treatments (P<0.05). Values given are
     averages of three replicates ± standard deviations.

The nanoparticles were similar in appearance in TEM images (Figure 5.4) as

slightly amorphous shapes, with the monomer nanoparticles (bottom-up) showing a

more spherical shape than either of the top-down synthesized particles. The more

amorphous shape of the top-down particles is due to the irregular polymer molecules

generated by the homogenization step of the process. Other studies utilizing the bottom-

up synthesis procedure displayed similarly spherical particle images (Ramanan and

others 2006; Wadajkar and others 2009). Wadajkar and others (2009) used a similar

bottom-up synthesis procedure and produced nanoparticles of a slightly smaller size and with less polydispersity, however these authors used sodium dodecyl sulfate (SDS) as a surfactant instead of PVA, which could have led to this difference. PVA was used in this study because it was found to produce particles with higher entrapment of CBE in preliminary testing, in comparison with particles produced with SDS as a surfactant. The bottom-up nanoparticles produced by Ramanan and others (2006) were very similar in size and size distribution to the particles produced in this study. The particle size of all particles appears slightly smaller in the TEM images than the sizes measured by laser light diffraction in the particle size analyzer, but due to the high level of polydispersity in the particle samples, there could simply be a wide range of particle sizes present in the samples. Fan and others (2008) displayed similar TEM images of slightly spherical, but irregular shapes for PNIPAAM nanoparticles synthesized using a top-down procedure. This author also showed an increase in particle size when PNIPAAM nanoparticles were loaded with hydrophobic material, versus unloaded control particles (Fan and others 2008). Amorphous nanoparticles of a similar size prepared via a top-down synthesis method were also reported by Chuang and others (2010), although this study utilized a PNIPAAM-co-polymer rather than pure PNIPAAM polymer. The synthesis and analysis methods were similar, leading to relevant comparisons of the results.
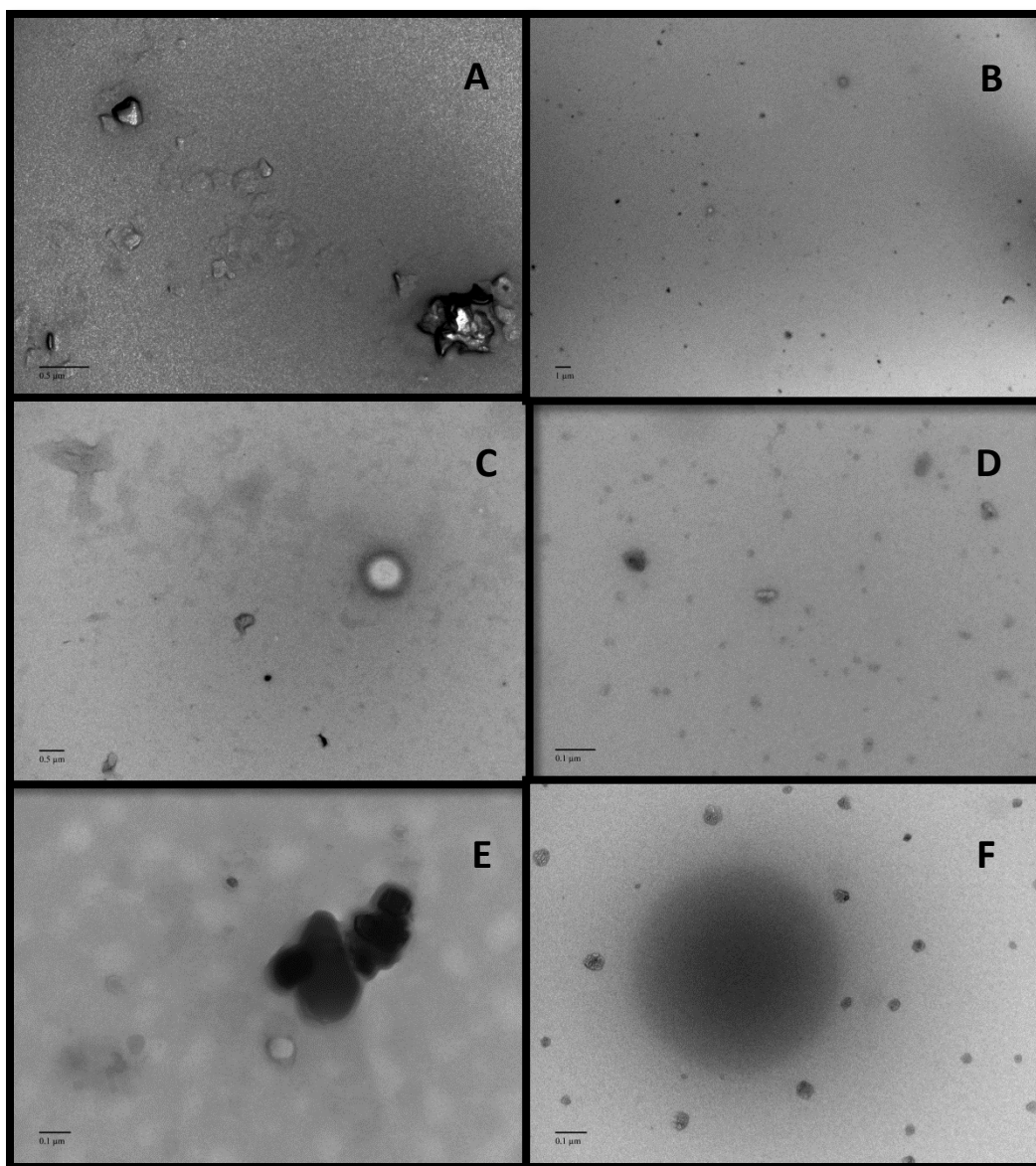
Figure 5.4 TEM images of PNIPAAM nanoparticles manufactured through different methods. (A) 10min top-down control (unloaded); (B) 10min top-down CBE; (C) 7min top-down control; (D) 7min top-down CBE; (E) Monomer bottom-up control; (F) Monomer bottom-up CBE. Observations were performed at 80 kV using magnifications ranging from 4,400 to 71,000x.

<u>Entrapment Efficiency and Drug Loading</u>

The entrapment efficiency for all the nanoparticles (Table 5.2) was similar and ranged from 86.78% for monomer particles (bottom-up process) to 91.46% for 10min particles (top-down process). A high level of entrapment was achieved regardless of the synthesis method, showing that the PNIPAAM provided a highly compatible form of encapsulation for hydrophobic material. PNIPAAM possesses both hydrophilic and hydrophobic groups in the polymer chain that lead to its LCST behavior (Phillips and others 2010; Gran 2011). The nanoparticles are loaded at a temperature above their LCST, so that the hydrophobic regions collapse around the hydrophobic CBE to minimize unfavorable aqueous interactions. A similarly high entrapment efficiency (73.7%) and drug loading (8.4%) of hydrophobic molecules within PNIPAAM nanoparticles were found by Fan and others (2008).

Similar to the entrapment efficiency results, the 7 and 10 min top-down PNIPAAM nanoparticles presented slightly higher drug loading values than the PNIPAAM nanoparticles synthesized by the bottom-up method. A drug loading of 100% CBE entrapment would be 2.56% for the top-down nanoparticles and 10.36% for the bottom-up particles, meaning the drug loading values for each of the particles were close to their maximum values.

Table 5.2 Entrapment efficiency values measured for cinnamon bark extract (CBE) in
PNIPAAM nanoparticles by spectrophotometry at 280 nm.

Nanoparticle	Average CBE entrapped (%)	Drug Loading (%)
7min CBE	90.24[a]±0.72	2.31[b]±0.02
10min CBE	91.46[a]±0.49	2.34[b]±0.01
Monomer CBE	86.78[a]±7.76	8.99[a]±0.80

Values given are averages of three replicates ± standard deviations. Different superscript
letters within a column represent significantly different values (P<0.05).

Cloud Point and Lower Critical Solution Temperature (LCST)

The LCST for the PNIPAAM hydrogel fell within the typical range (30-35°C) for

PNIPAAM polymers at 33.9°C via DSC determination (Schild 1992). The LCST

determined by the cloud point method was slightly higher at 34.8°C due to the slightly

lower sensitivity of this method (Table 5.3). It was necessary to use the cloud point

method for the nanoparticle LCST determination because the particles were protected by

a matrix of PVA that prevented high enough concentrations of particles to be placed in

the DSC pans. The cloud method allowed for larger volumes of particle suspensions,

resulting in more reliable and consistent LCST measurements. The monomer particles

had the lowest LCST at 33.5°C, while the 7min and 10min nanoparticles had the same

LCST values at 35.4°C. The cloud point method and DSC methods both reveal the

transition temperature through different data collection.

The DSC analysis determines the endothermic transition peak caused by the heat

required to break hydrogen bonds between water and the polymer, which occurs at the

transition temperature. Meanwhile, the cloud point method utilizes spectrophotometric

98

analysis to visualize the clouding of the polymer solution caused by the precipitation of the PNIPAAM at the transition temperature. Eeckman and others (2001) also measured both the cloud point and the LCST value of PNIPAAM polymer, and found the values of the transition temperature to be similar regardless of the method used to measure it and close to the values reported for the nanoparticles in this study. Other studies even use the term LCST when the transition temperature has been measured by the cloud point method, likely because both methods provide similar results (Kim and others 2005b; Zhang and others 2007).

Table 5.3 Lower critical solution temperatures (LCSTs) of PNIPAAM hydrogel and nanoparticles determined by differential scanning calorimetry (DSC) and the cloud point method.

Material	Cloud Point [°C]	LCST [°C]
PNIPAAM polymer	$_w34.8^a \pm 0.1$	$_w33.9$
Monomer Control nanoparticle (bottom-up)	$33.5^b \pm 0.1$	Nd
10 min Control nanoparticle (top-down)	$35.4^a \pm 0.1$	Nd
7 min Control nanoparticle (top-down)	$35.4^a \pm 0.1$	Nd

Values given are averages of three replicates ± standard deviations.
[a]Means within a column that are not followed by a common superscript letter are significantly different ($p<0.05$). [w]Means within a row, of the same parameter, that are not preceded by a common subscript letter are significantly different ($p<0.05$).
nd-not determined.

Controlled Release

The three temperatures used for the controlled release experiments were chosen as representative temperatures for the behavior of nanoparticles at temperatures above,

99

below, or near the LCST of the particles. All of the nanoparticles showed an initial burst release followed by a slower more gradual release (Figure 5.5). The initial burst was highest for the top-down synthesized nanoparticles at higher temperatures (35°C and 40°C). Above the LCST, the polymer nanoparticles exhibit a "squeeze out" of the active compound due to the collapse of the polymer matrix resulting in the larger initial burst of release at these temperatures (Gran 2011). Release after the polymer matrix has collapsed is governed primarily by diffusion through the tighter polymer matrix (Ritger and Peppas 1987a; Schild 1992). The CBE release from the monomer particles (bottom-up process) was extremely slow, especially at 25°C, where the concentration was too low to be measured over the course of the release study (data not shown). A study by Fan and others (2008) also found a larger burst release at temperatures above the LCST of the nanoparticles. All of the nanoparticles showed a low percentage of release after 5 days, indicating that the release would slowly continue over an extended period of time. This could potentially be beneficial for inhibiting foodborne pathogens over the course of the entire product shelf life, for example fresh and fresh-cut produce, which have a shelf life of 14-21 days. Zhang and others (2004b) also measured a slow, gradual release of active material from PNIPAAM hydrogels over the course of 96 hours; however, their analysis was on large pieces of polymer rather than nanoparticles. The polymer was crosslinked in a process similar to the polymer synthesis used for the top-down process,

100

and the total cumulative release ranged from 20 to 40% (Zhang and others 2004b), similar to the range of release from the top-down particles synthesized in this study. The PNIPAAM nanoparticles show excellent potential for encapsulating essential oils and protecting them from degradation or losses due to volatilization. The monomer (bottom-up) nanoparticles showed similar release profiles to those synthesized by Ramanan and others (2006) who found a low level of release from monomer nanoparticles with an initial burst followed by a more gradual release. This study also found a higher rate of release from particles placed in release media above the LCST than those maintained at a release temperature below the LCST (Ramanan and others 2006).

The release data points from the controlled release experiments fit well to the release equation proposed for spherical, swellable polymers (Eq. 5.2) as was expected for these nanoparticle systems (Table 5.4). All coefficients of determination (R^2) were greater than 0.95 and therefore were not shown in Table 5.4.
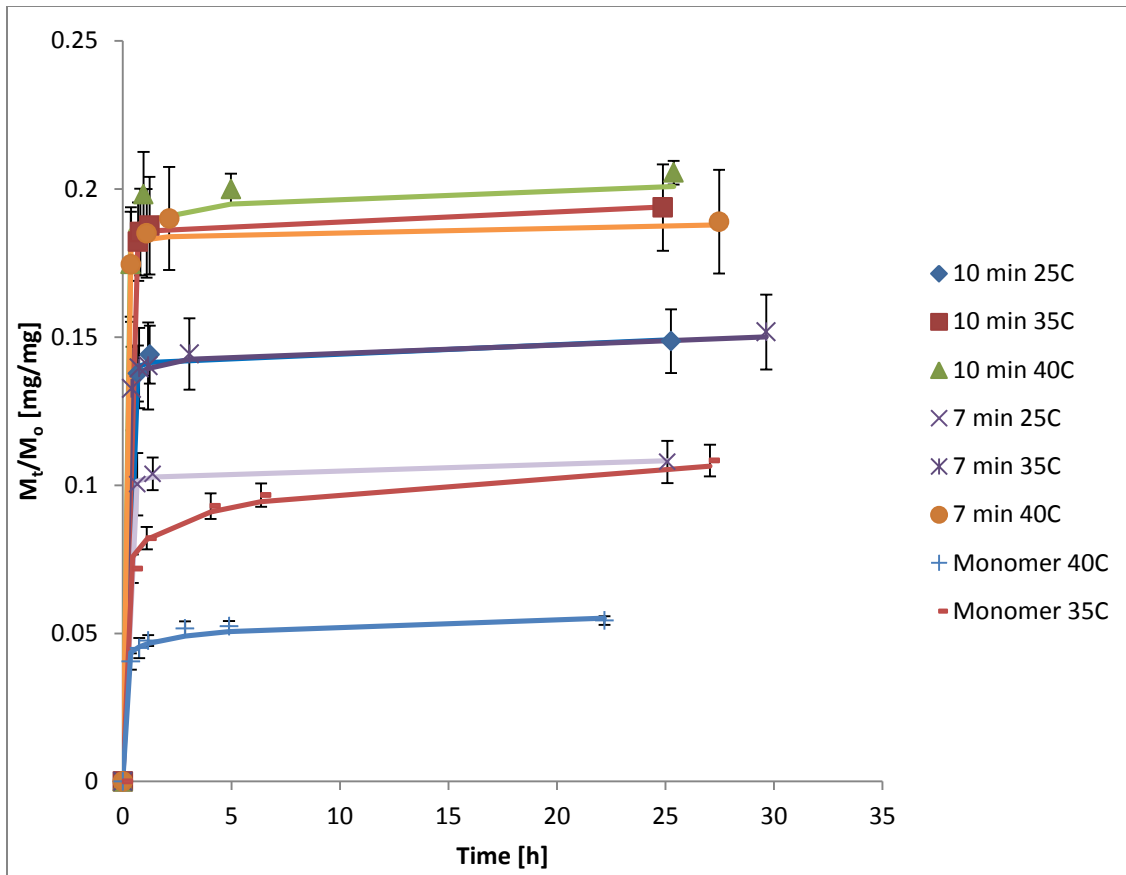
Figure 5.5 Controlled release profiles of PNIPAAM nanoparticles at different temperatures in 0.15M phosphate buffered saline (PBS, pH 7.4) fit to model release equation (solid lines). Raw data are represented by data points and error bars.

Table 5.4 Controlled release model rate coefficients (k) and diffusion constants (n) for PNIPAAM nanoparticles with entrapped CBE synthesized by bottom-up (monomer) and top-down processes (7 and 10 min).

| | Release Temperature | | | | | |
| | 25°C | | 35°C | | 40°C | |
Nanoparticle	k_r [s^{-n}]	n_r	k_r [s^{-n}]	n_r	k_r [s^{-n}]	n_r
10 min	3.77×10^{-4} $\pm$ (1.88×10^{-5})	0.59 $\pm$ (2.51×10^{-3})	5.85×10^{-4} $\pm$ (3.19×10^{-5})	0.61 $\pm$ (2.48×10^{-3})	6.34×10^{-4} $\pm$ (1.95×10^{-5})	0.62 $\pm$ (1.11×10^{-3})
7 min	2.60×10^{-4} $\pm$ (1.08×10^{-5})	0.57 $\pm$ (2.08×10^{-3})	5.44×10^{-4} $\pm$ (2.92×10^{-5})	0.61 $\pm$ (2.83×10^{-3})	5.51×10^{-4} $\pm$ (2.62×10^{-5})	0.61 $\pm$ (5.92×10^{-3})
Monomer	N/A	N/A	2.33×10^{-4} $\pm$ (8.05×10^{-6})	0.58 $\pm$ (1.72×10^{-3})	2.66×10^{-4} $\pm$ (6.02×10^{-6})	0.58 $\pm$ (1.09×10^{-3})

5.4.2 Minimum Inhibitory and Bactericidal Concentration (MIC) and (MBC)

The MIC values (Tables 5.5) for CBE encapsulated in both of the top-down PNIPAAM nanoparticles (7min CBE and 10min CBE) was very similar and significantly lower than the MIC for CBE encapsulated in the bottom-up PNIPAAM nanoparticles (monomer CBE) against both microorgansims (*Salmonella* and *Listeria*). This is likely a result of the much slower initial release from the monomer nanoparticles. The MIC experiments were conducted in a short time period (24h) that did not provide enough time for the monomer nanoparticles to release as much CBE into the growth media. The 10min CBE nanoparticles had the same MIC value against both *S.* Typhimurium and *L. monocytogenes*, while the 7min CBE nanoparticle had a slightly higher MIC against *L. monocytogenes*. Both the 7min and 10min CBE nanoparticles showed bactericidal activity against the *S.* Typhimurium at the same concentration as their MIC, but the concentrations tested against *L. monocytogenes* were not high enough to exhibit bactericidal activity. The reason for the higher MIC and MBC values for *L. monocytogenes* for all the nanoparticles is because Gram-positive bacteria are less susceptible to inhibition by essential oils (Walsh and others 2003). The primary mode of action for essential oils is through the cell membrane, and the Gram-positive cell membrane is more difficult for essential oils to access (Walsh and others 2003; Raybaudi-Massilia and others 2009). The 10min and 7min PNIPAAM particles both had lower MIC values than free CBE against both *S.* Typhimurium and *L. monocytogenes* found in a previous study, 400 µg/mL and 500 µg/mL, respectively (Hill and others 2013a). Similarly for the MBC values, a lower level of nanoparticles was effective

104

against the *Salmonella* than the *L. monocytogenes*. Bactericidal activity was achieved for

the 7 min and 10 min (top-down) nanoparticles for *Salmonella*, but the concentration of

monomer (bottom-up) nanoparticles tested, was not sufficiently high to kill all the

bacterial cells. Only the 7 min (top-down) nanoparticles exhibited bactericidal activity at

the concentrations tested against *L. monocytogenes*, as it is less susceptible to the

antimicrobial activity of essential oils as previously mentioned.

Table 5.5. MIC and MBC of CBE loaded PNIPAAM nanoparticles against *Salmonella enterica* Typhimurium LT2 and *Listeria monocytogenes* Scott A for CBE loaded PNIPAAM nanoparticles synthesized by bottom-up (monomer) and top-down processes (7 and 10 min).

Nanoparticle	MIC[1] [µg/mL]	MBC [µg/mL]
Salmonella enterica Typhimurium LT2		
7min CBE	345.79[a]	345.79[a]
10min CBE	347.09[b]	347.09[b]
Monomer CBE	2061.80[c]	>2061.80[2c]
Listeria monocytogenes Scott A		
7min CBE	461.06[a]	576.32[a]
10min CBE	347.09[b]	>578.48[2b]
Monomer CBE	1237.08[c]	>2061.80[c]

[1] Values are the lowest concentration of nanoencapsulated CBE for which a ≤0.05 OD630 change was observed after 24 h incubation at 35°C in tryptic soy broth. MIC and MBC values are given based on CBE concentration.
[2] Values preceded by a higher than (>) means that tested concentrations were not sufficient to determine the MIC or MBC values.
[a,b] Means within a column for the same bacterium which are not followed by a common superscript letter are significantly different ($P < 0.05$).

The hydrophobic nature of CBE makes its delivery to pathogen cites challenging in a aqueous environment. Nanoencapsulation in PNIPAAM improves the aqueous solubility of the essential oil and consequently, improves its delivery to microbial cells in aqueous media (Fan and others 2008; Ravichandran and others 2011). Once the essential oil is delivered to the pathogen cell, its hydrophobic character is advantageous in helping the antimicrobial material partition into the cell membrane (Burt 2004; Fan and others 2008). Without the protective PNIPAAM encapsulation, the CBE may have a tendency to coalesce is aqueous solution in order to minimize unfavorable hydrophobic interactions or even be lost to the atmosphere by volatilization (Lapidot and others 2002). In the case of the monomer (bottom-up) PNIPAAM particles, the encapsulation may in fact be too protective, thereby limiting the amount of CBE that is released initially. This resulted in the higher MIC values against the pathogens because not enough CBE was available to inhibit the cell growth. The increase in temperature above the LCST for the top-down particles caused a contraction of the polymer matrix that quickly forced out some of the entrapped CBE. This contraction created a larger "burst" of CBE release initially than the bottom-up nanoparticles. This helped inhibit the bacteria by quickly weakening the bacteria cells by delivering a large initial dose of antimicrobial to the pathogen sites, just as the environmental temperature is reaching the optimal range for pathogen growth (35°C).

5.5 Conclusions

Different methods of synthesis were compared for the production of temperature-responsive PNIPAAM particles to encapsulate CBE. The goal was to determine the best

106

method to synthesize particles to be used for antimicrobial controlled delivery, as no previous research has been conducted related to the use of PNIPAAM in this application. The top-down versus bottom-up synthesis methods yielded particles with significantly different characteristics, especially their release profiles and antimicrobial activities. The PNIPAAM particles synthesized via the top-down procedure had a much faster release which led to a greater antimicrobial activity. Both of the top-down nanoparticles performed similarly, so the 7 min homogenization time nanoparticle would be the best for this application, as the process time is shorter and little improvement was seen by using a slightly longer homogenization. This synthesis procedure also has more promise for use in the food industry because it allows for much more effective purification steps to remove potentially harmful monomers and reagents. The particles produced through the bottom-up procedure could be advantageous in applications were a robust encapsulation was necessary to protect a hydrophobic active compound over a longer period of time than what is needed for antimicrobial delivery.

CHAPTER VI

CHARACTERIZATION OF TEMPERATURE AND PH-RESPONSIVE POLY-N-ISOPROPYLACRYLAMIDE-CO-POLYMER NANOPARTICLES FOR THE RELEASE OF CINNAMON EXTRACT

6.1 Overview

Cinnamon bark extract (CBE) is a hydrophobic spice extract that is a powerful natural antimicrobial effective against foodborne pathogens. Chitosan and alginate are both pH-responsive biopolymers extracted from crustacean exoskeletons and brown algae, respectively. Poly-N-isopropylacrylamide (PNIPAAM) is a hydrogel that becomes hydrophobic at a lower-critical solution temperature. This study sought to combine these pH- and temperature-responsive polymers via crosslinking, in order to create a dual-stimuli responsive polymer for natural antimicrobial compounds delivery, improving their antimicrobial effects. Two co-polymers were synthesized to create two nanoparticles types: chitosan-co-PNIPAAM and alginate-co-PNIPAAM. Nanoparticles were formed from the resulting co-polymers using a self-assembly top-down process followed by glutaraldehyde crosslinking. These nanoparticles were then used as controlled delivery vehicles for CBE, whose rapid release could be triggered by specific external stimuli. Each particle was characterized for size, morphology, entrapment efficiency, release profile, lower-critical solution temperature, and minimum inhibitory and bactericidal concentrations against *Listeria monocytogenes* Scott A and *Salmonella enterica* Typhimirium LT2. Both nanoparticles showed amorphous shape and their

diameters varied (P<0.05) from 69 to 3277 nm based on polymer conformation due to external stimuli. For the same pH and temperature conditions, the chitosan-co-PNIPAAM nanoparticles were significantly more potent bacterial inhibitors against both pathogens and also exhibited a faster CBE release over time as well as slightly higher entrapment efficiency. The alginate-co-PNIPAAM nanoparticles were significantly smaller and exhibited a slow, gradual release over a long time period. Although both nanoparticles were able to effectively inhibit pathogen growth at lower (P<0.05) concentration than free CBE, the chitosan-co-PNIPAAM nanoparticles were more effective in delivering a natural antimicrobial with controlled release against foodborne pathogens. These results show that stimuli-responsive nanoparticles enhanced hydrophobic natural antimicrobial efficacy and could present important food safety applications.

6.2 Introduction

Cinnamon bark extract (CBE) is a highly effective antimicrobial of natural origin, which could provide a "label-friendly" way to inhibit bacterial growth and prevent foodborne pathogen outbreaks; however, it has a very low aqueous solubility and high volatility that limit its contact with foodborne pathogens which favor aqueous environments (Kim and others 1995; Valero and Salmeron 2003). Nanoencapsulation provides protection to the cinnamon extract and allows for careful design and control of the antimicrobial release. Essential oils have extremely low flavor thresholds, so care must be taken to minimize the amount added to food products (Burt 2004).

Encapsulation helps mask the sensory impact and also decreases the effective inhibitory concentration by increasing CBE solubility and improving its delivery to pathogen sites.

Chitosan and alginate are biodegradable polymers that respond to fluctuations in pH. Chitosan is extracted from the exoskeletons of crustaceans and has a pKa of 6.2, meaning it is positively charged in acidic to neutral solution and readily binds to negatively charged surfaces (Rabea and others 2003). At this pH chitosan shifts from being hydrophilic at pH below the pKa value to hydrophobic at pH values above its pKa (Stössel and Leuba 1984; Leuba and Stossel 1986). Chitosan is a long-chained molecule, and when it becomes hydrophobic, it contracts to minimize thermodynamically unfavorable interactions. Alginate exhibits similar behavior, but at opposing pH ranges. It is an anionic polysaccharide extracted from brown algae and has a pKa of approximately 3.5 (King 1988; Gu and others 2004). Above the pKa, alginate is hydrophilic and in environments that are below this pH, alginate is hydrophobic.

These polymers can be crosslinked with PNIPAAM, which responds to temperature stimuli, to create a dual-stimuli responsive polymer. Poly(N-isopropylacrylamide) (PNIPAAM) reacts reversibly at a lower critical solution temperature (LCST) that ranges from 30-35°C (Schild 1992). PNIPAAM's structure possesses hydrophilic and hydrophobic groups within its polymer chain which enables its temperature responsive behavior at the LCST (Gran 2011). Hydrogen-bonds form between water and the hydrophilic groups of the polymer at temperatures below the LCST, which results in a swollen hydrogel PNIPAAM. As the polymer is subjected to temperatures above the LCST, a weakening of the polymer-water hydrogen bonds

110

occurs and the polymer to polymer interactions among the hydrophobic groups predominate (Pelton 2000). Once temperatures are increased above the LCST, the polymer becomes hydrophobic and its polymer chains contract to minimize thermodynamically unfavorable interactions between the aqueous environment and the hydrophobic polymer groups (Schild 1992; Pelton 2000).

These alginate-PNIPAAM and chitosan-PNIPAAM co-polymers can then be used to encapsulate antimicrobial essential oils in order to control their release using environmental stimuli, both temperature and pH, and ultimately improve their efficacy. These co-polymers will contract in response to the external stimuli that induce hydrophobic behaviors. This polymer contraction (of one or both components of the co-polymers) will force out some of the active material entrapped within the polymer matrix, creating a burst release at the transition temperature or pH (Sershen and others 2000). The temperature range for PNIPAAM's LCST is similar to the optimal temperature range for microbial growth for several foodborne pathogens of interest, while the desired pH range for release can be designed by selecting either alginate or chitosan as the co-polymer. Although there have been several previous studies on the antimicrobial capabilities of essential oils (Kalemba and Kunicka 2003; Raybaudi-Massilia and others 2009), there has not been any previously reported work on developing a stimuli-responsive controlled release of antimicrobials for the food industry. A stimuli-responsive polymer could create a way to trigger an antimicrobial release when foods are stored at a pH or temperature that promotes microbial growth. Antimicrobials would be released when they are needed the most, rather than being

111

metabolized or degraded before they are in contact with pathogenic bacteria. While there have been numerous studies on the use of PNIPAAM, alginate, or chitosan to develop nanoparticle delivery systems, very little research has looked at combining chitosan or alginate with PNIPAAM to create a dual-stimuli responsive nanoparticle. Furthermore, thus far there have been no research studies comparing the response of alginate-PNIPAAM hydrogels to chitosan-PNIPAAM hydrogel materials. The goal of this study is to develop a stimuli-responsive nanoparticle system to more effectively inhibit bacteria growth and reduce the incidence of foodborne pathogen related illnesses associated with improper food handling or storage.

6.3 Materials & Methods

6.3.1 Materials

N-isopropylacrylamide (NIPAAM) was purchased from TCI America (Portland, OR). Poly(vinyl alcohol) (PVA) (87%, M_w 30-70 kDa), chitosan (M_w 190-310 kDa, 75-85% deacetylated chitin, viscosity $\leq$ 30 mPa.s), sodium alginate (M_w 120-190 kDa, mannuronate/gluronate (M/G) ratio = 1.56), N,N-methylene-bisacrylamide (MBA), glutaraldehyde (25%), and cinnamon bark extract (99%) (CBE) were purchased from Sigma Aldrich Co. (St. Louis, MO, U.S.A.). N,N,N',N'-tetramethyl-ethylenediamine (TEMED) was purchased from Alfa Aesar (Ward Hill, MA, U.S.A.). Ammonium persulfate was purchased from BDH Chemicals (London, England). All other reagents were of analytical grade.

6.3.2 Particle Synthesis

Alginate Co-Polymer Synthesis

Alginate-PNIPAAM polymer was synthesized by a semi-IPN (interpenetrating polymer network) method similar to that outlined by de Moura and others (2009) and Zhang and others (2005). First, 8 g of NIPAAM monomer were dissolved in 100mL of distilled water with 13% (w/w) sodium alginate, relative to NIPAAM. To this solution, 2% (w/w) N,N'-methylenebisacrylamide (MBA) was added as a crosslinker, followed by 1% (w/w) ammonium persulfate (APS) and 1% (w/w) TEMED to serve as redox initiators. Polymerization took place at 5°C for 24 hours in a glass vessel without any agitation, then the polymer was cut into small pieces and immersed in an excess of distilled water to remove residual monomers and reactants. The water was replaced with fresh distilled water every few hours over a 24 hour period. The hydrogel was then dried in a vacuum oven (Squared Lab Line Instruments, Melrose Park, Ill., U.S.A.) at room temperature and a pressure ≤ 13.3 kPa to remove all moisture. The dried polymer was stored at -20°C until needed for particle synthesis.

Chitosan Co-Polymer Synthesis

Chitosan-PNIPAAM polymer was prepared using a semi-IPN method similar to the method utilized by Lee and others (2004) and Lee and Chen (2001). Briefly, a 1M solution of NIPAAM was mixed with 3% (w/w) chitosan in 1% (w/w) acetic acid until the chitosan had completely dissolved. Then 3 mol% MBA (based on total monomers) was added to the solution, followed by 1% (w/w) APS and TEMED. This solution was poured into a shallow glass dish and allowed to polymerize at 5°C for 24 hours. The

crosslinked hydrogel was soaked in distilled water for 24 hours, replacing the water with

fresh water several times to remove any unreacted monomer. Following this purification

process, the polymer was dried in a vacuum oven at room temperature for 24 hours.

Dried polymer was stored at -20°C until needed for particle synthesis.

<u>Particle Synthesis</u>

A similar procedure was used to form both types of nanoparticles (Figure 6.1).

First, 1.5 mg/mL of dried PNIPAAM-co-polymer was suspended in 150 mL of 0.5%

(w/v) aqueous PVA solution with or without cinnamon bark extract (without for control

particles) and allowed to hydrate overnight without agitation. Following polymer

hydration, the solution was homogenized using an Ultra-Turrax T25 basic Ika (Works,

Inc., Wilmington, NC) at 9500 rpm for 7 minutes in order to break the polymer into

smaller particles. After homogenization, the solutions were placed in a shaking water

bath (VWR International, Radnor, PA) at 40°C and 150 rpm for 24 hours to allow the polymer to self-assemble into micelles. The chitosan-PNIPAAM and alginate-PNIPAAM micelles were then crosslinked with glutaraldehyde (2:1 molar ratio of glutaraldehyde to monomers) or calcium chloride (1% (w/v)), respectively, to generate IPN nanoparticles. The finished particles were then purified via ultrafiltration using a Millipore-Labscale[TM] TFF system fitted with a 50 kDa molecular weight cutoff Pellicon XL-Millipore (Millipore Co., Kankakee, IL) to remove excess reactants and free cinnamon extract. The nanoparticles were ultrafiltered with an inlet pressure of 25 psi and outlet pressure of approximately 5-10 psi, using 300 mL of water and 100 mL of the retentate was collected. After filtration, the particles were lyophilized at -50°C and 1.45 x 10^{-4} psi vacuum for 24 hours in a Labconco Freeze Dry-5 unit (Labconco, Kansas City, MO). Dried nanoparticles were stored at -20°C until they were needed for analysis.
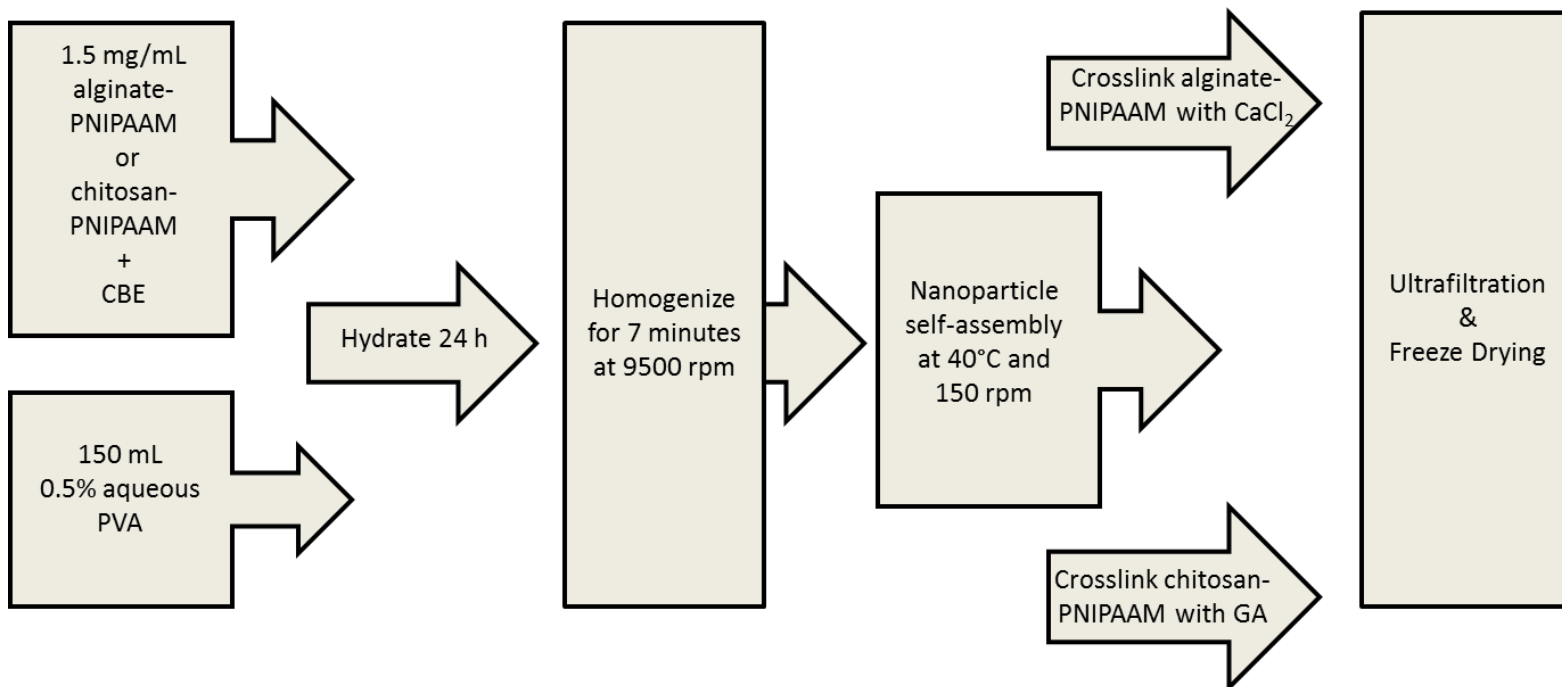
Figure 6.1. Schematic diagram of the self-assembly synthesis procedure for alginate-PNIPAAM or chitosan-PNIPAAM nanoparticles.

6.3.3 Particle Characterization

Particle Size and Morphology

Aqueous suspensions of each nanoparticle were analyzed for size distribution and polydispersity index (PDI) using a Delsa™ Nano C Particle Analyzer (Beckman Coulter, Brea, CA). Nanoparticles were suspended in distilled water (neutral pH) at a concentration of 50 mg/mL and sonicated at 70 W (Cole Parmer sonicator 8890, Vernon Hill, IL) for 15 minutes prior to analysis using 1 cm path length plastic cuvettes at a scattering angle of 165°, with a pinhole set to 50 µm, and a refractive index of 1.3328 for 120 continuous accumulation times. Particle size attributes were analyzed at 25°C and 40°C to observe the impact of heating the particles above the LCST.

Aqueous suspensions of nanoparticles were viewed using a FEI Morgagni Transmission Electron Microscope (TEM) (FEI Company, Hillsboro, OR) at the School of Veterinary Medicine and Biomedical Sciences of Texas A&M University (College Station, TX). All particles were viewed at room temperature (below the LCST) and neutral pH, due to equipment and material limitations. The microscope employed was not capable of maintaining elevated temperatures, so the reversible nature of the polymer transition at the LCST prevents viewing at different temperatures. Suspended particles were placed on 300 mesh copper grids and stained with a 2% (w/v) uranyl acetate aqueous stain (Electron Microscopy Sciences, Hatfield, PA) to provide contrast under magnification. Excess liquid on the mesh was removed with filter paper and the grid was allowed to dry before viewing under 10,000 to 100,000 times magnification. Observations were performed at 80 kV.

Entrapment Efficiency (EE) and Drug Loading (DL)

The entrapment efficiency of and drug loading of each nanoparticle were measured indirectly by determining the amount of CBE that was present in the permeate collected during ultrafiltration. It was assumed that any CBE that did not pass through the filter membrane was entrapped within particles. The amount of CBE present in the permeate was measured spectrophotometrically at 280 nm (Shimadzu UV-1601 spectrophotometer, Columbia, MA) in a 1 cm path length quartz cuvette. The EE and DL were calculated according to Equation (6.1) and (6.2), respectively (Gomes and others 2011b; Iannitelli and others 2011):

$$ EE = \frac{amount\ of\ active\ compound\ entrapped}{initial\ active\ compound\ amount} x100 \qquad [6.1] $$

$$ DL = \frac{amount\ of\ active\ compound\ entrapped}{amount\ of\ particles\ produced} x100 \qquad [6.2] $$

Cloud Point and Lower Critical Solution Temperature (LCST)

The LCST values of the PNIPAAM, chitosan-PNIPAAM, and alginate-PNIPAAM hydrogels were measured using differential scanning calorimetry in a Pyris 6 Perkin Elmer instrument (Pyris 5.0 Software, Boston, MA). Hydrogel samples were submerged in water (neutral pH) and allowed to swell to equilibrium before DSC measurements were taken. Roughly 10 mg of swollen PNIPAAM was placed into 40 µL aluminum pans and sealed with one hole in their lids and scanned from 25°C to 50°C at a rate of 3°C per minute under nitrogen atmosphere (Zhang and others 2004b). The onset of the endothermal peak was considered the LCST.

118

The cloud point method (Kim and others 2005b) was used to find the thermal transition temperature of the control and CBE encapsulating co-polymer nanoparticles. A 0.1% (w/w) aqueous solution of particles (neutral pH) was prepared for each type of nanoparticle and three wells of a 96-well plate were filled with 200 µL of each nanoparticle suspension. Absorbance of the particle solutions was measured at 450 nm using a 96-well plate reader equipped with temperature control (VERSAmax Tunable Microplate Reader, Molecular Devices, Sunnyvale, CA). The cloud point was defined as the inflection point on a plot of absorbance versus temperature for each nanoparticle suspension as the temperature was increased from 25°C to 50°C at a rate of 2°C every 10 minutes. The cloud point of the PNIPAAM-co-polymer hydrogels were also measured to ensure the cloud point method and DSC method produced comparable results.

Controlled Release

Controlled release experiments were conducted at 25°C, 35°C, and 45°C to determine the rate of CBE release below, above, or near the LCST of the particles. The release was measured at these temperatures in release media of pH 3 and pH 7.4 to determine the particle response to differing pH stimuli because chitosan and alginate are pH-responsive. Nanoparticles were suspended in phosphate buffered saline (PBS, 0.15M, pH 3 or 7.4) to achieve a 1.0 mg/mL concentration of particles (sink conditions) in 15 mL conical tubes. The pH of the acidic PBS was adjusted with 0.5M hydrochloric acid. The particle suspensions were placed in a shaking water bath (VWR International, Radnor, PA) set at 100 rpm and the desired temperature. At predetermined time intervals, 1 mL samples were removed and centrifuged at 23506g for 15 minutes to

precipitate any nanoencapsulant material prior to spectrophotometric analysis of the supernatant at 280 nm.

The controlled release profile could be modeled by a semi-empirical equation (6.3) described by Korsmeyer and others (1986) that accounts for both Fickian diffusion and transport due to swelling effects (termed "non-Fickian Type II transport"):

$$\frac{M_t}{M_\infty} = kt^n \qquad [6.3]$$

where M_t/M_∞ is the percent of antimicrobial released at time t (s), k is a rate constant (1/s), and n is the diffusional exponent (dimensionless). The release mechanism from swellable particles differs from a purely Fickian model since the release is governed by the polymer's swelling behavior as well as the diffusion rate of the antimicrobial through the polymer matrix (Arifin and others 2006).

6.3.4 Minimum Inhibitory and Bactericidal Concentration (MIC and MBC)

Bacterial Cultures

Salmonella enterica serovar Typhimurium LT2 and *Listeria monocytogenes* strain Scott A were obtained from Texas A&M University Food Microbiology Laboratory (College Station, TX). *S*. Typhimurium and *L. monocytogenes* were resuscitated in tryptic soy broth (TSB) and tryptose phosphate broth (TPB) (Becton, Dickinson and Co., Sparks, MD), respectively, by two identical consecutive transfers and incubating for 24 hours aerobically at 35°C. The bacterial cultures were maintained on TSA slants stored at 4°C for no more than 3 months. Transfers from slants were conducted similarly to the resuscitation method to prepare microorganisms for analysis.

<u>Antimicrobial Activity</u>

Minimum inhibitory concentrations (MICs) for the Chitosan-PNIPAAM and Alginate-PNIPAAM nanoparticles were measured using a broth dilution assay (Brandt and others 2010). Growth curves for each strain were performed at 35°C to correlate plate counts with optical density values at 630 nm (OD630) measured with an Epoch microplate spectrophotometer (BioTek® Instruments, Inc., Winooski, VT). Bacterial inocula were incubated 20-22 h and then serially diluted in double-strength TSB (2x TSB) or TPB (2x TPB), as appropriate, to achieve an initial inoculum of approximately 3.0 $\log_{10}$ CFU/mL in each sample well while providing the appropriate amount of nutrients upon dilution. Initial inocula were enumerated via spread plating on tryptic soy agar (TSA) or Modified Oxford agar (MOX) and incubated for 24 h at 35°C. Aliquots of 100-µL of all antimicrobial solutions and solvent blanks were spread plated on TSA at the beginning of the experiment to ensure their sterility.

The MIC experiments were carried out in 96 well microtiter plates (sterilized 300 µl capacity – MicroWell, NUNC, Thermo-Fisher Scientific, Waltham, MA). The nanoparticles were placed in the microtiter plates as aqueous suspensions in concentrations ranging from 5,000 to 25,000 µg/mL for both pathogens. Equal volumes (100 µL) of nanoparticle solution and bacterial inoculum in 2x broth were loaded into each test well. Negative controls were prepared with nanoparticle solutions and sterile 2x broth to account for baseline OD630 readings. Positive controls were also prepared containing inoculum and sterile distilled water or control nanoparticles to ensure nanoparticle encapsulate materials had no inhibitory effect on bacterial growth. Once all

solutions were added to the plates, they were covered with a mylar plate sealer (Thermo Fisher Scientific), shaken gently, and OD630 of the wells was read (0 h). The microtiter plates were incubated (24 h at 35°C) and shaken gently before OD630 readings were taken again to observe bacterial growth or inhibition in the presence of the nanoparticles over the course of the typical bacterial growth cycle. Antimicrobial test wells that showed ≤0.05 change in OD630 after 24 h of incubation were considered "inhibited" by the antimicrobial (after appropriate baseline adjustments) for that time period. The MIC for each nanoparticle and pathogen was considered to be the lowest concentration of antimicrobial that inhibited growth for all test replicates (Brandt and others 2010).

Any wells that exhibited inhibition of the test microorganism after 24 h were then tested for bactericidal activity by spreading 100 μL from each well onto TSA plates and incubating for 24 h at 35°C. If no colonies were observed on the plate surfaces following incubation for all replicates, the treatment concentration was considered bactericidal. The lowest concentration of nanoparticles demonstrating bactericidal activity across all replicates was considered the MBC.

6.3.5 Statistical Analysis

All determinations were made in triplicate as independent experiments. All statistical analyses were performed using JMP v. 9 Software (SAS Institute, Cary, NC). Differences between variables were tested for significance using one-way analysis of variance (ANOVA) and significantly different means ($p<0.05$) were separated using Tukey's Honestly Significant Differences (HSD) test. Controlled release data were fit to model using JMP software and the non-linear modeling procedure to determine rate

constants (k) and diffusional coefficients (n). The model constants were analyzed for goodness of fit using the non-linear procedure to determine coefficients of determination (R^2).

6.4 Results & Discussion

6.4.1 Particle Characterization

<u>Particle Size and Morphology</u>

The morphology of both the alginate and chitosan-PNIPAAM nanoparticles appeared to be amorphous structures in TEM images (Figure 6.2). The chitosan-PNIPAAM particles were larger (P<0.05) chained structures, as anticipated, considering the large structure of chitosan polymers. The chitosan used in this study possesses a medium range molecular weight for chitosan polymers, ranging from 190-310 kDa and a high degree of deacetylation (75-85%). Alginate has a significantly smaller molecular size ranging from 120-190 kDa, leading to smaller polymer nanoparticles, as seen in previous study of chitosan and alginate nanoparticles (Douglas and Tabrizian 2005).

Particle size analysis also showed the alginate-PNIPAAM nanoparticles to be significantly smaller than the chitosan-PNIPAAM nanoparticles (Table 6.1) at temperatures above and below the LCST for each particle, much like the TEM images. The TEM images showed similar particle sizes to those determined by laser diffraction in the particle size analyzer, with the alginate-PNIPAAM particles appearing smaller than the chitosan-PNIPAAM particles and the unloaded (control) particles appearing smaller than those that contained entrapped CBE in the images. For both alginate-PNIPAAM and chitosan-PNIPAAN nanoparticles, the unloaded control particles were

smaller in diameter than their CBE-containing counterparts at temperatures above the LCST. This phenomenon occurred because the polymers contract and collapse the micelles when heated above their LCST, and the unloaded nanoparticles had no CBE to prevent total collapse of the micelles (Fan and others 2008).

All particle suspensions were found to have a heterogeneous particle size distribution, reflected in the PDI values greater than 0.1. The TEM images also demonstrated the wide range of particle sizes present in the alginate-PNIPAAM and chitosan-PNIPAAM particle solutions. The chitosan-PNIPAAM nanoparticles synthesized by (Fan and others 2008) also showed a wide particle size distribution; however, their average diameter was smaller than the chitosan-PNIPAAM particles synthesized in this study. No previous studies have synthesized nanoparticles from alginate-PNIPAAM, they have only investigated the bulk alginate-PNIPAAM hydrogel.
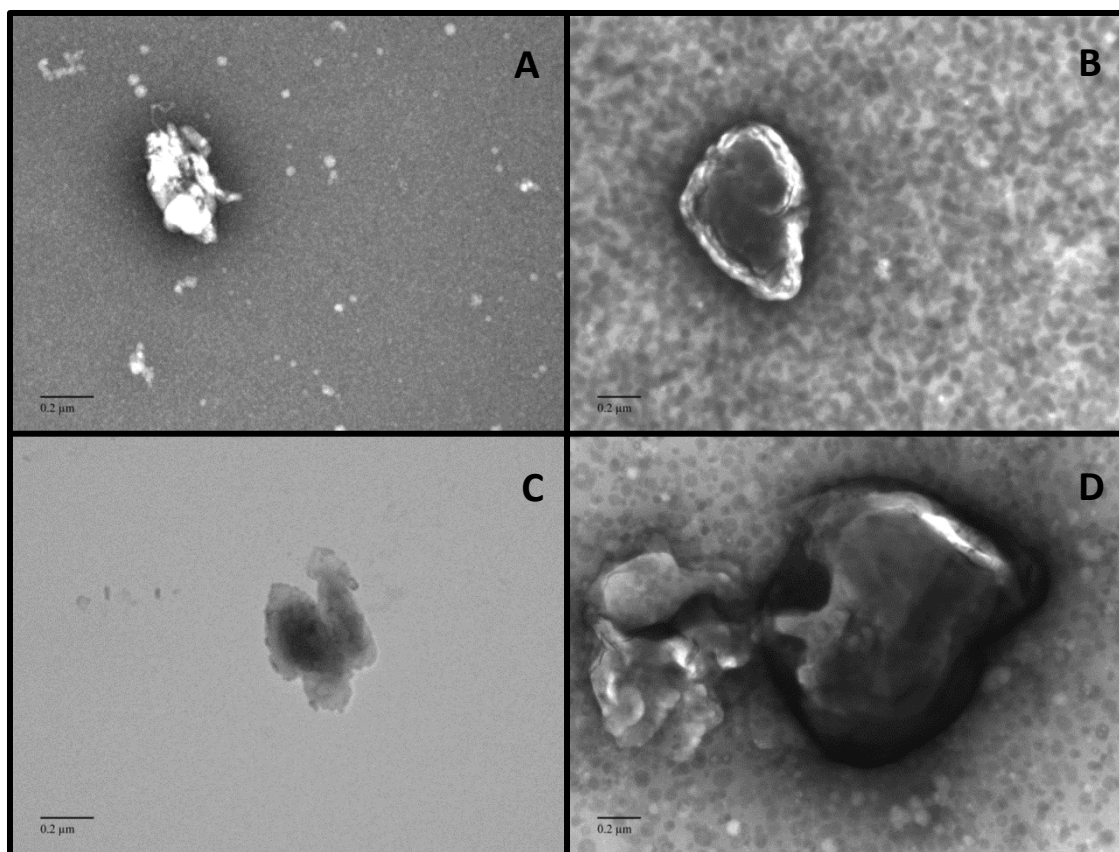
Figure 6.2. Transmission electron microscope (TEM) images of PNIPAAM-co-polymer nanoparticles. (A) alginate-PNIPAAM control (unloaded); (B) alginate-PNIPAAM CBE; (C) chitosan-PNIPAAM control; (D) chitosan-PNIPAAM CBE. Observations were performed at 80 kV using magnifications ranging from 36,000 to 44,000x.

Table 6.1. Comparison of average particle diameter and polydispersity index (PDI) for control (unloaded) and CBE entrapped alginate-PNIPAAM and chitosan-PNIPAAM nanoparticles below (25°C) and above the LCST (40°C).

Particle	Average Diameter [nm]		PDI	
	25°C	40°C	25°C	40°C
Chitosan-PNIPAAM Control	$_w$7526.80^a (84.29)	$_x$3179.58^a (1703.13)	$_w$0.81^{ab} (1.04)	$_w$0.48^a (0.03)
Chitosan-PNIPAAM CBE	$_w$9920.18^a (3927.58)	$_x$4580.40^a (496.11)	$_w$0.57^b (0.30)	$_w$0.54^a (0.13)
Alginate-PNIPAAM Control	$_w$110.07^c (46.30)	$_w$69.42^c (15.67)	$_w$1.15^a (0.04)	$_x$0.15^b (0.05)
Alginate-PNIPAAM CBE	$_w$955.78^b (33.07)	$_w$918.79^b (71.57)	$_w$1.08^a (0.02)	$_x$0.49^{ab} (0.43)

[a]Means within a column that are not followed by a common superscript letter are significantly different ($p<0.05$). $_w$Means within a row, of the same parameter, that are not preceded by a common subscript letter are significantly different ($p<0.05$).

Entrapment Efficiency and Drug Loading

The entrapment efficiency was slightly higher in the chitosan-PNIPAAM nanoparticles than the alginate-PNIPAAM nanoparticles, but not significantly higher (Table 6.2). Although the level of entrapment was similar, the chitosan particles were more effective bacterial inhibitors. This is likely due to the fact that chitosan itself has some antimicrobial capabilities (Rabea and others 2003). Similar entrapment efficiencies were not surprising because both biopolymers were co-polymerized with PNIPAAM and self-assembly was conducted at the same temperature and pH for both co-polymers. Fan and others (2008) found slightly lower values of entrapment efficiency and drug loading

of a hydrophobic drug in chitosan-PNIPAAM nanoparticles synthesized via a similar method, while Chuang and others (2009) found even lower values of EE and DL for a hydrophilic drug in a similar chitosan-PNIPAAM nanoparticle. Shi and others (2006) synthesized alginate-PNIPAAM spheres encapsulating a hydrophobic drug at similar levels of EE and DL; however, these spheres were much larger than nano-scale delivery systems. PNIPAAM is the temperature-responsive component of the co-polymers, so its response to the temperature above the LCST during the self-assembly process governed the formation of the particle micelles and the entrapment of the CBE within the capsules. The elevated temperature during the self-assembly process caused the PNIPAAM to contract and form micelles around the hydrophobic CBE to minimize unfavorable interactions with the aqueous environment. Alginate and chitosan both respond to pH, which was kept stable (7.4) along with the temperature during the particle manufacture process.

The alginate-PNIPAAM and chitosan-PNIPAAM nanoparticles presented high DL values, as they did with the entrapment efficiency values. A drug loading of 100% CBE entrapment would be 2.56% for the alginate-PNIPAAM nanoparticles and 1.43% for the chitosan-PNIPAAM nanoparticles, meaning the drug loading values for each of the particles were close to their maximum values. The drug loading maximum is higher for the alginate-PNIPAAM nanoparticles due to the higher M_w of chitosan.

Table 6.2. Entrapment efficiency and drug loading values measured for cinnamon bark extract (CBE) in chitosan- and alginate- PNIPAAM nanoparticles by spectrophotometry at 280 nm.

Nanoparticle	Entrapment Efficiency [%]	Drug Loading [%]
Chitosan-PNIPAAM CBE	75.58[a] ± 9.46	1.93[a]±0.24
Alginate-PNIPAAM CBE	74.50[a] ± 8.13	1.07[b]±0.12

[a]Means within a column that are not followed by a common superscript letter are significantly different (p<0.05).

Cloud Point and Lower Critical Solution Temperature (LCST)

The LCST for PNIPAAM hydrogel was measured in a previous study and fell within the typical range (30-35°C) for PNIPAAM polymers at 33.9°C via DSC determination (Schild 1992). The LCST of the alginate-PNIPAAM and chitosan-PNIPAAM hydrogels also fell within this range, at 32.5°C and 31.2°C, respectively. The LCSTs determined by the cloud point method were slightly higher at 33.8°C for alginate-PNIPAAM and 34.2°C for chitosan-PNIPAAM (Table 6.3). The small differences in the LCST values determined by each method are attributable to the lower sensitivity of the cloud point method (Eeckman and others 2001). The cloud point method was used to determine the LCSTs for the nanoparticles because they were protected by a matrix of PVA that prevented sufficient volumes of particles to be placed in the DSC pans for accurate analysis. The cloud method allowed for larger aliquots of particle suspensions, enabling consistent LCST measurements. The cloud point and DSC methods reveal the transition temperature through different means of data collection.

The DSC analysis measures the heat required to break hydrogen bonds between water and the polymer, which occurs at the transition temperature and results in an endothermic peak on the thermogram. The cloud point method monitors the precipitation of the PNIPAAM as it passes through the transition temperature using spectrophotometric analysis to visualize the changes in solution turbidity. Eeckman and others (2001) measured the cloud point and LCST values of PNIPAAM polymer, and found similar transition temperature values, irrespective of the method used to measure it and the values were similar to those reported for the nanoparticles in this study. The alginate-PNIPAAM control particles had the lowest LCST at 31.8°C, while the alginate-PNIPAAM CBE nanoparticles had a slightly higher LCST value at 32.6°C. Authors Vasile and others (2009) measured a similar range of LCST values for alginate-PNIPAAM hydrogels, that varied based upon the amount of alginate present in the polymer matrix. The chitosan-PNIPAAM control and CBE particles had slightly higher LCST values, at 33.9°C and 34.7°C, respectively. Chitosan-PNIPAAM hydrogels synthesized by Verestiuc and others (2004) showed a similar transition temperature within the typical range for PNIPAAM polymers. None of the co-polymers or nanoparticles exhibited transition temperatures drastically different than the PNIPAAM hydrogel. The PNIPAAM is the temperature-responsive element of these co-polymers, so this behavior should not deviate significantly from the temperature response of PNIPAAM itself.

Table 6.3. Cloud point and lower critical solution temperatures (LCSTs) of chitosan- and alginate-PNIPAAM hydrogel and nanoparticles (control and CBE loaded).

Material	Cloud Point [°C]	LCST [°C]
Alginate-PNIPAAM hydrogel*	$_w33.8^{ab}$ (0.65)	$_z32.45$ (0.55)
Alginate-PNIPAAM control	31.8^c (0.78)	-
Alginate-PNIPAAM CBE	32.6^{bc} (0.29)	-
Chitosan-PNIPAAM hydrogel*	$_w34.2^{ab}$ (0.78)	$_z31.16$ (0.47)
Chitosan-PNIPAAM control	33.9^{ab} (0.61)	-
Chitosan-PNIPAAM CBE	34.7^a (0.50)	-

[a]Means within a column that are not followed by a common superscript letter are significantly different ($p<0.05$). [w]Means within a row, of the same parameter, that are not preceded by a common subscript letter are significantly different ($p<0.05$). *Hydrogels consist of the bulk co-polymer materials synthesized before being used to manufacture nanoparticles.

Controlled Release

The release profiles of both the alginate and chitosan-co-PNIPAAM

nanoparticles (Figures 6.3 and 6.4) were highly dependent upon the release media

conditions, as was anticipated. For the chitosan-PNIPAAM particles, the release was

governed primarily by temperature, while the release for the alginate-PNIPAAM

particles was more heavily dependent upon the pH of the release media. The fact that the

alginate-PNIPAAM nanoparticles respond more dramatically to changes in pH would

lead us to believe that the co-polymer that comprises these particles has a higher level of

alginate present in the co-polymer matrix. Conversely, the observation that the chitosan-PNIPAAM nanoparticle release responds more to changes in release media temperature, suggests that there is more PNIPAAM present in the chitosan-PNIPAAM co-polymer matrix. The chitosan M_w (190-310 kDa) is higher than the M_w of alginate (120-190 kDa), which may have provided more sites for NIPAAM monomer to attach and build the polymer matrix. Different types of polymer crosslinking agents were used to form the nanoparticle micelles, based on which type of co-polymer was being used. The alginate-PNIPAAM nanoparticles were stabilized with calcium chloride, which crosslinks alginate immediately and could have potentially led to the formation of an exterior layer of alginate in the alginate-PNIPAAM nanoparticles. If the alginate is present on the exterior of the micelle, then its expansion or contraction will more dramatically impact the release of active material than if the PNIPAAM is expanding or contracting on the interior of the polymer micelles (Chuang and others 2010). The chitosan-PNIPAAM micelles were crosslinked with glutaraldehyde, which crosslinks amine groups in PNIPAAM and chitosan effectively (Chuang and others 2009). This may have led to co-polymer micelles with more heterogeneous polymer structures than those formed by the alginate-PNIPAAM polymers.

The chitosan-PNIPAAM polymer likely has a higher percentage of PNIPAAM than chitosan in its matrix, as it is the temperature-responsive component of the co-polymer, and the burst release from these particles was significantly larger at 35°C, which is above the LCST. Above the LCST, the PNIPAAM will contract to force out a quick release of CBE before continuing to slowly release the CBE by diffusion through

the polymer matrix. The initial release of CBE is approximately four times the magnitude at 35°C than at 25°C, because the particle does not contract below the LCST, leaving the release to be governed primarily by diffusion. At both temperatures, the release is slightly higher when the release media is at a pH of 7.4 than pH 3.0. The chitosan polymer chains will also be contracting at pH 7.4, contributing to the initial burst release of the nanoparticles as they are added to the release media (Rabea and others 2003). The chitosan contracts as its amine groups are deprotonated in pH environments above the pKa, causing it to be hydrophobic (Chuang and others 2010).
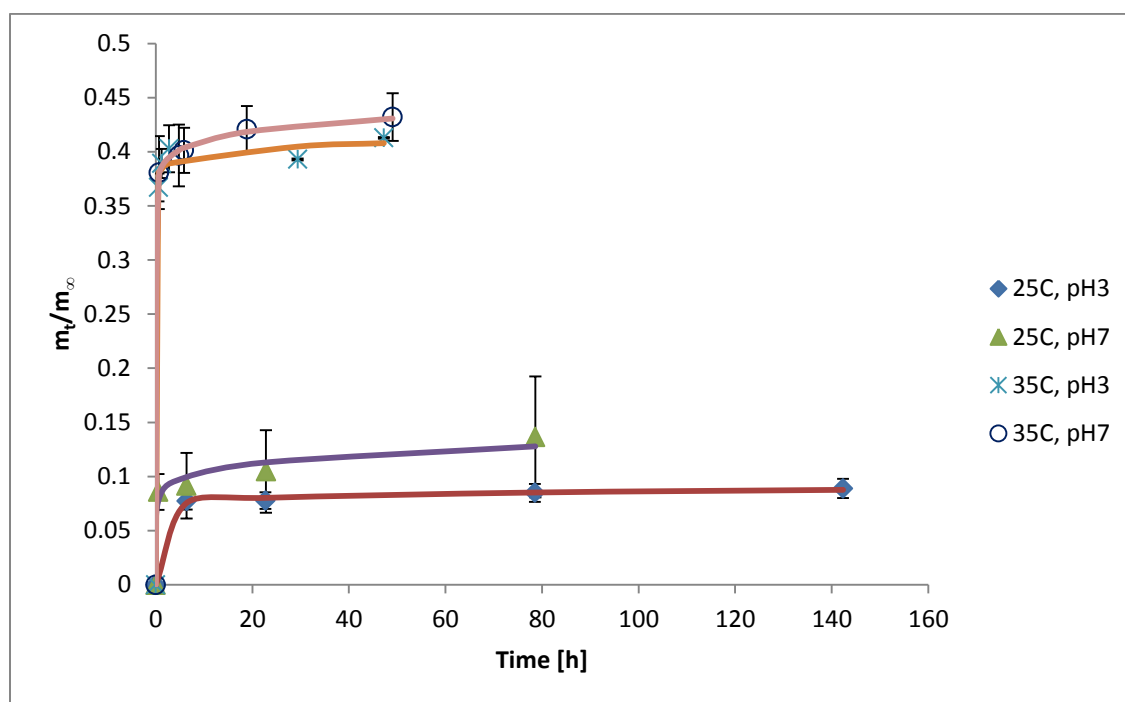
Figure 6.3. Controlled release profiles of chitosan-PNIPAAM nanoparticles at different temperatures in 0.15M phosphate buffered saline (PBS) adjusted to pH 3.0 and pH 7.4, fit to model release equation (solid lines). Raw data are represented by data points and error bars.
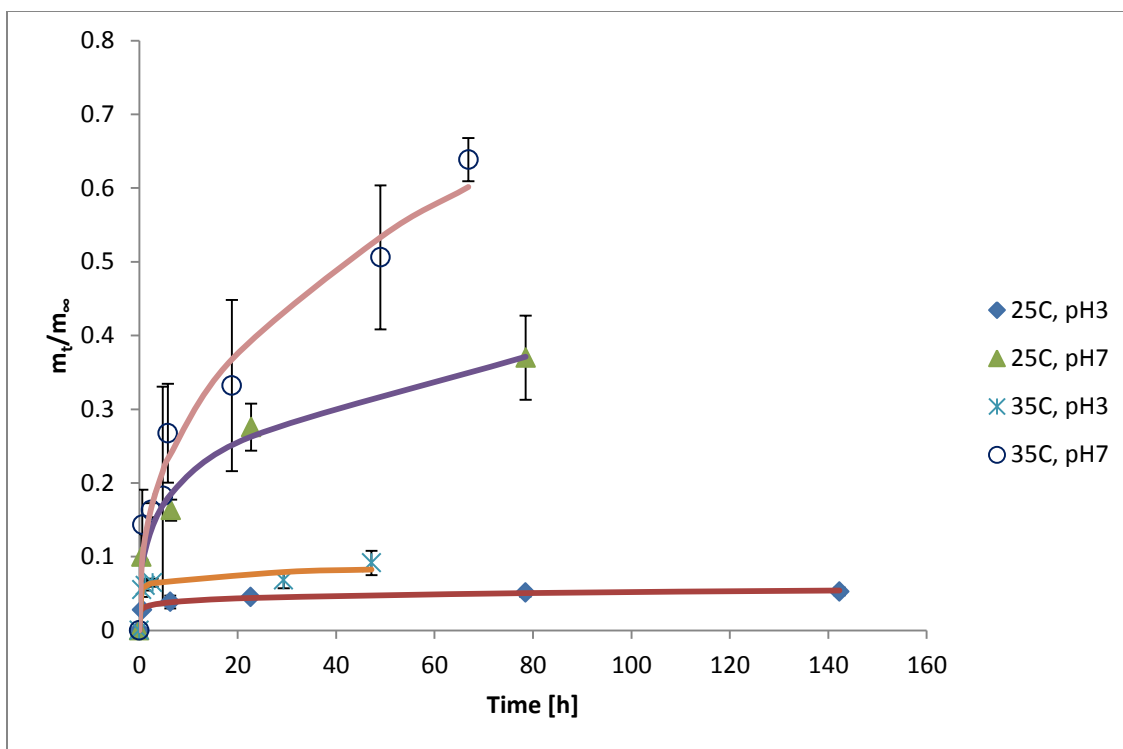
Figure 6.4. Controlled release profiles of alginate-PNIPAAM nanoparticles at different temperatures in 0.15M phosphate buffered saline (PBS) adjusted to pH 3.0 and pH 7.4, fit to model release equation (solid lines). Raw data are represented by data points and error bars.

The alginate-PNIPAAM particle release was more significantly affected by a shift in the release media pH, indicating that this co-polymer behavior is governed primarily by alginate, the pH responsive polymer, rather than PNIPAAM. Vasile and others (2009) also noted a dramatic increase in release from alginate-PNIPAAM nanoparticles as the pH was increased; however, they did not measure release at different temperatures to provide a basis for the comparison in this respect. Another reason for the high rate of diffusion-governed release at pH 7.4 from alginate-PNIPAAM nanoparticles is a result of the environmental pH being well above the pKa of 3.5 for

alginate. As the pH incrementally increases, the alginate molecules become highly

hydrophilic and the hydrogel polymer matrix becomes swollen and opens more pores to

diffusion. In contrast with the chitosan-PNIPAAM nanoparticles, the release of CBE was

higher when the alginate is hydrophilic at pH 7.4 than at pH 3.0, where it is hydrophobic

(Gu and others 2004). The burst release for these nanoparticles was much lower

($P < 0.05$) than for the chitosan-PNIPAAM nanoparticles, but the subsequent release

governed by diffusion was much higher ($P < 0.05$) due to the more open nature of the

polymer matrix as a swollen hydrogel (de Moura and others 2009; Vasile and others

2009). Lee and Chen (2001) noted that the diffusion rate slowed from chitosan-

PNIPAAM hydrogels as the ratio of chitosan to PNIPAAM increased as was seen in this

study and explains the lower diffusion rate in the chitosan-PNIPAAM particles than the

alginate-PNIPAAM particles. The release was again higher at 35°C than 25°C for both

pHs, as the PNIPAAM contracts and contributes a burst of CBE release into the

medium. Shi and others (2006) and de Moura and others (2009) also found a similar

relationship between release, temperature, and pH conditions for alginate-PNIPAAM

spheres loaded with indomethacin. A previous study working with controlled release of a

hydrophobic drug from chitosan-PNIPAAM particles found release profiles that were

highly dependent upon the environmental pH and temperature and with a similar

response to the release found in this study (Fan and others 2008). This study prepared

chitosan-PNIPAAM co-polymer at a similar ratio of the two polymers to that which was

used in the present study. Similarly, these authors showed the release of entrapped

material was more impacted by a change in temperature than a change in pH. This study

134

found that release was highest at a pH of 6.9, but there was little difference among release rates at pH values above or below 6.9 (Fan and others 2008). The co-polymer synthesis procedure could be refined in order to design the ratio of each stimuli-responsive component within the polymer matrix. In this way, a nanoparticle can be designed to fit a specific set of release parameters that are the most effective for antimicrobial delivery in any food system under various potential storage conditions.

The raw data from the controlled release experiments fit well to the release equation proposed for spherical, swellable polymers (Eqn. 6.3) as was expected for these nanoparticle systems (Table 6.4). The rate coefficients and diffusion constants are slightly lower than those determined by Vasile and others (2009) for a slightly more soluble encapsulated material (vanillin). All coefficients of determination (R^2) were greater than 0.95, indicating an excellent fit to the proposed release model.

Table 6.4. Controlled release model rate coefficients (k) and diffusion constants (n) for alginate- and chitosan-PNIPAAM nanoparticles with entrapped CBE.

		Alginate-PNIPAAM CBE			Chitosan-PNIPAAM CBE		
		k_r [s^{-n}]	n_r	R^2	k_r [s^{-n}]	n_r	R^2
25°C	pH 3.0	1.39×10^{-4} $\pm$ (1.46×10^{-5})	0.55 $\pm$ (5.05×10^{-3})	1	1.78×10^{-4} $\pm$ (3.59×10^{-5})	0.56 $\pm$ (3.61×10^{-3})	1
	pH 7.4	3.81×10^{-4} $\pm$ (6.32×10^{-5})	0.60 $\pm$ (0.01)	0.99	2.60×10^{-4} $\pm$ (4.64×10^{-5})	0.58 $\pm$ (0.01)	0.97
35°C	pH 3.0	2.83×10^{-4} $\pm$ (2.63×10^{-5})	0.58 $\pm$ (4.60×10^{-3})	0.96	9.90×10^{-4} $\pm$ (1.76×10^{-5})	0.64 $\pm$ (8.49×10^{-4})	1
	pH 7.4	5.28×10^{-4} $\pm$ (1.33×10^{-4})	0.62 $\pm$ (0.01)	0.97	6.46×10^{-4} $\pm$ (9.30×10^{-5})	0.62 $\pm$ (4.02×10^{-3})	1

6.4.2 Minimum Inhibitory and Bactericidal Concentration (MIC and MBC)

The MIC values for the alginate-PNIPAAM and chitosan-PNIPAAM encapsulated CBE (Table 6.5) were lower ($P<0.05$) for both *S.* Typhimurium and *L. monocytogenes* than the MIC values found for free CBE in a previous study (400 and 500 µg/mL, respectively) (Hill and others 2013a). The MIC values for chitosan-PNIPAAM, at 192 µg/mL for *S.* Typhimurium and 385 µg/mL for *L. monocytogenes*, were slightly lower than those found for alginate-PNIPAAM due to the inherent antimicrobial properties of chitosan. Although the control chitosan-PNIPAAM nanoparticles did not present inhibitory activity, the bacterial growth in contact with these particles was lower than the levels of growth present in either of the bacteria controls or the alginate-PNIPAAM control particles.

The MIC experiments were conducted at 35°C and a neutral pH, so the release profiles of the antimicrobial particles would have been similar to those measured at 35°C and pH 7.4. For the chitosan-PNIPAAM particles would have a large burst of antimicrobial as soon as the medium reached 35°C, which would deliver a high dose of antimicrobial to the pathogens right as they are reaching their ideal growth temperature. This would increase the antimicrobial efficacy of the nanoparticles by delivering their highest dose before the bacteria is able to reach its exponential growth phase. The release profile for the alginate-PNIPAAM nanoparticles in the MIC experiment was more slow and gradual than the release of antimicrobial from chitosan-PNIPAAM nanoparticles. This slower release could contribute to the higher MIC value determined for the alginate-PNIPAAM particles. The MIC values for both nanoparticles were lower

137

for *S.* Typhimurium than for *L. monocytogenes*, because Gram-positive bacteria are less

susceptible to inhibition by essential oils (Walsh and others 2003). The antimicrobial

activity of essential oils is a result of its action on the microbial cell membrane, which is

more accessible to essential oils in Gram-negative bacteria (Walsh and others 2003;

Raybaudi-Massilia and others 2009).

Table 6.5. MIC and MBC values of CBE loaded alginate- and chitosan-PNIPAAM
nanoparticles against *Salmonella enterica* Typhimurium LT2 and *Listeria
monocytogenes* Scott A.

Nanoparticle	*Salmonella spp.*		*Listeria spp.*	
	MIC[1] [µg/mL]	MBC [µg/mL]	MIC [µg/mL]	MBC [µg/mL]
Alginate-PNIPAAM CBE	264[a]	>661.18[2]	397[a]	>661.18
Chitosan-PNIPAAM CBE	192[b]	>481.2	385[b]	>481.2

[1] Values are the lowest concentration of nanoencapsulated CBE for which a ≤0.05
OD630 change was observed after 24 h incubation at 35°C in tryptic soy broth. MIC
and MBC values are given based on CBE concentration.
[2] Values preceded by a higher than (>) means that tested concentrations were not
sufficient to determine the MIC or MBC values.

No MBC values were determined for these two nanoparticles, as the

concentrations tested were not sufficient to kill all the bacteria present. Higher

concentrations of alginate or chitosan-PNIPAAM encapsulated CBE would likely result

in bactericidal activity. Chitosan-PNIPAAM and alginate-PNIPAAM co-polymers have

not previously been tested as vehicles for delivery of antimicrobial compounds for food

products, but have been studied for pharmaceutical delivery applications (Ju and others

2001; de Moura and others 2009; Chuang and others 2010).

6.5 Conclusions

The antimicrobial activity found in this study shows potential for a controlled delivery system of essential oils for the food industry that could improve the antimicrobial efficacy of essential oils while minimizing their sensory impact. The release profiles of the co-polymer nanoparticles appeared to be highly dependent upon the ratio of pH and temperature-responsive polymers present in the final polymer matrix. The polymer that predominantly governs the release, determines whether the antimicrobial release is primarily affected by temperature or pH stimuli. This study shows that it is possible to engineer dual stimuli-responsive co-polymers that release antimicrobials in response to specific environmental conditions, and consequently enhance antimicrobials efficacy in adverse storage conditions. The results of this study showed the chitosan-PNIPAAM nanoparticles to have a higher release rate of antimicrobial material and a more effective antimicrobial activity than the alginate-PNIPAAM nanoparticles in an optimal environment for bacteria growth. In a lower temperature environment, the alginate-PNIPAAM nanoparticles would have a higher release rate than chitosan-PNIPAAM nanoparticles and potentially superior antimicrobial activity. An antimicrobial delivery system that reacts to potentially dangerous storage environments for food products could improve the food safety and prevent potentially dangerous foodborne outbreaks.

CHAPTER VII

EFFECTS OF THE APPLICATION OF NANOENCAPSULATED CINNAMON EXTRACT ON MICROBIAL SAFETY AND QUALITY OF FRESH-CUT ROMAINE LETTUCE

7.1 Overview

The quality and safety of fresh-cut romaine lettuce treated with free and nanoencapsulated cinnamon bark extract (CBE) was assessed in this study. A challenge study was conducted to compare the antimicrobial efficacy of different types of nanoencapsulated CBE, including: beta-cyclodextrin (BCD), poly-(D,L-lactide-co-glycolide) (PLGA), and chitosan co-polymer with poly-N-isopropylacrylamide (PNIPAAM). The most effective antimicrobial compound against *Listeria monocytogenes* Scott A was the chitosan-PNIPAAM encapsulated CBE, with a ~2 $\log_{10}$ CFU/g reduction (P<0.05) versus the other treatments when fresh-cut lettuce was stored at both 5°C and 10°C for 15 days. This nanoparticle was compared to a control and free CBE for its effects on the quality of fresh-cut romaine lettuce over a 15 day shelf life at 5°C. The parameters measured to assess the quality of fresh-cut lettuce were: color, texture, moisture content, headspace gases, chlorophyll and carotenoid content, total aerobic plate count, and consumer acceptance. The differences in quality parameters between the control and the treated samples were not significantly different to consider the treatments unacceptable for most quality attributes. Only on the final day of storage, the consumers rated the chitosan-PNIPAAM treated lettuce just below an acceptable

level in terms of appearance and overall product acceptance. The lower scores for the chitosan-PNIPAAM samples were most likely the result of increased moisture from the treatment, rather than a result of the particles themselves. Longer drying times after nanoparticle application would likely improve consumer acceptance of the treated lettuce. The antimicrobial nanoparticles were effective at the concentrations tested, but the antimicrobial and quality impact could be improved by increasing the concentration of nanoparticles applied to the lettuce surface.

7.2 Introduction

Fresh-cut produce has increased in popularity in recent years due to the increasingly busy lifestyles of average consumers. These products provide convenient and ready-to-eat way to include fresh fruits and vegetables in the consumer diet; however, fresh-cut produce is more susceptible to microbial decay and decreased shelf-life (Raybaudi-Massilia and others 2009). Once the leaf tissue is wounded, the respiration rates increase, moisture loss is accelerated, and microorganisms can more easily penetrate the lettuce cell structure to shorten shelf life (Kim and others 2005a). Aside from quality loss issues, fresh-cut lettuce is also more susceptible to pathogen contamination because there is no lethal processing step in fresh-cut produce preparation. Chlorinated water washes, refrigerated storage, and modified atmosphere packaging are the primary methods used for extending fresh-cut produce shelf life (Prakash and others 2000). These methods are not sufficient for protecting against potential contamination by psychrotrophic pathogens, such as *Listeria monocytogenes* (Prakash and others 2000; Harris and others 2003). In fact, a California grower was

141

forced to recall several varieties of fresh-cut lettuce products in 2012 due to contamination by *L. monocytogenes* (USFDA 2012b).

Spice extracts have been found to serve as highly effective inhibitors of foodborne pathogens (Kalemba and Kunicka 2003; Kong and others 2007; Raybaudi-Massilia and others 2009). Cinnamon bark extract (CBE) contains *trans*-cinnamaldehyde, eugenol, and benzoic acid, which all inhibit bacterial growth by various unique mechanisms of action (Burt 2004; Davidson and Taylor 2007). CBE has effectively inhibited the growth of various foodborne pathogens, but its high volatility and extremely low solubility make challenging to deliver to the sites of microbial cells in aqueous media (Hill and others 2013a; Valero and Salmeron 2003; Ayala-Zavala and others 2008).

Nanoencapsulation is a means of protecting the CBE, improving the CBE solubility, and controlling its delivery to pathogen sites. Encapsulation also has the potential to lessen the sensory impact attributed to spice extracts, which have an extremely low flavor threshold (Kalemba and Kunicka 2003). Three nanoencapsulates (BCD, PLGA, and chitosan-PNIPAAM) were tested as antimicrobial delivery systems against free CBE for the inhibition of *Listeria monocytogenes* on fresh-cut romaine lettuce. One of the materials used for encapsulation in this study was a co-polymer of poly-N-isopropylacrylamide (PNIPAAM) and chitosan. PNIPAAM is a thermally-responsive polymer that transitions from hydrophilic to hydrophobic at a lower critical solution temperature (LCST) (Schild 1992). Chitosan is pH-sensitive and is hydrophilic in acidic solutions and hydrophobic in alkaline solutions (Prabaharan 2008). This co-

polymer creates a nanocapsule that responds to temperature and/or pH stimuli with a burst release of antimicrobial material as the polymer contracts (Schild 1992; Lee and others 2004).

BCD was also used to improve the delivery of CBE by forming inclusion complexes with this hydrophobic essential oil. BCD is an enzymatically modified starch molecule that is capable of forming inclusion complexes with hydrophobic molecules (Mourtzinos and others 2008). Cyclodextrins can mask the flavor of CBE while also protecting it against oxidation or heat damage, which allows the CBE to remain effective as an antimicrobial agent under an array of environmental conditions for longer time periods (Hedges and others 1995;Weiss and others 2006). Once the CBE is within the inclusion complexes, their sensory impact on romaine lettuce can be reduced and its water solubility can be increased. This improved aqueous solubility provides increased contact time between the CBE and pathogens to inhibit their growth, making foods safer for human consumption. The final nanocapsule was formed with PLGA, a biocompatible polymer widely used in the pharmaceutical industry to protect active ingredients from harsh environments and improve their delivery and uptake (Weiss and others 2006). PLGA can be used to encapsulate hydrophobic active materials through a relatively simple process, and prevents the sensory impact of the CBE.

The goal of this study was to test the efficacy of BCD, PLGA, and PNIPAAM-Chitosan nanoparticles with entrapped CBE as a way to improve delivery of CBE to foodborne pathogens on fresh cut romaine lettuce while monitoring their effect on produce quality. Many studies have tested natural antimicrobials *in vitro*, but not their

143

performance on the surface of produce. It is extremely important not only to guarantee food safety, but also to maintain the quality of the fresh produce once the antimicrobials are applied, as consumers will reject produce that is adversely affected by the application of antimicrobials.

7.3 Materials & Methods

7.3.1 Materials

N-isopropylacrylamide (NIPAAM) was purchased from TCI America (Portland, OR). Poly(vinyl alcohol) (PVA) (87%, M_w 30-70 kDa), chitosan (M_w 190-310 kDa, 75-85% deacetylated chitin, viscosity $\leq$ 30 mPa.s), sodium alginate M_w 120-190 kDa, mannuronate/gluronate (M/G) ratio = 1.56), N,N-methylene-bisacrylamide (MBA), glutaraldehyde (25%), and cinnamon bark extract (CBE) (99%) were purchased from Sigma Aldrich Co. (St. Louis, MO). N,N,N',N'-tetramethyl-ethylenediamine (TEMED) was purchased from Alfa Aesar (Ward Hill, MA). Ammonium persulfate was purchased from BDH Chemicals (London, England). Whole heads of organic romaine lettuce was purchased from the local supermarket in College Station, Texas. All other reagents were of analytical grade.

7.3.2 Nanoparticle Synthesis

Beta-cyclodextrin (BCD) Particles

The inclusion complexes containing cinnamon bark extract were prepared via the freeze-drying method (Karathanos and others 2007). BCD and cinnamon bark extract were mixed in an aqueous solution in a 1:1 molecular ratio at concentrations of 16 mM each. The mixture was magnetically stirred in a sealed container for 24 h at room

temperature (25°C) to allow for complex formation and prevent loss of volatiles to the atmosphere. After mixing, the solution was frozen and lyophilized at -50°C and 7.5 μmHg in a Labconco Freeze Dryer-5 (Kansas City, MO) for approximately 48 h or until all moisture had been sublimated. Calculations for mixing the 1:1 molecular aqueous solutions were based upon the concentrations of active compound present (*trans*-cinnamaldehyde). The dried particles were collected and stored in a dessicator at -20°C until needed for analysis for no more than one month.

Poly(D,L-lactide-co-glycolide) (PLGA) Particles

      Nanoparticles were formed using the emulsion evaporation method similar to the method outlined by Gomes and others (2011). First, the organic phase was created by dissolving 50 mg of poly-(D,L-lactide-co-glycolide) (PLGA) into 2 mL dichloromethane along with 16% (w/w) cinnamon bark extract relative to PLGA. The organic phase was added drop-wise to 20 mL of aqueous 0.5% (w/w) polyvinyl alcohol (PVA) solution in nanopure water. This mixture was emulsified for 2 minutes at 9500 rpm using an Ultra-Turrax T25 basic Ika (Works, Inc., Wilmington, NC). The emulsion was sonicated in an ice bath for 30 minutes at 70 W (Cole Parmer sonicator 8890, Vernon Hill, IL), before removing the dichloromethane using a rotoevaporator (Buchi R-210 Rotavapor, Buchi Co., New Castle, DE) for 20 minutes under vacuum (0.97 psi). Once synthesized, the nanoparticles were purified by ultrafiltration to remove excess PVA and non-encapsulated cinnamon bark extract. A Millipore-Labscale[TM] TFF system fitted with a 50 kDa molecular weight cutoff Pellicon XL-Millipore (Millipore Co., Kankakee, IL) was used. The nanoparticles were ultrafiltered with 200 mL of water and 50 mL of the

retentate was collected. Inlet pressure was 25 psi and outlet pressure in the system was

5-10 psi. After ultrafiltration, nanoparticles were kept at -20°C overnight then

lyophilized at -50°C and 1.45 x 10^{-4} psi vacuum for 24 hours in a Labconco Freeze Dry-

5 unit (Labconco, Kansas City, MO). D(+)-trehalose was added to the nanoparticle

solution prior to freezing to act as a cryoprotectant at a 1:1 ratio relative to the PLGA.

The dried particles were collected and stored in a dessicator at -20°C until needed for

analysis. Particles were not stored for more than one month before they were used for

analysis.

PNIPAAM-co-chitosan Particles

      Chitosan-PNIPAAM polymer was synthesized using a semi-IPN

(Interpenetrating Polymer Network) method similar to the method described by Lee and

others (2004) and Lee and Chen (2001). Briefly, a 1M solution of NIPAAM was mixed

with 3% w/w chitosan in 1% w/w acetic acid until the chitosan had completely

dissolved. Next, 3% mol MBA (based on total monomers) was added to the solution

followed by 1% w/w APS and TEMED. This solution was poured into a shallow glass

dish and allowed to polymerize at 5°C for 24 hours without agitation. The crosslinked

hydrogel was soaked in distilled water for 24 hours, replacing the water with fresh water

every 4-5 hours to remove any unreacted monomer. Following this purification process,

the polymer was dried in a vacuum oven (Squared Lab Line Instruments, Melrose Park,

Ill., U.S.A.) at room temperature and a pressure ≤ 13.3 kPa for 24 hours. Dried polymer

was stored at -20°C until needed for particle synthesis.

To form nanoparticles, 1.5 mg/mL of dried PNIPAAM-co-polymer was suspended in 150 mL of 0.5% w/v aqueous PVA solution with cinnamon bark extract and allowed to hydrate overnight. Following polymer hydration, the solution was homogenized using an Ultra-Turrax T25 basic Ika (Works, Inc., Wilmington, NC) at 9500 rpm for 7 minutes to break the polymer into smaller particles. Once the solutions were homogenized, they were placed in a shaking water bath (VWR International, Radnor, PA) at 40°C and 150 rpm for 24 hours to allow self-assembly into micelles. The micelles were then crosslinked with glutaraldehyde, at a 2:1 molar ratio of glutaraldehyde to PNIPAAM, to stabilize the particles. The finished particles were then purified via ultrafiltration similarly to the PLGA synthesis procedure to remove excess reactants, and lyophilized at -50°C and 1.45×10^{-4} psi vacuum for 24 hours in a Labconco Freeze Dry-5 unit (Labconco, Kansas City, MO). Dried nanoparticles were stored at -20°C until they were needed for analysis for no more than one month.

7.3.3 Challenge Study

<u>Bacterial Cultures</u>

Listeria monocytogenes strain Scott A was obtained from Texas A&M University Food Microbiology Laboratory (College Station, TX). This pathogen was chosen because it was found to be more resistant to inhibition by cinnamon bark extract in previous studies (Hill and others 2013a). Its behavior can be used to predict the "worst case scenario" for microbial contamination. *L. monocytogenes* was resuscitated in tryptose phosphate broth (TPB) (Becton, Dickinson and Co., Sparks, MD), by two identical consecutive transfers and incubating for 24 hours aerobically at 35°C. The

bacterial cultures were maintained on tryptic soy agar (TSA) slants stored at 4°C for no more than 3 months. Transfers from slants were conducted similarly to the resuscitation method to prepare microorganisms for analysis.

<u>Inoculation and Lettuce Preparation</u>

Whole heads of organic romaine lettuce were purchased from the local supermarket and kept refrigerated (4°C) until needed (within 24 hours). The advertised sell by date was 14 days after packaging. All leaves showing signs of decay, cuts, or bruises were removed and discarded along with the basal portion of the head. Whole leaves were washed in 200 ppm chlorine for 5 minutes, followed by rinsing in sterile distilled water for 1 minute. Leaves were then spun dry in a kitchen centrifuge (OXO Intl., New York, NY, USA) for 2 minutes. Whole leaves were inoculated with *L. monocytogenes* culture in order to minimize bacterial internalization. The bacteria were diluted in sterile 0.1% peptone to achieve an inoculum of approximately 7 $\log_{10}$ CFU/mL. Lettuce leaves were submerged in the culture for 10 minutes, then placed on a metal drying rack inside a biosafety cabinet to air dry for 30 minutes to allow time for bacterial attachment onto the leaves. After 30 minutes, the leaves were spun dry in the kitchen centrifuge for 5 minutes. The inoculated leaves were aseptically cut into 4 cm^2 pieces, using a square stainless steel cookie cutter (Wilton Brands, Woodridge, IL, U.S.A.) and placed on metal drying racks to be treated with antimicrobial solutions within 1 hour of their preparation.

<u>Treatment Application</u>

Free CBE, CBE entrapped in beta-cyclodextrin, PLGA encapsulated CBE, and CBE encapsulated in PNIPAAM-co-chitosan nanoparticles were sprayed onto the cut lettuce pieces (approximately 1 mL/leaf). The nanoparticles were suspended in water at a predetermined concentration for each particle: 400 µg/mL for CBE, 2,500 µg/mL for BCD, 20,000 µg/mL for PLGA, and 20,000 µg/mL for chitosan-PNIPAAM. The concentrations of each treatment applied to the leaves were determined by their minimum inhibitory concentration against *Listeria monocytogenes* found by an *in vitro* assay in liquid media previously studied (Hill and others 2013a; Hill and others 2013b). Inoculated, untreated leaves were used as a positive control and non-inoculated, untreated leaves as a negative control. The leaves were uniformly sprayed on one side, dried for 15 minutes in a biological safety cabinet, and then sprayed on the opposite side. Treated leaves were weighed into 10 g samples and placed in sterile stomacher bags (18 oz Whirl Pak® bags, Nasco Inc., Atlanta, GA, U.S.A.). Three samples for each temperature, treatment, and sample time point were stored at 5°C and 10°C for 15 days and analyzed immediately after preparation, and at 2h, 8h, 24h, 3 days, 5 days, 7 days, and 15 days. These temperatures were used to mimic ideal and slightly abusive storage conditions, respectively.

<u>Sample Analysis and Bacteria Enumeration</u>

At each sample time, stomacher bags were removed from storage and diluted with 90 mL of sterile 0.1% w/v peptone before stomaching at 230 rpm for 1 minute. Blended samples were serially diluted using 0.1% w/v peptone and spread plated onto

PALCAM agar (selective medium for *Listeria* spp.) to enumerate the level of bacterial contamination present with or without antimicrobial treatment. To enumerate background microflora, negative controls were spread plated onto TSA. Plates were incubated for 48 hours at 35°C before counting the colony growth. This experiment was completed in triplicate and all replicate samples were plated in duplicate.

7.3.4 Shelf Life Study

<u>Produce Preparation</u>

The lettuce samples (10g) were prepared identically to those used in the challenge study, except without the pathogen inoculation step and stored at 5°C in sterile stomacher bags (18 oz Whirl Pak® bags, Nasco Inc., Atlanta, GA, U.S.A.) before being analyzed on the day of sample preparation, and then after 5, 10, and 15 days of storage. Only the PNIPAAM-chitosan nanoparticles and free CBE were applied to the lettuce leaves for the shelf life study. The PNIPAAM-chitosan nanoparticles were used because they were the most effective treatment in the challenge study and free CBE was tested as a positive control.

<u>Moisture Content</u>

Samples were dried at 60-65C in a vacuum oven (<13.3 kPa) (Squared Lab Line Instruments, Melrose Park, IL, USA) for 12-14 hours, until constant weights were achieved, following AOAC method 930.04 (Helrich 1990). Each sample consisted of approximately 2 g of lettuce (control or treatment) placed in an aluminum pan.

<u>Color</u>

The color changes were evaluated using a Labscan XE (16437) colorimeter (HunterLab, Inc., Reston, VA, USA) with the Universal Version 3.73 software (HunterLab, Inc., Reston, VA, USA). The measuring aperture was 36 mm and D65/10 was the illuminant/viewing geometry. Standard white and black plates were used to calibrate the colorimeter before measurements were taken. Five leaves were measured for each treatment at each time point and the mean values were calculated to determine the color coordinates according to the CIELAB system. These coordinates are L^* (lightness), a^* (red-green intensity), and b^* (yellow-blue intensity). The leaf color was quantified on the three-dimensional standard color space.

<u>Headspace Analysis</u>

Hermetically sealed jars (236.59 mL, Ball Mason Jars, Broomfield, CO, USA) were used to measure changes in headspace gases throughout the shelf life study at 5°C. Small holes were drilled in the metal lids and sealed with a rubber stopper that the needle of the analyzer could pass through without creating a leak in the container. The rubber stoppers were sealed with silicon sealant to ensure a hermetically sealed container. Lettuce pieces were weighed in 5 g samples and placed into the glass jars and sealed for the entire storage study (without loss of any gases to the atmosphere). On the day of sample preparation (Day 0), the jars were allowed to equilibrate for 2 hours before taking headspace measurements. Subsequent measurements were taken at storage days 5, 10, and 15 using a MOCON headspace analyzer (Model 650, Dual Headspace

Analyzer, Minneapolis, MN, USA). Measurements were carried out at room temperature (Mantilla and others 2012).

Texture Analysis

Leaf firmness was measured using a Kramer Shear Press with 5 blades (TA-91) attached to a TA-XT2 Texture Analyzer (Texture Technologies Corporation, Scarsdale, NY). This probe is frequently used to quantify the firmness of leafy vegetables, which require a low magnitude force to cut through (Han and others 2004; Gomes and others 2008). Ten cut leaf samples were stacked on the sample holder with the veins perpendicular to the blades (internal dimensions 82 x 63 x 89 mm^3) and the 5 flat-plate plunger (1.5 mm blade width) was forced through the leaves. The blades were adjusted to a height 65 mm above the base of the five flat-plate plunger and moved at a rate of 1 mm/s. The maximum force (N) and work (J) until shear were recorded by Texture Expert software, version 2.55 (Texture Technologies Corporation, Scarsdale, NY). Five measurements were taken for each treatment at each storage time point.

Chlorophyll and Carotenoid Contents

Chlorophyll and carotenoid contents were extracted and quantified according to a procedure outlined by Lichtenthaler (1987). Briefly, lettuce samples were frozen at −20°C then lyophilized for 24 hours (Labconco Freeze Dry-5, Labconco, St. Louis, MO). Freeze dried leaves were crushed, and then 100 mg of sample was suspended in 10 mL of 80% acetone (v/v) and protected from light while the extraction took place for 24 hours. Extracts were filtered and the volumes increased to 25 mL with more 80% acetone. These solutions were analyzed spectrophotometrically (Thermo Fisher

Scientific Genesys 10S UV-Vis Spectrophotometer, Waltham, MA) at 470nm, 646.8nm, and 663.2nm in a 1 cm path length cuvette. Absorbance values were used to calculate the level of carotenoids and chlorophylls present according to the equations provided by Lichtenthaler (1987). Values were expressed in terms of percentage of lettuce dry weight.

<u>Total Aerobic Plate Count</u>

The total aerobic plate counts were measured in triplicate, on days 0, 5, 10, and 15. Samples from each treatment weighing 10g were placed in sterile stomacher bags with 90 mL of 0.1% peptone and pummeled at 230 rpm for 60 seconds. Blended samples were serially diluted and enumerated on petrifilms (3M aerobic plate count, St. Paul, MN). Petrifilms were incubated for 48 hours at 35°C before counting the colony growth. Results were reported as CFU/g of lettuce (AOAC 1990).

<u>Sensory Analysis</u>

Panelists were recruited from Texas A&M University campus (n=50), consisting of staff, undergraduate, and graduate students, to participate in a consumer panel. Each panelist was instructed to visually examine each sample for color, appearance, aroma, and overall quality and rate each attribute on a 9-point hedonic scale, where 1=dislike extremely and 9=like extremely. New samples were examined on days 1, 5, and 13 to give an idea of the lettuce quality over the course of its typical shelf life. A mean score of 5 or greater was considered acceptable for each sample attribute. Samples of approximately 10 g were placed in sealed plastic containers (Ziploc brand with Smart

Snap Seal, 591 mL) labeled with random 3 digit sample codes and presented to panelists (3 samples total) on each day (Carr and others 1999).

7.3.5 Statistical Analysis

All determinations were made in triplicate as independent experiments. The experiment was based on a completely randomized design with equal replications. All statistical analyses were performed using JMP v. 9 Software (SAS Institute, Cary, NC). Differences between variables were tested for significance using one-way analysis of variance (ANOVA) and significantly different means ($p<0.05$) were separated using Tukey's Honestly Significant Differences (HSD) test.

7.4 Results & Discussion

7.4.3 Challenge Study

The purpose of a challenge study was to test how a new antimicrobial technology functions in the environment where it would be applied, in this case fresh-cut romaine lettuce. In order to test the most adverse conditions for the nanoparticles, *Listeria monocytogenes* was used as the test organism because it was less susceptible to inhibition by cinnamon bark extract and nanoparticles containing CBE in preliminary studies than gram-negative bacteria (Hill and others 2013a). Three different types of nanoparticles were tested, as well as free CBE to compare their abilities to inhibit *L. monocytogenes* on the surface of cut romaine lettuce at ideal storage temperature (5°C) and slightly abusive storage temperature (10°C). The survival of the microorganism on fresh-cut romaine lettuce over the course of 15 days is shown in Figures 7.1 and 7.2. Pathogen growth was higher on the lettuce stored at 10°C than at 5°C because the higher

154

temperature is more suitable for bacterial growth (Oliveira and others 2010). It is recommended that most fresh produce be stored at 5°C or lower because microorganisms exhibit slower growth rates at these cooler storage temperatures; however, in practice this is not always the case (Oliveira and others 2010). Refrigeration temperatures are not sufficient to kill the pathogens or force them into dormancy.

The PNIPAAM-chitosan nanoparticles were the most effective treatment (P<0.05) for inhibiting microbial growth at both temperatures, followed by the BCD-CBE particles, then the free CBE, and finally the PLGA-CBE particles. There was a larger difference in efficacy between the BCD-CBE and the free CBE or PLGA-CBE at 5°C than at 10°C, where all three of these treatments yielded similar levels of log reductions (approximately 1 log) by the end of storage due to similar levels of entrapped CBE and release profiles. The antimicrobials were more readily released from the nanocapsules at the higher temperature (10°C), but the bacteria were also able to grow at a faster rate. However, this increased release is accompanied by an increased level of volatilization of the CBE for both the free CBE and the CBE release from BCD.

The higher effectiveness of PNIPAAM-chitosan nanoparticles is likely because chitosan also has some antimicrobial capabilities, which improved the inhibition of the pathogen growth (Rabea and others 2003). During previous *in vitro* antimicrobial assay experiments, the control chitosan-PNIPAAM nanoparticles did not present inhibitory activity; however, the bacteria in contact with these particles exhibited lower levels of growth than either of the bacteria growth controls (*Listeria monocytogenes* and *Salmonella enterica* serovar Typhimurium). All of the treatments showed an initially lower ($P<0.05$) microbial load on the lettuce than the untreated control, demonstrating their antimicrobial activities, but not all treatments were able to maintain this differential. This early behavior is likely due to the burst release of antimicrobial material from nanoparticles seen in preliminary *in vitro* release studies, but as time passes the CBE volatilizes and the bacteria that were only inhibited, not killed, were able to recover as the release slows and stabilizes.

Figure 7.1. Survival of *Listeria monocytogenes* on fresh-cut romaine lettuce stored at 5°C for 15 days. Lettuce was sprayed with cinnamon bark extract (CBE), PNIPAAM-chitosan with entrapped CBE (Chito-CBE), CBE encapsulated in poly-(D,L-lactide-co-glycolide) (PLGA-CBE), and CBE beta-cyclodextrin inclusion complexes (BCD-CBE).
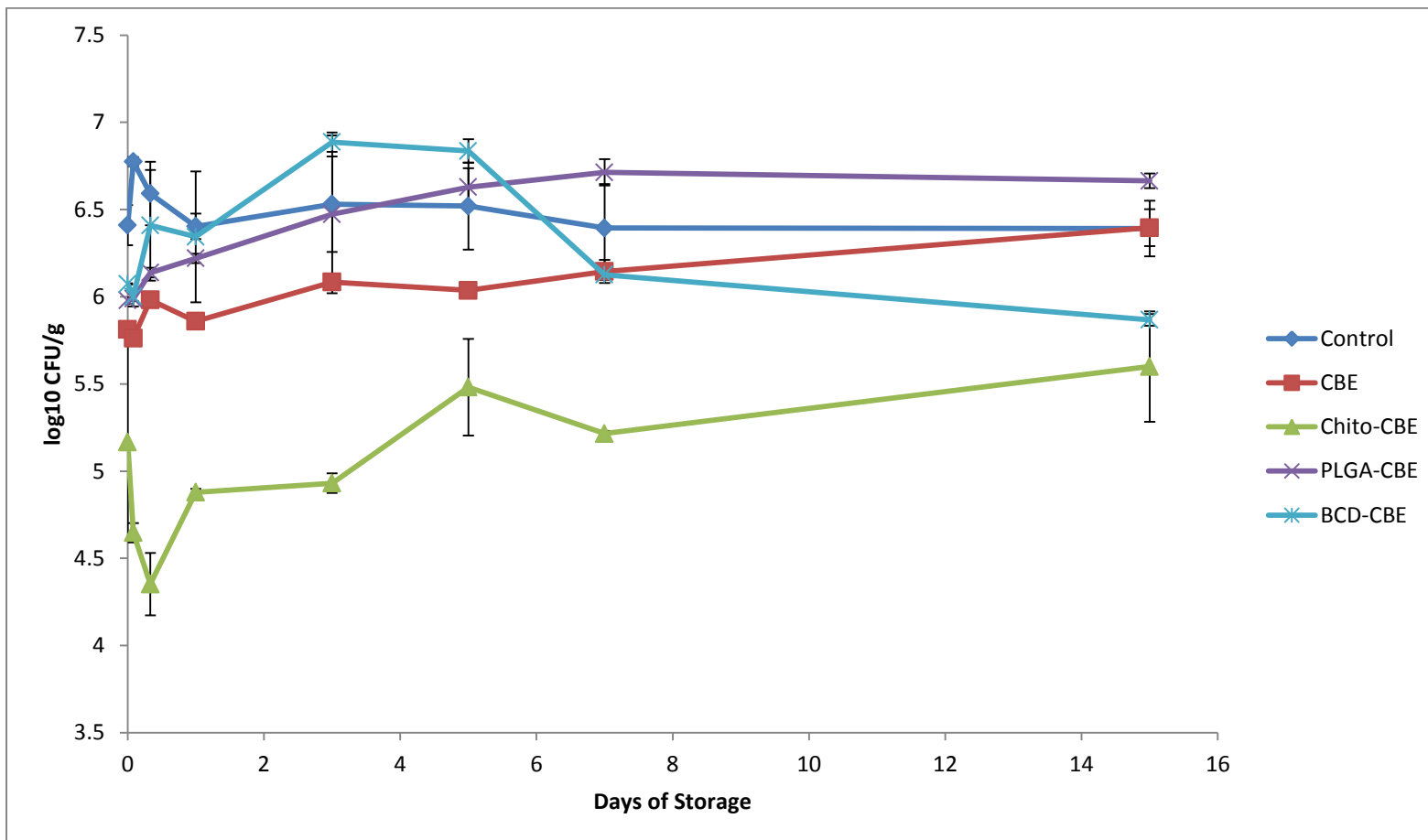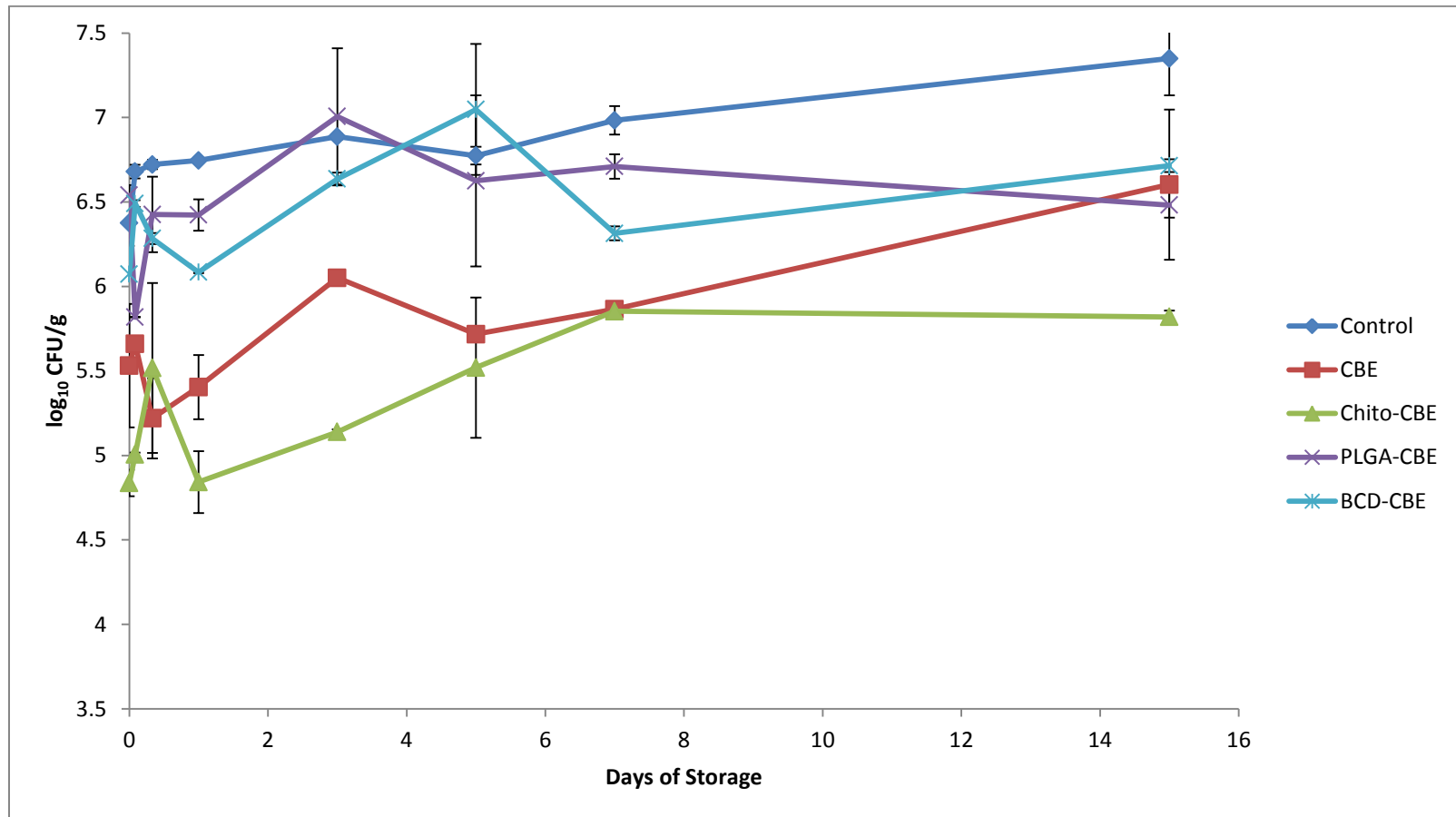
Figure 7.2. Survival of *Listeria monocytogenes* on fresh-cut romaine lettuce stored at 10°C for 15 days. Lettuce was sprayed with cinnamon bark extract (CBE), chitosan-PNIPAAM with entrapped CBE (Chito-CBE), CBE encapsulated in poly-(D,L-lactide-co-glycolide) (PLGA-CBE), and CBE beta-cyclodextrin inclusion complexes (BCD-CBE).

The dosage levels of the nanoparticle and CBE treatments were kept low (at the minimum inhibitory concentration (MIC)) to mimic realistic application levels that could be used in industry without negatively impacting the organoleptic properties of the fresh-cut lettuce. The MIC values for each particle treatment detailed previously were accounting for the entire particle weights. The concentration of active CBE present in each particle (166 µg/mL for BCD, 299.23 µg/mL for PLGA, 461.06 µg/mL for chitosan-PNIPAAM) varies based on synthesis procedures and type of encapsulate material. The amount of CBE present in each of the nanoparticles was lower than the amount of free CBE used. The particles also exhibit slightly different release profiles, that govern how quickly or slowly all of the CBE is released onto the lettuce. At higher concentrations, the reduction in the bacteria population would likely be more dramatic as seen in previous studies (Gomes and others 2011a); however, it would be detrimental to lettuce quality parameters. The free CBE was most effective at the beginning of storage, where it showed a 2 $\log_{10}$ reduction in *Listeria* growth, but then its high volatility (vapor pressure 2.7 Pa at 20°C) allowed it to evaporate over time, and allow more bacterial growth, so that there was only a 1 $\log_{10}$ reduction compared to the control by the end of storage. The PLGA-CBE showed a similar trend, but only exhibited a 1 $\log_{10}$ growth reduction because it tends to release most of the CBE within 24 hours. Since the PLGA nanocapsules had a lower MIC (for active CBE entrapped), there is less CBE initially present than the free CBE, which explains the rise in the bacterial load above the level seen in the free CBE treated lettuce. The BCD-CBE actually became more effective (P<0.05) at inhibiting the bacteria over time, with the bacteria populations dropping

159

approximately 1 $\log_{10}$ compared with the control after 5 days for both storage temperatures. The BCD releases CBE based on an equilibrium with the environment rather than due to diffusion, so it can continue to release more CBE as more of it interacts with the microorganisms or evaporates from the surface of the leaves and the relative humidity within the package increases (Higuchi and Connors 1965; Ayala-Zavala and others 2008). The PNIPAAM-chitosan-CBE nanocapsules were able to maintain a relatively consistent level of bacterial inhibition (approximately 2 $\log_{10}$ reduction) over the entire storage time. At higher concentrations, the PNIPAAM-chitosan-CBE particles and BCD particles could improve the safety of fresh-cut produce while creating little or no quality changes on the fresh-cut lettuce products. The visual appearance of the lettuce samples for all treatments became less appealing over storage, with visible decay and browning occurring more rapidly in samples stored at 10°C than 5°C (Figure 7.3).
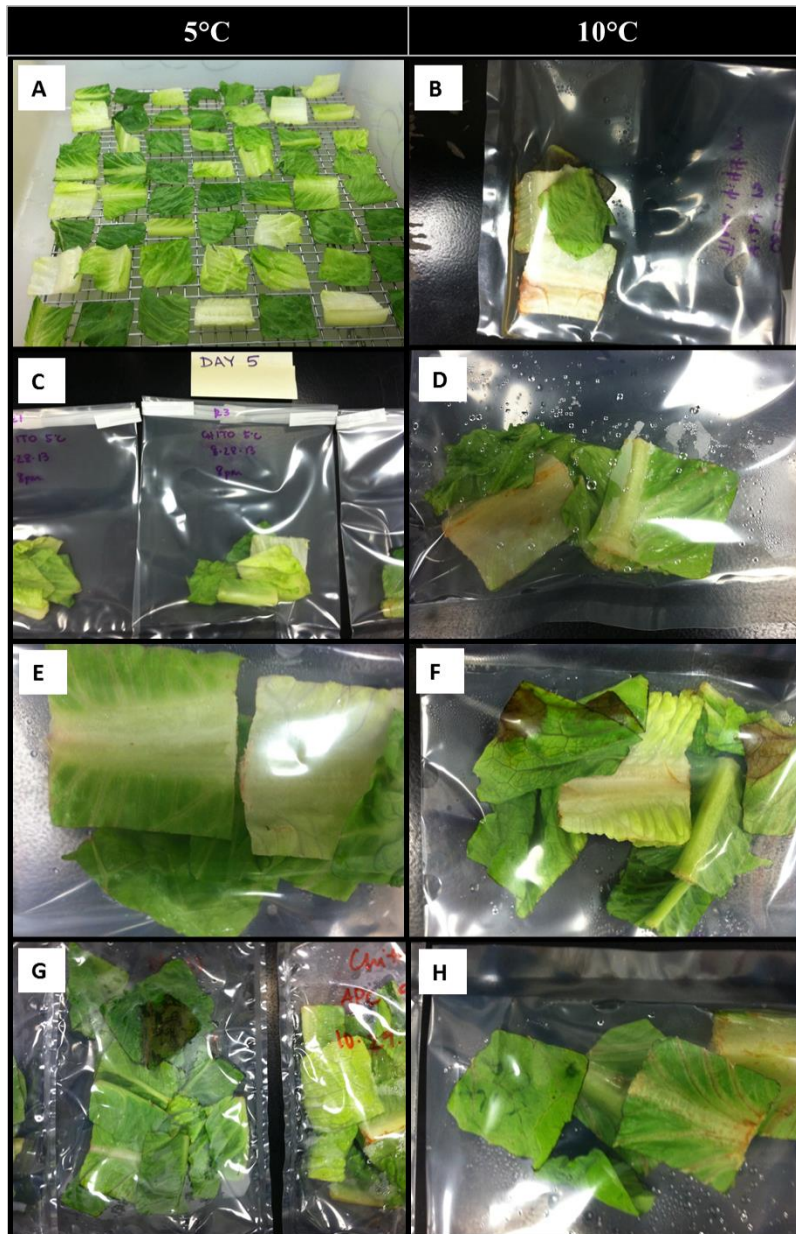
Figure 7.3. Fresh-cut romaine lettuce inoculated with *Listeria monocytogenes* Scott A stored at 5°C and 10°C for 15 days. A- control 0 days storage; B- treated with cinnamon bark extract (CBE), stored at 10°C for 15days; C- treated with Chitosan-PNIPAAM-CBE (Chito-CBE), stored at 5°C for 5days; D- treated with BCD, stored at 10°C for 15days; E- treated with BCD, stored at 5°C for 15days; F- treated with poly-(D,L-lactide-co-glycolide) (PLGA), stored at 10°C for 15days; G- treated with Chito-CBE, stored at 5°C for 15days; H- treated with Chito-CBE, stored at 10°C for 7days.

7.4.4 Shelf Life Study

<u>Moisture Content</u>

The moisture content of the lettuce leaves (Table 7.1) decreased (P>0.05) throughout the storage time of the study for all treatments, as water migrated from the leaves into the packaging. The moisture content was not significantly different among treatments, nor was it significantly lower on the last day of storage from the time of sample preparation. These findings were not surprising, as the antimicrobial treatments do not provide any type of physical barrier to prevent moisture loss. The moisture content measured on day 0 was typical for romaine lettuce, which possesses an average moisture content of approximately 94% according to the USDA nutrient database (USDA 2013).

Table 7.1. Moisture content (wet basis) of fresh-cut romaine lettuce controls and lettuce treated with cinnamon bark extract (CBE) and chitosan-PNIPAAM nanoparticles (chito-CBE) over 15 days of storage at 5°C.

Treatment/Day	% Moisture			
	0	**5**	**10**	**15**
Control	$_w93.96^a$ (5.15)	$_w91.30^a$ (3.43)	$_w88.19^a$ (6.18)	$_w84.15^a$ (6.05)
CBE	$_w93.90^a$ (4.24)	$_w92.27^a$ (0.70)	$_w87.29^a$ (3.84)	$_w88.91^a$ (2.58)
Chito-CBE	$_w90.36^a$ (0.48)	$_w87.27^a$ (6.87)	$_w86.32^a$ (6.72)	$_w81.61^a$ (6.36)

[a]Means within a column that are not followed by a common superscript letter are significantly different (p<0.05).
[w]Means within a row that are not preceded by a common subscript letter are significantly different (p<0.05).

<u>Color</u>

The color of the leaves did change over time, but only the a* parameter (red-green intensity) of the control changed significantly (P<0.05) with time (Table 7.2). The a* values increased (P<0.05) over the course of the shelf life study, indicating a decrease in green intensity, which occurs upon the degradation of chlorophyll (Bolin and Huxsoll 1991).This change indicates that the chitosan-PNIPAAM nanoparticles and CBE did help protect the leaves from color change compared with the control. The L* values (lightness) decreased for most treatments over time, but none significantly, indicating the leaves became slightly darker with longer storage times which can occur as microbial spoilage progresses or moisture content decreases (Prakash and others 2000). Significant differences in color attributes among treatments within the same day can be attributed to the heterogeneous nature of romaine lettuce color from leaf to leaf, as samples tended to follow the same trend in color changes (Bolin and Huxsoll 1991). The b* parameter (blue-yellow intensity) did not vary significantly throughout storage. Overall, color was not significantly affected (P>0.05) by the application of antimicrobial treatments.

Table 7.2. CIELAB L*a*b* color parameters of fresh-cut romaine lettuce controls and lettuce treated with cinnamon bark extract (CBE) and chitosan-PNIPAAM nanoparticles (Chito-CBE) over 15 days of storage at 5°C.

Treatment/Day	L^*			
	0	5	10	15
Control	$_w33.28^a$ (1.16)	$_w32.26^a$ (1.52)	$_w31.49^a$ (1.59)	$_w32.38^a$ (1.78)
CBE	$_w32.46^a$ (2.01)	$_w32.10^a$ (2.70)	$_w31.91^a$ (3.47)	$_w32.00^a$ (3.70)
Chito-CBE	$_w29.23^b$ (1.10)	$_w29.66^a$ (1.43)	$_w29.43^a$ (1.52)	$_w29.41^a$ (1.72)
	a^*			
Control	$_z-7.07^b$ (0.09)	$_z-7.01^b$ (0.20)	$_z-6.93^b$ (0.14)	$_w-6.50^a$ (0.19)
CBE	$_w-6.67^{ab}$ (0.26)	$_w-6.43^{ab}$ (0.40)	$_w-6.36^{ab}$ (0.45)	$_w-6.33^a$ (0.52)
Chito-CBE	$_w-6.28^a$ (0.35)	$_w-6.11^a$ (0.47)	$_w-5.99^a$ (0.41)	$_w-5.99^a$ (0.37)
	b^*			
Control	$_w13.11^a$ (0.34)	$_w12.96^a$ (0.47)	$_w13.12^a$ (0.64)	$_w12.22^a$ (0.84)
CBE	$_w12.77^a$ (1.37)	$_w12.12^{ab}$ (1.71)	$_w12.11^{ab}$ (1.96)	$_w12.19^a$ (2.19)
Chito-CBE	$_w10.99^b$ (0.76)	$_w10.74^b$ (1.00)	$_w10.57^b$ (0.97)	$_w10.66^a$ (0.95)

[a]Means within a column that are not followed by a common superscript letter are significantly different ($p < 0.05$).

[w]Means within a row that are not preceded by a common subscript letter are significantly different ($p < 0.05$).

Headspace Analysis

As respiration occurs throughout storage life, typically the percentage of CO_2 increases, while the percentage of O_2 decreases. It was hoped that the CBE and nanoparticle treatments would slow down the respiration rates of the leaves, thus improving their quality during storage and potentially extending their shelf life; however, differences in headspace gases were only significant on the first day of storage, with the chitosan-PNIPAAM nanoparticles showing the lowest ($P<0.05$) level of CO_2 and the highest level of O_2 present in the headspace (Table 7.3). Subsequently, all samples behaved similarly with steadily increasing concentrations of CO_2 gases throughout storage. Several other studies on quality changes in fresh-cut romaine lettuce noted similar trends of increasing concentrations of CO_2 as shelf-life progressed (Prakash and others 2000; Kim and others 2005a; Oliveira and others 2010). Increasing levels of CO_2 and decreasing concentrations of O_2 tend to intensify browning on cut leaf surfaces (Prakash and others 2000). Extensive browning on the samples was observed by the end of the storage study, which tends to lead to lower consumer acceptance of lettuce products. Although the respiration rate was not measured directly, the similar trends in changing headspace composition among the treatments and the control samples indicate the respiration rates were similar for all samples. The application of the antimicrobial treatments did not make a significant impact ($P>0.05$) on the quality of the lettuce with respect to the gas atmosphere composition within the packages throughout storage.

Table 7.3. Headspace gas measurements over 15 days of storage at 5°C for fresh-cut romaine lettuce controls and lettuce treated with cinnamon bark extract (CBE) and chitosan-PNIPAAM (Chito-CBE) nanoparticles.

Treatment/Day	%CO$_2$			
	0	**5**	**10**	**15**
Control	$_z0.48^a$ (0.05)	$_y2.08^b$ (0.25)	$_x3.28^a$ (0.25)	$_w3.73^a$ (0.19)
CBE	$_z0.50^a$ (0.08)	$_y2.13^b$ (0.17)	$_x3.05^a$ (0.40)	$_w4.00^a$ (0.70)
Chito-CBE	$_z0.10^b$ (0.00)	$_w3.13^a$ (0.62)	$_w3.98^a$ (1.13)	$_w4.35^a$ (1.53)
	%O$_2$			
Control	$_w20.20^b$ (0.08)	$_x18.48^a$ (0.19)	$_y17.28^a$ (0.26)	$_z16.65^a$ (0.24)
CBE	$_w19.98^c$ (0.10)	$_x18.45^a$ (0.17)	$_y17.38^a$ (0.50)	$_z16.15^a$ (0.68)
Chito-CBE	$_w20.85^a$ (0.06)	$_z17.58^a$ (0.80)	$_z16.63^a$ (1.47)	$_z15.95^a$ (2.05)

[a]Means within a column that are not followed by a common superscript letter are significantly different (p<0.05).
[w]Means within a row that are not preceded by a common subscript letter are significantly different (p<0.05).

Texture Analysis

The force and work required to shear the lettuce leaves (Figures 7.4 and 7.5) increased (P<0.05) over the course of the storage time for both treated samples but not for the control. The damage to the leaf tissue caused by cutting the lettuce for sample preparation can cause the uninjured cells to produce lignin and suberin to prevent water loss, which would increase the force and work needed to shear the leaves (Rittinger and others 1987; Jacobsson and others 2004). Typically, as leaves are stored, the force

166

required to cut them decreases. The force and work required to shear the control and CBE samples did not differ (P>0.05) throughout the entire storage, with the exception of the first day of the study when samples were initially prepared. The force required to cut through the chitosan-PNIPAAM treated leaves was significantly higher (P<0.05) than the control and CBE-treated samples on all storage days after the initial sample preparation day. This suggests that the chitosan-PNIPAAM nanoparticles did help minimize microbial decay initially, which can contribute to overall tissue softening (Devlieghere and others 2004; Baur and others 2005). Aside from antimicrobial effects, other studies found chitosan improved the texture of fresh cut lettuce and berries by providing structural reinforcement (Ghaouth and others 1991; Devlieghere and others 2004). The same trend was noted for the work required to cut through the lettuce samples.
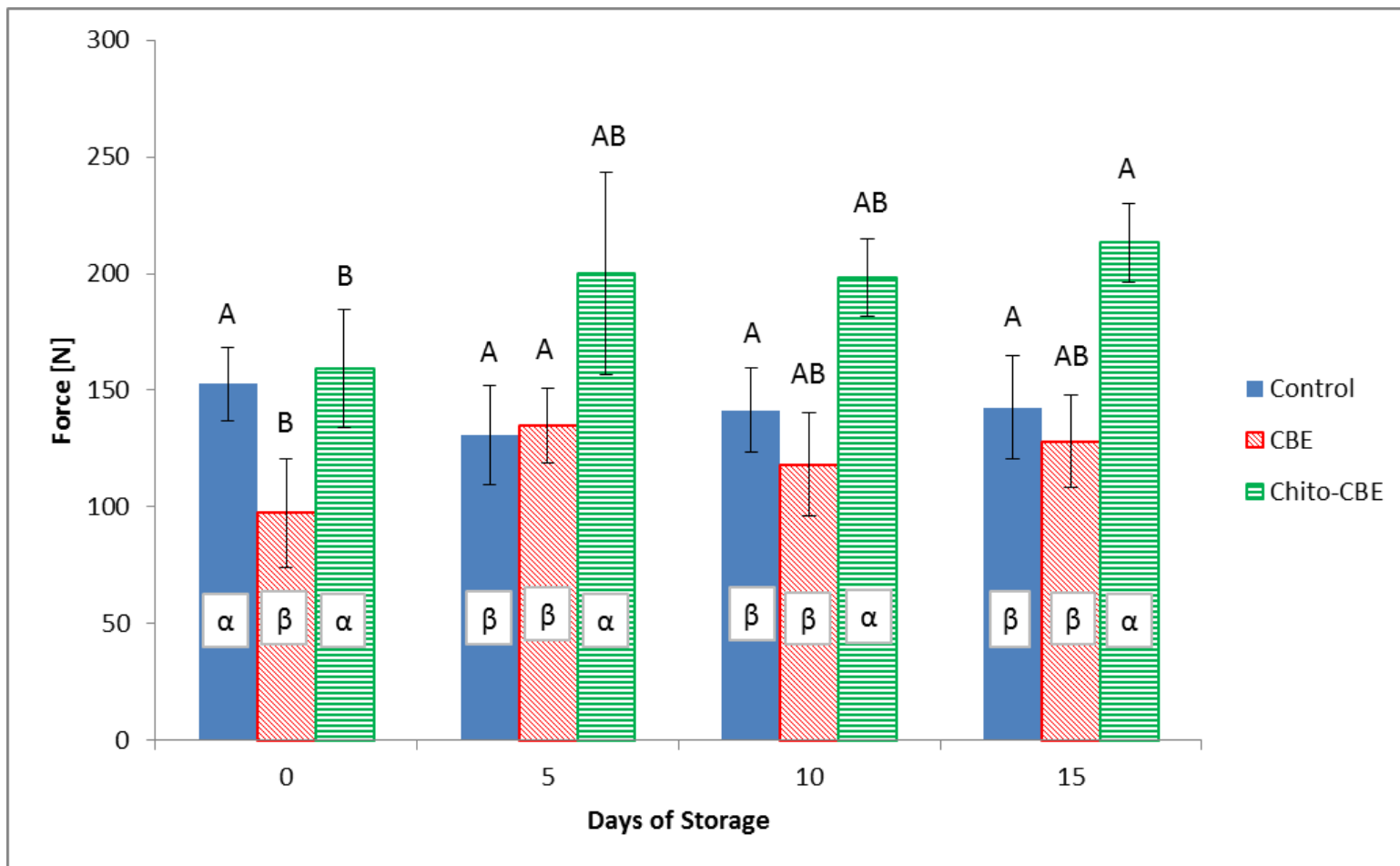
Figure 7.4. Total force required to cut through fresh-cut romaine lettuce controls and lettuce treated with cinnamon bark extract (CBE) and chitosan-PNIPAAM (Chito-CBE) nanoparticles over 15 days of storage at 5°C. [A]Columns within the same treatment that do not have a common letter above them are significantly different (p<0.05). [α]Columns within the same storage day that do not contain a common Greek letter are significantly different (p<0.05).

168

Figure 7.5. Total work required to cut through fresh-cut romaine lettuce controls and lettuce treated with cinnamon bark extract (CBE) and chitosan-PNIPAAM (Chito-CBE) nanoparticles over 15 days of storage at 5°C. [A]Columns within the same treatment that do not have a common letter above them are significantly different (p<0.05). [α]Columns within the same storage day that do not contain a common Greek letter are significantly different (p<0.05).

169

<u>Chlorophyll and Carotenoid Contents</u>

The level of chlorophyll and carotenoids was on the same order of magnitude to those previously reported (Fontes and others 1997; Kim and others 2007; Martín-Diana and others 2008) and decreased ($P<0.05$) throughout storage for all samples (Figure 7.6 and 7.7). The control samples showed the most significant decrease for both chlorophylls and carotenoids by the last day of storage, while the CBE samples remained the most stable, and the chitosan-PNIPAAM samples decreased ($P<0.05$) by a smaller amount than the controls. This trend of decreasing chlorophyll values was confirmed by the results of the color analysis, which showed decreasing a* values (indicating decreasing in green color). Overall, the treatments did not negatively impact or accelerate the natural degradation trend of the chlorophyll and carotenoid compounds. The different initial levels of these compounds among treatments can be attributed to the natural variation among romaine lettuce leaves, as they range in green intensity (which is a result of chlorophyll content) and carotenoid content. The breakdown of chlorophyll leads to the yellowing of leaves, which is an important quality indicator in leafy green vegetables, so it was important that the antimicrobial treatments not promote chlorophyll break-down (Burton 1982; Prakash and others 2000). Green leafy vegetables are an important source of carotenoids, which are phytonutrients with antioxidant capacity (Kim and others 2007). Therefore, it was important that the levels of these nutrients were not impacted by the antimicrobial treatments, as they provide important health benefits and quality attributes.

170
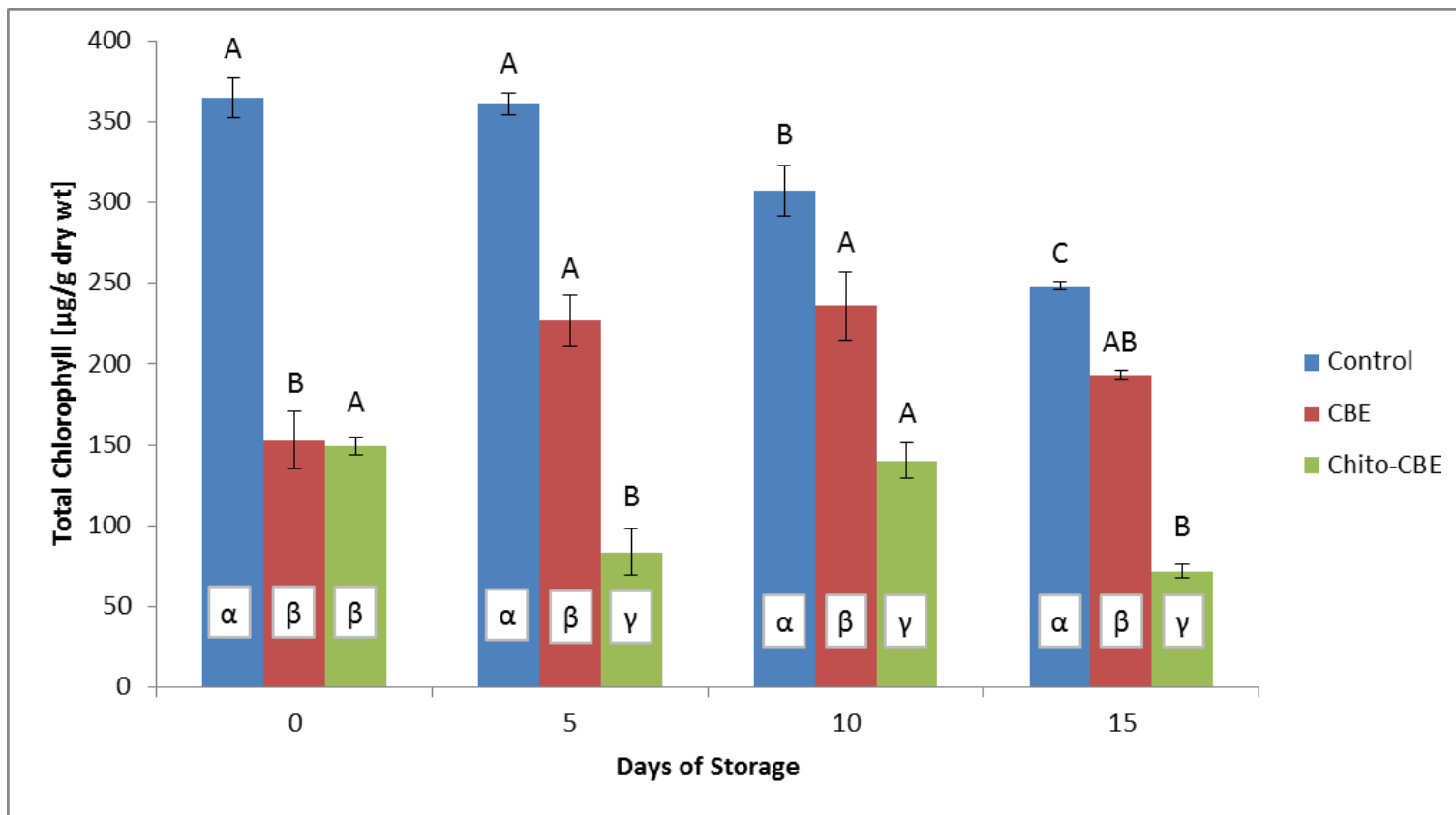
Figure 7.6. Amount of total chlorophyll measured throughout 15 days of storage on fresh-cut romaine lettuce treated with cinnamon bark extract (CBE) and chitosan-PNIPAAM (Chito-CBE) nanoparticles and their untreated controls. Measurements were based on the amount of dried leaf weight. [A]Columns within the same treatment that do not have a common letter above them are significantly different ($p<0.05$). [α]Columns within the same storage day that do not contain a common Greek letter are significantly different ($p<0.05$).

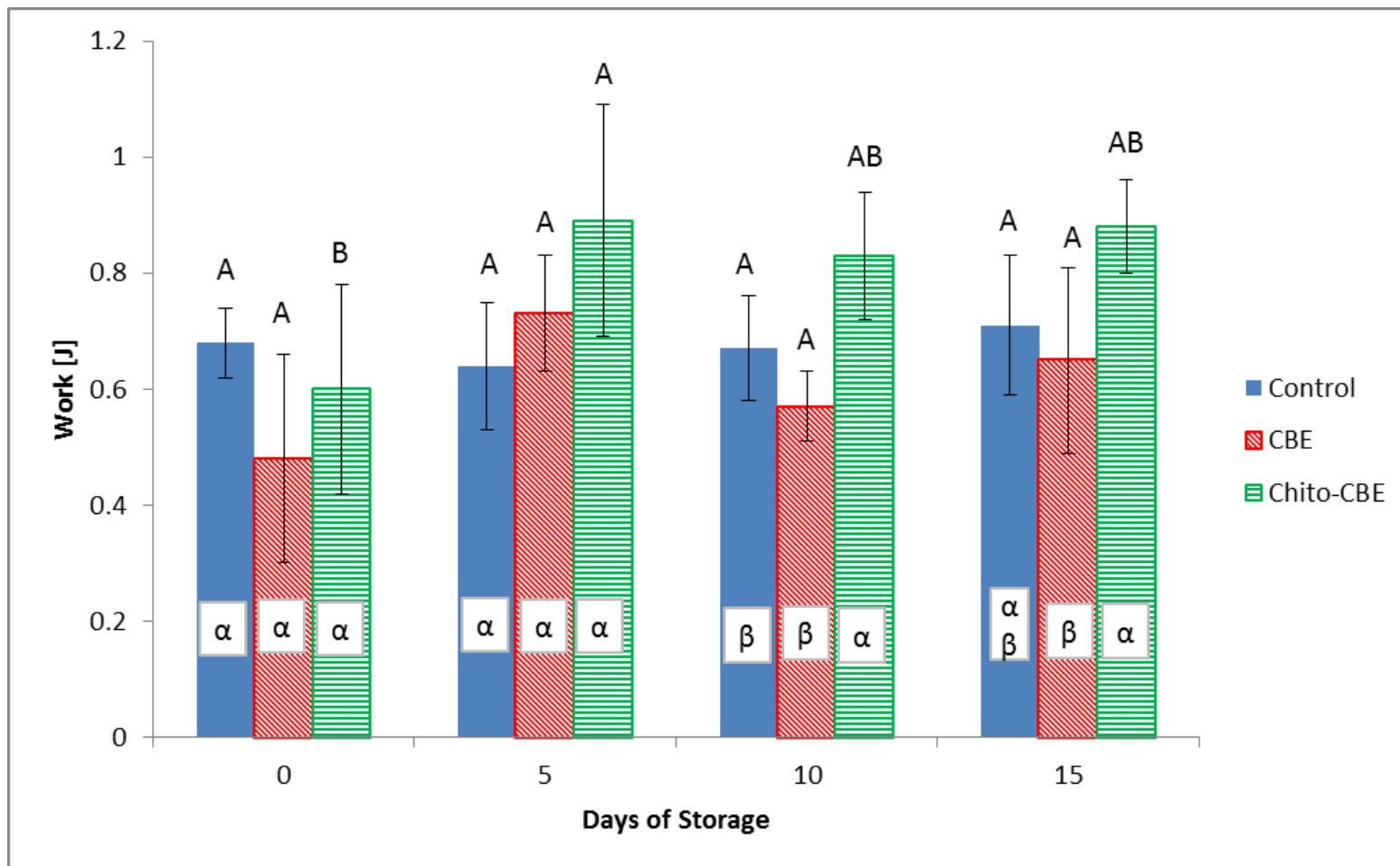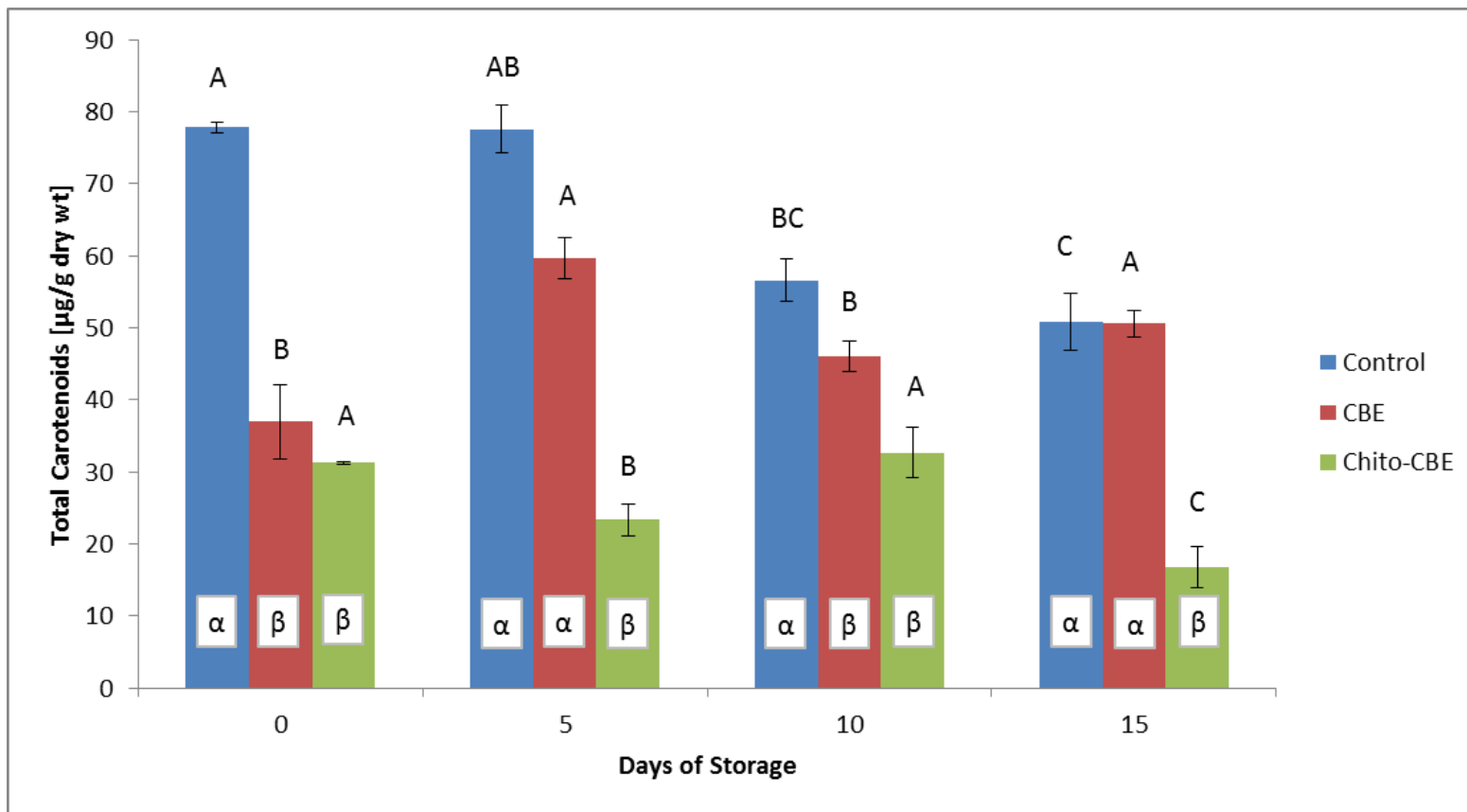Figure 7.7. Amount of total carotenoids measured throughout 15 days of storage on fresh-cut romaine lettuce treated with cinnamon bark extract (CBE) and chitosan-PNIPAAM (Chito-CBE) nanoparticles and their untreated controls. Measurements were based on the amount of dried leaf weight. [A]Columns within the same treatment that do not have a common letter above them are significantly different ($p<0.05$). [α]Columns within the same storage day that do not contain a common Greek letter are significantly different ($p<0.05$).

Initially, the microbial load on the chitosan-PNIPAAM treated lettuce was significantly lower than the control and CBE treated samples by approximately 3 $\log_{10}$ CFU/g of samples, as seen in Figure 7.8. However, by day 5 of storage, the aerobic plate counts had increased (P<0.05) to approximately the same level. The low microbial loads on the chitosan-PNIPAAM samples at the beginning of storage indicate that the nanoparticles were initially effective at inhibiting microbial growth, but the treatment concentration was not high enough to provide a sustained release at an effective antimicrobial concentration. Although not regulated in the United States, it is generally accepted that the maximum acceptable microbial load is 7 $\log_{10}$ CFU/g of produce by the end use date (Prakash and others 2000; Artés and others 2007). By this standard, all samples were acceptable in terms of microbiological quality by the end of storage and the chitosan-CBE particles could potentially extend the microbiological shelf-life beyond the typical 15 days. The natural microflora growth was inhibited significantly

less than the *Listeria* pathogens were by the antimicrobial treatments. Several studies have shown that natural microflora is not as readily inhibited by essential oils as pathogenic microorganisms (Raybaudi-Massilia and others 2009). They generally required longer exposure times to reach the same levels of inhibition, or are less effectively inhibited by essential oils (Ponce and others 2008; Raybaudi-Massilia and others 2009). Previous studies have found that microbial spoilage in green leafy vegetables is dominated primarily by Gram-negative microorganisms, rather than lactic acid bacteria or yeast, due to a low concentration of sugars present (Ponce and others 2011). These microorganisms are present at consistently lower levels and grow at slower rates than Gram-negative bacteria (Ponce and others 2011). The state of cell growth occurring impacts the antimicrobial efficacy of essential oils, as dividing cells are more susceptible to penetration by essential oils (Bakkali and others 2008), so less active and slower growing native microflora were likely less susceptible to inhibition by CBE.
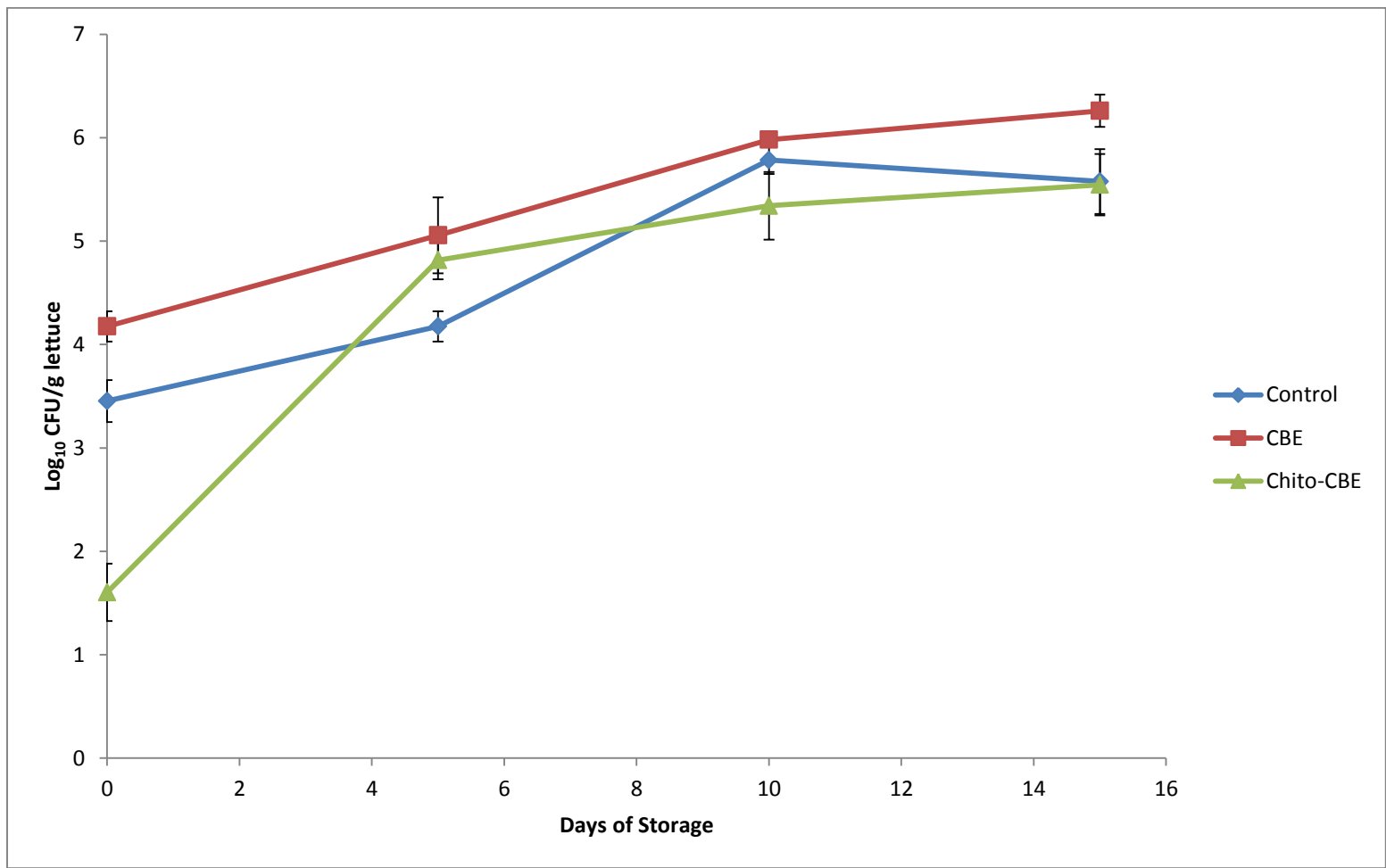
Figure 7.8. Total aerobic plate counts measured throughout 15 days of storage on fresh-cut romaine lettuce controls and treated with cinnamon bark extract (CBE) and chitosan-PNIPAAM (Chito-CBE) nanoparticles.

Consumer panelists rated all samples as acceptable (rating over 5) on the first day of storage, but did rate the controls slightly higher in all categories than the CBE or chitosan-PNIPAAM treated samples (Table 7.4). On the fifth day of storage, panelists still found all samples acceptable, but rated the chitosan-PNIPAAM samples lower ($P<0.05$) in all categories with the exception of aroma. By the last storage day, the chitosan-PNIPAAM lettuce was rated just below ($P<0.05$) an acceptable level in the appearance and overall categories. At this point, these samples showed more wilting and browning than the control and CBE samples (Figure 7.9). The chitosan-PNIPAAM and CBE treatments both introduce more moisture onto the lettuce surface, which can promote microbial decay and wilting on the leaves and lead to lower consumer acceptance (Allende and others 2004). The chitosan tended to retain the moisture on the leaf surface more than the CBE after the drying period, which is likely why the chitosan-

PNIPAAM leaves wilted and browned at a faster rate than the other samples. A longer drying time after the chitosan-PNIPAAM treatment could potentially improve the consumer acceptance of these samples and delay the onset of microbial decay and leaf browning. Cutting the leaves, rather than using whole leaves for the study also increased the amount of browning and wilting that occurred on the samples. Once the leaves are damaged, the natural protection of the epidermis is removed and they are more susceptible to microbial decay and browning (Artés and others 2007). The visible browning and wilting was the primary factor that led to lower consumer acceptance, rather than as a result of the antimicrobial treatments themselves. There were no comments made during the sensory study in reference to a cinnamon aroma or a visible indication of the nanoparticle treatments. Panelists consistently scored aroma of all samples as acceptable, demonstrating that the antimicrobial treatments had no negative impact on this sensory parameter.

Table 7.4. Consumer acceptance panel ratings of fresh-cut romaine lettuce controls and treated with cinnamon bark extract (CBE) or encapsulated CBE in chitosan-PNIPAAM (Chito-CBE) nanoparticles over 13 days of storage at 5°C.

Day/Treatment	Control	CBE	Chito-CBE
Color			
1	$_w7.46^a$ (1.24)	$_z6.59^b$ (1.47)	$_{wz}6.82^a$ (1.81)
5	$_y6.26^b$ (1.61)	$_w7.22^a$ (1.11)	$_z5.53^b$ (1.35)
13	$_w6.53^b$ (1.75)	$_w6.61^{ab}$ (1.36)	$_z5.24^b$ (1.48)
Appearance			
1	$_w7.16^a$ (1.41)	$_z6.04^b$ (1.79)	$_z5.89^a$ (2.03)
5	$_y6.32^b$ (1.62)	$_w7.16^a$ (1.09)	$_z5.23^{ab}$ (1.27)
13	$_w6.14^b$ (1.78)	$_w6.39^b$ (1.59)	$_z4.23^b$ (1.48)
Aroma			
1	$_w6.45^a$ (1.49)	$_z5.68^a$ (1.86)	$_{wz}5.95^a$ (1.72)
5	$_w5.94^{ab}$ (1.33)	$_w6.32^a$ (1.32)	$_w5.83^a$ (1.31)
13	$_w5.76^b$ (1.58)	$_w5.80^a$ (1.36)	$_z5.07^b$ (1.31)
Overall Quality			
1	$_w7.13^a$ (1.31)	$_z5.98^b$ (1.70)	$_z6.04^a$ (1.80)
5	$_y6.30^b$ (1.49)	$_w7.14^a$ (1.05)	$_z5.28^{ab}$ (1.35)
13	$_w6.33^b$ (1.56)	$_w6.47^{ab}$ (1.54)	$_z4.47^b$ (1.41)

[a]Means within a column that are not followed by a common superscript letter are significantly different (p<0.05).
[w]Means within a row that are not preceded by a common subscript letter are significantly different (p<0.05).
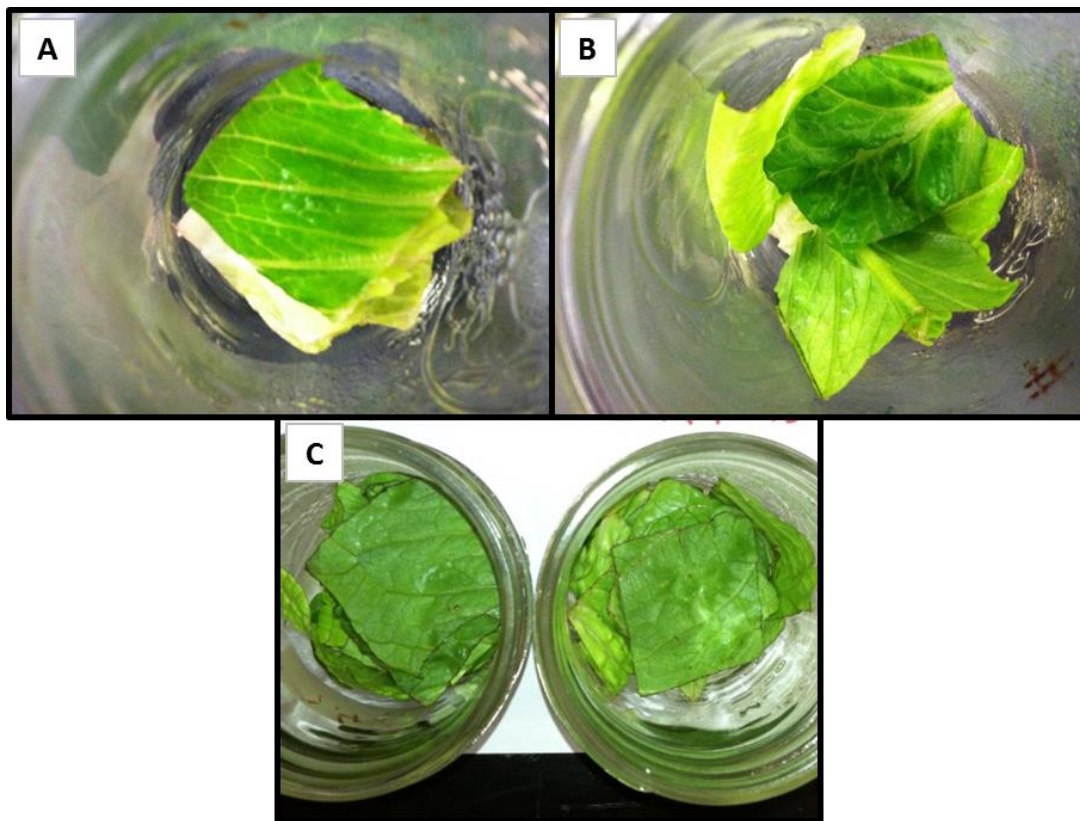
Figure 7.9. Appearance of fresh-cut romaine lettuce with or without antimicrobial treatments (A-Control, B-CBE, C-chitosan-PNIPAAM-CBE nanoparticles) after 15 days of storage at 5°C.

7.5 Conclusions

The chitosan-PNIPAAM nanoparticles with entrapped CBE were effective inhibitors of microbial growth, both pathogens and spoilage microorganisms. However, the level of inhibition was not quite high enough to ensure safety in the case of a pathogen outbreak, but did extend the shelf life of fresh-cut romaine lettuce. The concentrations of antimicrobials applied to fresh-cut lettuce were kept intentionally low to avoid imparting any detrimental changes on the quality attributes that would prevent consumer acceptance; however, the level of antimicrobial application could likely be

increased without imparting any changes to the quality or sensorial attributes of romaine lettuce. A higher level of antimicrobial application would increase the level of inhibition on the lettuce and better ensure produce safety. The goal was to test the impact of these antimicrobial compounds at levels that would be meaningful and acceptable in a food processing environment. Future studies should be conducted to determine the threshold application level of all of the antimicrobials tested in fresh-cut romaine lettuce, as higher concentrations will lead to improved antimicrobial activity.

CHAPTER VIII

CONCLUSIONS

This research explored the effects of nanoencapsulation on the antimicrobial efficacy of essential oils (cinnamon bark and clove bud extracts) and their active compounds (*trans*-cinnamaldehyde and eugenol) on Gram-positive and Gram-negative foodborne pathogens. Through the experimentation on the antimicrobials and various encapsulation matrices, the following conclusions were reached:

1. Whole spice extracts proved more effective as bacterial inhibitors against both Gram-positive and Gram-negative bacteria in *in vitro* testing. This phenomenon was true for both free essential oils and encapsulated essential oils. Of the antimicrobials tested, cinnamon bark extract was the most effective antimicrobial compound against *Salmonella enterica* serovar Typhimurium LT2 and *Listeria* spp.

2. Beta-cyclodextrin (BCD) creates inclusion complexes with hydrophobic essential oils and active compounds that increased their solubility and improved their stability. The improved solubility facilitated better delivery of the antimicrobials to pathogen sites in aqueous media, which led to more effective bacteria inhibition over free antimicrobials.

3. Cinnamon bark extract was encapsulated in poly (DL-lactide-co-glycolide) (PLGA), which delayed its release compared with BCD inclusion complex particles. Prolonged release and increased aqueous solubility improved the

antimicrobial efficacy of CBE, even up to 72 hours in liquid media under ideal growth environments for pathogen growth.

4. A synthesis procedure was developed for manufacturing temperature-responsive nanoparticles from poly(N-isopropylacrylamide) (PNIPAAM) hydrogel. A bottom-up procedure using NIPAAM monomer was compared with a top-down procedure using crosslinked PNIPAAM hydrogel particulates.

5. The PNIPAAM nanoparticles synthesized via the top-down procedure were more effective delivery systems for CBE as antimicrobials against foodborne pathogens than those synthesized via the bottom-up procedure.

6. PNIPAAM was combined with chitosan and alginate to create nanoparticles that respond to temperature and pH stimuli. These nanoparticles had different release profiles when subjected to different pH and temperature environments. The chitosan-PNIPAAM nanoparticles were the most effective antimicrobials at 35°C, which is an optimal temperature for microbial growth.

7. All of the nanoparticles synthesized in this research study were subjected to a challenge study on the surface of fresh-cut romaine lettuce against *L. monocytogenes*. The chitosan-PNIPAAM nanoparticles with entrapped CBE were the most effective antimicrobials at both 5 and 10°C on romaine lettuce.

8. The chitosan-PNIPAAM nanoparticles were applied to fresh-cut romaine lettuce to confirm the antimicrobials do not negatively impact quality attributes of food products. The fresh-cut lettuce was minimally affected by

the antimicrobial treatments. Most quality parameters tested did not show

significant differences when compared to an untreated control.

CHAPTER IX

RECOMMENDATIONS FOR FURTHER STUDY

Recommendations for future research on nanoencapsulation strategies to enhance fresh and fresh-cut produce safety:

1. Quantify the release rate of antimicrobials in a variety of food applications, temperatures, and different release environments that reflect typical storage conditions.

2. Study essential oils in combination with other "natural" antimicrobials (e.g. nisin, benzoic acid, acetic acid, etc.) to create a highly effective antimicrobial cocktail that imparts no sensory impact to food products, while delivering a high level of bacterial inhibition.

3. Examine the application of a mixture of different controlled delivery systems that will improve antimicrobial efficacy by delivering antimicrobials throughout different stages of product processing and shelf life, due to their varied release profiles.

4. Incorporate antimicrobial nanoparticles into a packaging film as an alternate delivery system that does not require direct antimicrobial application on to food products.

5. Utilize nanoencapsulate technology in a biosensor to detect and inhibit pathogens in fresh produce.

REFERENCES

Allende A, Aguayo E, Artés F. 2004. Microbial and sensory quality of commercial fresh processed red lettuce throughout the production chain and shelf life. Int J Food Microbiol 91(2):109-17.

Amalaradjou MAR, Venkitanarayanan K. 2011a. Effect of *trans*-cinnamaldehyde on reducing resistance to environmental stresses in *Cronobacter sakazakii*. Foodborne Pathog Dis 8(3):403-9.

Amalaradjou MAR, Venkitanarayanan K. 2011b. Effect of *trans*-cinnamaldehyde on inhibition and inactivation of *Cronobacter sakazakii* biofilm on abiotic surfaces. J Food Prot 74(2):200-8.

Amalaradjou MAR, Hoagland TA, Venkitanarayanan K. 2009. Inactivation of *Enterobacter sakazakii* in reconstituted infant formula by *trans*-cinnamaldehyde. Int J Food Microbiol 129(2):146-9.

Anderson JM, Shive MS. 1997. Biodegradation and biocompatibility of PLA and PLGA microspheres. Adv Drug Deliv Rev 28(1):5-24.

AOAC Association of Official Analytical Chemists. 1990. Official method 990.12. Aerobic Plate Count in Foods. Official Methods of Analysis (13th ed). Washington, D.C.: AOAC International.

Arifin DY, Lee LY, Wang CH. 2006. Mathematical modeling and simulation of drug release from microspheres: Implications to drug delivery systems. Adv Drug Deliv Rev 58(12-13):1274-325.

Artés F, Gómez P, Artés-Hernández F. 2007. Physical, physiological and microbial deterioration of minimally fresh processed fruits and vegetables. Food Sci Technol Int 13(3):177-88.

Astete CE, Sabliov CM. 2006. Synthesis of poly (DL-lactide-Co-glycolide) nanoparticles with entrapped magnetite by emulsion evaporation method. Particul Sci Technol 24(3):321-8.

Astete CE, Kumar CSSR, Sabliov CM. 2007. Size control of poly (d, l-lactide-co-glycolide) and poly (d, l-lactide-co-glycolide)-magnetite nanoparticles synthesized by emulsion evaporation technique. Colloids Surf A 299(1):209-16.

Astete CE, Sabliov CM. 2006. Synthesis and characterization of PLGA nanoparticles. J Biomater Sci, Polym Ed 17(3):247-89.

Astray G, Gonzalez-Barreiro C, Mejuto J, Rial-Otero R, Simal-Gandara J. 2009. A review on the use of cyclodextrins in foods. Food Hydrocoll 23(7):1631-40.

Ayala-Zavala JF, Soto-Valdez H, González-León A, Alvarez-Parrilla E, Martín-Belloso O, González-Aguilar GA. 2008. Microencapsulation of cinnamon leaf (*Cinnamomum zeylanicum*) and garlic (*Allium sativum*) oils in β-cyclodextrin. J Incl Phenom Macrocycl Chem 60(3):359-68.

Ayala-Zavala J, Del-Toro-Sánchez L, Alvarez-Parrilla E, González-Aguilar G. 2008. High Relative Humidity In-Package of Fresh-Cut Fruits and Vegetables: Advantage or Disadvantage Considering Microbiological Problems and Antimicrobial Delivering Systems? J Food Sci 73(4):R41-7.

Bakkali F, Averbeck S, Averbeck D, Idaomar M. 2008. Biological effects of essential oils–A review. Food Chem Toxicol 46(2):446-75.

Baur S, Klaiber R, Wei H, Hammes WP, Carle R. 2005. Effect of temperature and chlorination of pre-washing water on shelf-life and physiological properties of ready-to-use iceberg lettuce. Innovative Food Sci Emerg Technol 6(2):171-82.

Benita S. 2006. Microencapsulation: methods and industrial applications. 2nd ed. Boca Raton, FL: CRC Press Taylor and Francis Group.

Blanco M, Alonso M. 1997. Development and characterization of protein-loaded poly(lactide-co-glycolide) nanospheres. Eur J Pharm Biopharm 43(3):287-94.

Bolin H, Huxsoll C. 1991. Effect of Preparation Procedures and Storage Parameters on Quality Retention of Salad-cut Lettuce. J Food Sci 56(1):60-2.

Brackman G, Defoirdt T, Miyamoto C, Bossier P, Van Calenbergh S, Nelis H, Coenye T. 2008. Cinnamaldehyde and cinnamaldehyde derivatives reduce virulence in *Vibrio spp*. by decreasing the DNA-binding activity of the quorum sensing response regulator LuxR. BMC Microbiol 8(1):149.

Brandt AL, Castillo A, Harris KB, Keeton JT, Hardin MD, Taylor TM. 2010. Inhibition of *Listeria monocytogenes* by food antimicrobials applied singly and in combination. J Food Sci 75(9):M557-63.

Burt S. 2004. Essential oils: their antibacterial properties and potential applications in foods--a review. Int J Food Microbiol 94(3):223-53.

Burton WG. 1982. Post-harvest physiology of food crops. London, UK.: Longman Group Ltd.

Carlotti M, Sapino S, Cavalli R, Trotta M, Trotta F, Martina K. 2007. Inclusion of cinnamaldehyde in modified γ-cyclodextrins. J Incl Phenom Macrocycl Chem 57(1):445-50.

Carr BT, Meilgaard M, Civille GV. 1999. Sensory evaluation techniques. Washington, D.C.: CRC Press.

Centers for Disease Control and Prevention (CDC). 2012. Reports of Salmonella Outbreak Investigations from 2012. Last accessed on 03.01.14. http://www.cdc.gov/salmonella/outbreaks-2012.html

Centers for Disease Control and Prevention (CDC). 2011a. Surveillance for foodborne disease outbreaks--United States, 2008. Morb Mortal Wkly Rep 60(35):1197-202.

Centers for Disease Control and Prevention (CDC). 2011b. Vital signs: incidence and trends of infection with pathogens transmitted commonly through food--foodborne diseases active surveillance network, 10 U.S. sites, 1996-2010. Morb Mortal Wkly Rep 60(22):749-55.

CFR. 2009. Code of Federal Regulations. Title 21, Part 172.515. Food additives permitted for direct addition to food for human consumption: Synthetic flavoring substances and adjuvants. 3, 56-63.

Choi MJ, Ruktanonchai U, Soottitantawat A, Min SG. 2009a. Morphological characterization of encapsulated fish oil with β-cyclodextrin and polycaprolactone. Food Res Int 42(8):989-97.

Choi MJ, Soottitantawat A, Nuchuchua O, Min SG, Ruktanonchai U. 2009b. Physical and light oxidative properties of eugenol encapsulated by molecular inclusion and emulsion-diffusion method. Food Res Int 42(1):148-56.

Chuang CY, Don TM, Chiu WY. 2010. Synthesis and characterization of stimuli-responsive porous/hollow nanoparticles by self-assembly of chitosan-based graft copolymers and application in drug release. J Polym Sci, Part A: Polym Chem 48(11):2377-87.

Chuang CY, Don TM, Chiu WY. 2009. Synthesis of chitosan-based thermo-and pH-responsive porous nanoparticles by temperature-dependent self-assembly method and their application in drug release. J Polym Sci, Part A: Polym Chem 47(19):5126-36.

Chun J, You S, Lee M, Choi M, Min S. 2012. Characterization of β-cyclodextrin self-aggregates for eugenol encapsulation. J Food Eng 8(2):1-19.

Cohen S, Yoshioka T, Lucarelli M, Hwang LH, Langer R. 1991. Controlled delivery systems for proteins based on poly (lactic/glycolic acid) microspheres. Pharm Res 8(6):713-20.

Crank J. 1975. The mathematics of diffusion. Second ed. New York, NY: Oxford University Press.

Davidson P, Taylor T. 2007. Chemical preservatives and natural antimicrobial compounds. In: Doyle PM, Beuchat LR, & Montville TJ, editors. Food microbiology: Fundamentals and Frontiers. 3rd ed. Washington, D.C.: ASM Press, p 520-56.

de Moura MR, Ahmad Aouada F, Favaro SL, Radovanovic E, Forti Rubira A, Muniz EC. 2009. Release of BSA from porous matrices constituted of alginate–Ca^2 and PNIPAAm-interpenetrated networks. Mater Sci Eng C Mater Biol Appl 29(8):2319-25.

Del Toro-Sánchez C, Ayala-Zavala J, Machi L, Santacruz H, Villegas-Ochoa M, Alvarez-Parrilla E, González-Aguilar G. 2010. Controlled release of antifungal volatiles of thyme essential oil from β-cyclodextrin capsules. J Incl Phenom Macrocycl Chem 67(3):431-41.

Devlieghere F, Vermeulen A, Debevere J. 2004. Chitosan: antimicrobial activity, interactions with food components and applicability as a coating on fruit and vegetables. Food Microbiol 21(6):703-14.

Domadia P, Swarup S, Bhunia A, Sivaraman J, Dasgupta D. 2007. Inhibition of bacterial cell division protein FtsZ by cinnamaldehyde. Biochem Pharmacol 74(6):831-40.

Donsì F, Annunziata M, Sessa M, Ferrari G. 2011. Nanoencapsulation of essential oils to enhance their antimicrobial activity in foods. LWT Food Sci Technol 44(9):1908-14.

Douglas KL, Tabrizian M. 2005. Effect of experimental parameters on the formation of alginate–chitosan nanoparticles and evaluation of their potential application as DNA carrier. J Biomater Sci, Polym Ed 16(1):43-56.

Doyle MP, Beuchat LR. 2007. Food Microbiology: Fundamentals and Frontiers. 3rd ed. Washington, DC, USA: ASM Press.

Eeckman F, Amighi K, Moës AJ. 2001. Effect of some physiological and non-physiological compounds on the phase transition temperature of thermoresponsive polymers intended for oral controlled-drug delivery. Int J Pharm 222(2):259-70.

Fan L, Wu H, Zhang H, Li F, Yang T, Gu C, Yang Q. 2008. Novel super pH-sensitive nanoparticles responsive to tumor extracellular pH. Carbohydr Polym 73(3):390-400.

Fontes P, Pereira P, Conde R. 1997. Critical chlorophyll, total nitrogen, and nitrate-nitrogen in leaves associated to maximum lettuce yield. J Plant Nutr 20(9):1061-8.

Friedman M, Henika PR, Levin CE, Mandrell RE. 2004. Antibacterial activities of plant essential oils and their components against *Escherichia coli* O157: H7 and *Salmonella enterica* in apple juice. J Agric Food Chem 52(19):6042-8.

Ghaouth A, Arul J, Ponnampalam R, Boulet M. 1991. Chitosan coating effect on storability and quality of fresh strawberries. J Food Sci 56(6):1618-20.

Gill A, Holley R. 2004. Mechanisms of bactericidal action of cinnamaldehyde against *Listeria monocytogenes* and of eugenol against *L. monocytogenes* and *Lactobacillus sakei*. Appl Environ Microbiol 70(10):5750-5.

Gill A, Holley R. 2006a. Disruption of *Escherichia coli, Listeria monocytogenes* and *Lactobacillus sakei* cellular membranes by plant oil aromatics. Int J Food Microbiol 108(1):1-9.

Gill A, Holley R. 2006b. Inhibition of membrane bound ATPases of *Escherichia coli* and *Listeria monocytogenes* by plant oil aromatics. Int J Food Microbiol 111(2):170-4.

Gomes C, Moreira RG, Castell-Perez E. 2011a. Microencapsulated Antimicrobial Compounds as a Means to Enhance Electron Beam Irradiation Treatment for Inactivation of Pathogens on Fresh Spinach Leaves. J Food Sci 76(6):E479-88.

Gomes C, Moreira RG, Castell-Perez E. 2011b. Poly (DL-lactide-co-glycolide)(PLGA) nanoparticles with entrapped *trans*-cinnamaldehyde and eugenol for antimicrobial delivery applications. J Food Sci 76N24.

Gomes C, Moreira R, Castell-Perez M, Kim J, Da Silva P, Castillo A. 2008. E-Beam irradiation of bagged, ready-to-eat spinach leaves (Spinacea oleracea): an engineering approach. J Food Sci 73(2):E95-E102.

Gran ML. 2011. Metal-polymer nanoparticulate systems for externally-controlled delivery. [dissertation]. Austin, TX: The University of Texas at Austin.

Gu F, Amsden B, Neufeld R. 2004. Sustained delivery of vascular endothelial growth factor with alginate beads. J Controlled Release 96(3):463-72.

Hammer KA, Carson CF. 2011. Antibacterial and Antifungal Activities of Essential Oils. In: Thormar H, editor. Lipids and Essential Oils as Antimicrobial Agents. Wiley Online Library. p 255-306.

Han J, Gomes-Feitosa CL, Castell-Perez E, Moreira RG, Silva PF. 2004. Quality of packaged romaine lettuce hearts exposed to low-dose electron beam irradiation. LWT Food Sci Technol 37(7):705-15.

Harris L, Farber J, Beuchat L, Parish M, Suslow T, Garrett E, Busta F. 2003. Outbreaks associated with fresh produce: incidence, growth, and survival of pathogens in fresh and fresh-cut produce. Compr Rev Food Sci Food Safety 278-141.

Hedges AR, Shieh WJ, Sikorski CT. 1995. Use of cyclodextrins for encapsulation in the use and treatment of food products. In: Risch S & Reineccius G, editors. Encapsulation and Controlled Release of Food Ingredients. ACS Publications. p 60-73.

Helander IM, Alakomi HL, Latva-Kala K, Mattila-Sandholm T, Pol I, Smid EJ, Gorris LGM, Von Wright A. 1998. Characterization of the action of selected essential oil components on Gram-negative bacteria. J Agric Food Chem 46(9):3590-5.

Helrich K. 1990. Official methods of Analysis of the AOAC. Volume 2. Association of Official Analytical Chemists Inc.

Higuchi T, Connors KA. 1965. Phase-solubility techniques. Adv Anal Chem Instrum 4(2):117–212.

Hill LE, Gomes C, Taylor TM. 2013a. Characterization of Beta-cyclodextrin Inclusion Complexes Containing Essential Oils (*trans*-Cinnamaldehyde, Eugenol, Cinnamon Bark, and Clove Bud Extracts) for Antimicrobial Delivery Applications. LWT Food Sci Technol 51(1):86-93.

Hill LE, Taylor TM, Gomes C. 2013b. Antimicrobial Efficacy of Poly (DL-lactide-co-glycolide)(PLGA) Nanoparticles with Entrapped Cinnamon Bark Extract against Listeria monocytogenes and Salmonella typhimurium. J Food Sci 78(4):N626-32.

Iannitelli A, Grande R, Stefano AD, Giulio MD, Sozio P, Bessa LJ, Laserra S, Paolini C, Protasi F, Cellini L. 2011. Potential Antibacterial Activity of Carvacrol-Loaded Poly (DL-lactide-co-glycolide)(PLGA) Nanoparticles against Microbial Biofilm. International Journal of Molecular Sciences 12(8):5039-51.

Jacobsson A, Nielsen T, Sjöholm I. 2004. Effects of type of packaging material on shelf-life of fresh broccoli by means of changes in weight, colour and texture. Eur Food Res Technol 218(2):157-63.

Jay JM, Loessner MJ, Golden DA. 2005. Modern food microbiology. 7th ed. New York, NY: Springer Science.

Johny AK, Darre M, Donoghue A, Donoghue D, Venkitanarayanan K. 2010. Antibacterial effect of *trans*-cinnamaldehyde, eugenol, carvacrol, and thymol on *Salmonella Enteritidis* and *Campylobacter jejuni* in chicken cecal contents in vitro. J Appl Poult Res 19(3):237-44.

Johny AK, Darre M, Hoagland T, Schreiber D, Donoghue A, Donoghue D, Venkitanarayanan K. 2008. Antibacterial effect of *trans*-cinnamaldehyde on *Salmonella Enteritidis* and *Campylobacter jejuni* in chicken drinking water. J Appl Poult Res 17(4):490-7.

Ju HK, Kim SY, Lee YM. 2001. pH/temperature-responsive behaviors of semi-IPN and comb-type graft hydrogels composed of alginate and poly (N-isopropylacrylamide). Polymer 42(16):6851-7.

Juven B, Kanner J, Schved F, Weisslowicz H. 1994. Factors that interact with the antibacterial action of thyme essential oil and its active constituents. J Appl Microbiol 76(6):626-31.

Kalemba D, Kunicka A. 2003. Antibacterial and antifungal properties of essential oils. Curr Med Chem 10(10):813-29.

Karathanos VT, Mourtzinos I, Yannakopoulou K, Andrikopoulos NK. 2007. Study of the solubility, antioxidant activity and structure of inclusion complex of vanillin with beta-cyclodextrin. Food Chem 101(2):652-8.

Kim H, Fonseca JM, Choi J, Kubota C. 2007. Effect of methyl jasmonate on phenolic compounds and carotenoids of romaine lettuce (Lactuca sativa L.). J Agric Food Chem 55(25):10366-72.

Kim J, Marshall MR, Wei C. 1995. Antibacterial activity of some essential oil components against five foodborne pathogens. J Agric Food Chem 43(11):2839-45.

Kim JH, Lee SB, Kim SJ, Lee YM. 2002. Rapid temperature/pH response of porous alginate-g-poly (N-isopropylacrylamide) hydrogels. Polymer 43(26):7549-58.

Kim JG, Luo Y, Saftner RA, Gross KC. 2005a. Delayed modified atmosphere packaging of fresh-cut Romaine lettuce: Effects on quality maintenance and shelf-life. J Am Soc Hort Sci 130(1):116-23.

Kim KH, Kim J, Jo WH. 2005b. Preparation of hydrogel nanoparticles by atom transfer radical polymerization of N-isopropylacrylamide in aqueous media using PEG macro-initiator. Polymer 46(9):2836-40.

King AH. 1988. Flavor encapsulation with alginates. In: Risch S & Reineccius G, editors. Flavor Encapsulation. ACS Publications. p 122-5.

Klouda L, Mikos AG. 2008. Thermoresponsive hydrogels in biomedical applications. Eur J Pharm Biopharm 68(1):34-45.

Kong B, Wang J, Xiong YL. 2007. Antimicrobial activity of several herb and spice extracts in culture medium and in vacuum-packaged pork. J Food Prot 70(3):641-7.

Korsmeyer RW, Lustig SR, Peppas NA. 1986. Solute and penetrant diffusion in swellable polymers. I. Mathematical modeling. J Polym Sci, Part B: Polym Phys 24(2):395-408.

Kuan C, Yee-Fung W, Yuen K, Liong M. 2012. Nanotech: propensity in foods and bioactives. Crit Rev Food Sci Nutr 52(1):55-71.

Kumari A, Yadav SK, Yadav SC. 2010. Biodegradable polymeric nanoparticles based drug delivery systems. Colloids Surf, B 75(1):1-18.

Kwon J, Yu C, Park H. 2003. Bacteriocidal effects and inhibition of cell separation of cinnamic aldehyde on *Bacillus cereus*. Lett Appl Microbiol 37(1):61-5.

Lambert R, Skandamis PN, Coote PJ, Nychas GJE. 2001. A study of the minimum inhibitory concentration and mode of action of oregano essential oil, thymol and carvacrol. J Appl Microbiol 91(3):453-62.

Lapidot T, Walker MD, Kanner J. 2002. Can apple antioxidants inhibit tumor cell proliferation? Generation of H_2O_2 during interaction of phenolic compounds with cell culture media. J.Agric.Food Chem. 50(11):3156-60.

Lee C, Wen C, Lin C, Chiu W. 2004. Morphology and temperature responsiveness–swelling relationship of poly (N-isopropylamide–chitosan) copolymers and their application to drug release. J Polym Sci, Part A: Polym Chem 42(12):3029-37.

Lee W, Chen Y. 2001. Studies on preparation and swelling properties of the N-isopropylacrylamide/chitosan semi-IPN and IPN hydrogels. J Appl Polym Sci 82(10):2487-96.

Leuba J, Stossel P. 1986. Chitosan and other polyamines: antifungal activity and interaction with biological membranes. In: Gooday GW, Jeuniaux C, & Muzzarelli R, editors. Chitin in nature and technology. New York, NY: Springer. p 215-22.

Li M, Muthaiyan A, A OBryan C, E Gustafson J, Li Y, G Crandall P, C Ricke S. 2011. Use of natural antimicrobials from a food safety perspective for control of *Staphylococcus aureus*. Curr Pharm Biotechnol 12(8):1240-54.

Lichtenthaler HK. 1987. [34] Chlorophylls and carotenoids: Pigments of photosynthetic biomembranes. Meth Enzymol 148350-82.

Loftsson T, Masson M, Brewster ME. 2004. Self-association of cyclodextrins and cyclodextrin complexes. J Pharm Sci 93(5):1091-9.

Mainardes RM, Evangelista RC. 2005. PLGA nanoparticles containing praziquantel: effect of formulation variables on size distribution. Int J Pharm 290(1):137-44.

Mantilla N, Castell-Perez M, Gomes C, Moreira R. 2012. Multilayered antimicrobial edible coating and its effect on quality and shelf-life of fresh-cut pineapple (*Ananas comosus*). LWT Food Sci Technol 5137-43.

Martín-Diana AB, Rico D, Barry-Ryan C. 2008. Green tea extract as a natural antioxidant to extend the shelf-life of fresh-cut lettuce. Innovative Food Sci Emerg Technol 9(4):593-603.

Mohammadi G, Valizadeh H, Barzegar-Jalali M, Lotfipour F, Adibkia K, Milani M, Azhdarzadeh M, Kiafar F, Nokhodchi A. 2010. Development of azithromycin-PLGA nanoparticles: Physicochemical characterization and antibacterial effect against Salmonella typhi. Colloids and Surfaces B: Biointerfaces 80(1):34-9.

Mourtzinos I, Kalogeropoulos N, Papadakis S, Konstantinou K, Karathanos V. 2008. Encapsulation of Nutraceutical Monoterpenes in β-Cyclodextrin and Modified Starch. J Food Sci 73(1):S89-94.

Mourtzinos I, Salta F, Yannakopoulou K, Chiou A, Karathanos VT. 2007. Encapsulation of olive leaf extract in β-cyclodextrin. J Agric Food Chem 55(20):8088-94.

Mu L, Feng SS. 2003. PLGA/TPGS nanoparticles for controlled release of paclitaxel: effects of the emulsifier and drug loading ratio. Pharm Res 20(11):1864-72.

Neradovic D, Soga O, Van Nostrum C, Hennink W. 2004. The effect of the processing and formulation parameters on the size of nanoparticles based on block copolymers of poly (ethylene glycol) and poly (*N*-isopropylacrylamide) with and without hydrolytically sensitive groups. Biomaterials 25(12):2409-18.

Oliveira M, Usall J, Solsona C, Alegre I, Viñas I, Abadias M. 2010. Effects of packaging type and storage temperature on the growth of foodborne pathogens on shredded 'Romaine' lettuce. Food Microbiol 27(3):375-80.

Panyam J, Labhasetwar V. 2003. Biodegradable nanoparticles for drug and gene delivery to cells and tissue. Adv Drug Deliv Rev 55(3):329-47.

Panyam J, Williams D, Dash A, Leslie-Pelecky D, Labhasetwar V. 2004. Solid-state solubility influences encapsulation and release of hydrophobic drugs from PLGA/PLA nanoparticles. J Pharm Sci 93(7):1804-14.

Pelton R. 2000. Temperature-sensitive aqueous microgels. Adv Colloid Interface Sci 85(1):1-33.

Phillips MA, Gran ML, Peppas NA. 2010. Targeted nanodelivery of drugs and diagnostics. Nano Today 5(2):143-59.

Ponce Cevallos PA, Buera MP, Elizalde BE. 2010. Encapsulation of cinnamon and thyme essential oils components (cinnamaldehyde and thymol) in β-cyclodextrin: Effect of interactions with water on complex stability. J Food Eng 99(1):70-5.

Ponce A, Roura SI, Moreira MR. 2011. Essential oils as biopreservatives: different methods for the technological application in lettuce leaves. J Food Sci 76(1):M34-40.

Ponce AG, Roura SI, del Valle CE, Moreira MR. 2008. Antimicrobial and antioxidant activities of edible coatings enriched with natural plant extracts: *In vitro* and *in vivo* studies. Postharvest BiolTechnol 49(2):294-300.

Prabaharan M. 2008. Review paper: chitosan derivatives as promising materials for controlled drug delivery. J Biomater Appl 23(1):5-36.

Prakash A, Guner A, Caporaso F, Foley D. 2000. Effects of Low-dose Gamma Irradiation on the Shelf Life and Quality Characteristics of Cut Romaine Lettuce Packaged under Modified Atmosphere. J Food Sci 65(3):549-53.

Pray LA, Yaktine AL. 2009. Nanotechnology in food products: workshop summary. Washington, D.C.: Natl Academy Pr.

Qi ZH, Hedges AR. 1995. Use of cyclodextrins for flavors. ACS Symposium 610231-43.

Rabea EI, Badawy ME, Stevens CV, Smagghe G, Steurbaut W. 2003. Chitosan as antimicrobial agent: applications and mode of action. Biomacromolecules 4(6):1457-65.

Ramanan RMK, Chellamuthu P, Tang L, Nguyen KT. 2006. Development of a temperature-sensitive composite hydrogel for drug delivery applications. Biotechnol Prog 22(1):118-25.

Ravichandran M, Hettiarachchy NS, Ganesh V, Ricke SC, Singh S. 2011. Enhancement of Antimicrobial Activities of Naturally Occurring Phenolic Compounds by Nanoscale Delivery Against *Listeria Monocytogenes*, *Escherichia Coli* O157: H7 and *Salmonella* Typhimurium in Broth and Chicken Meat System. J Food Saf 31(4):462-71.

Raybaudi-Massilia RM, Mosqueda-Melgar J, Soliva-Fortuny R, Martín-Belloso O. 2009. Control of pathogenic and spoilage microorganisms in fresh-cut fruits and fruit juices by traditional and alternative natural antimicrobials. Compr Rev Food Sci Food Safety 8(3):157-80.

Rekharsky MV, Inoue Y. 1998. Complexation thermodynamics of cyclodextrins. Chem Rev 98(5):1875-918.

Ritger PL, Peppas NA. 1987a. A simple equation for description of solute release II. Fickian and anomalous release from swellable devices. J Control Release 5(1):37-42.

Ritger PL, Peppas NA. 1987b. Transport of penetrants in the macromolecular structure of coals: 4. models for analysis of dynamic penetrant transport. Fuel 66(6):815-26.

Rittinger P, Biggs A, Peirson D. 1987. Histochemistry of lignin and suberin deposition in boundary layers formed after wounding in various plant species and organs. Can J Bot 65(9):1886-92.

Schild H. 1992. Poly (N-isopropylacrylamide): experiment, theory and application. Prog Polym Sci 17(2):163-249.

Seo E, Min S, Choi M. 2010. Release characteristics of freeze-dried eugenol encapsulated with β-cyclodextrin by molecular inclusion method. J Microencapsul 27(6):496-505.

Sershen S, Westcott S, Halas N, West J. 2000. Temperature-sensitive polymer–nanoshell composites for photothermally modulated drug delivery. J Biomed Mater Res 51(3):293-8.

Shi J, Alves NM, Mano JF. 2006. Drug Release of pH/Temperature-Responsive Calcium Alginate/Poly (N-isopropylacrylamide) Semi-IPN Beads. Macromol biosci 6(5):358-63.

Sikkema J, De Bont J, Poolman B. 1994. Interactions of cyclic hydrocarbons with biological membranes. J Biol Chem 269(11):8022.

Song C, Labhasetwar V, Murphy H, Qu X, Humphrey W, Shebuski R, Levy R. 1997. Formulation and characterization of biodegradable nanoparticles for intravascular local drug delivery. J Control Release 43(2):197-212.

Stella VJ, He Q. 2008. Cyclodextrins. Toxicol Pathol 36(1):30-42.

Stössel P, Leuba J. 1984. Effect of chitosan, chitin and some amino sugars on growth of various soilborne phytopathogenic fungi. J Phytopathol 111(1):82-90.

Swaminathan B, Cabanes D, Zhang W, Cossart P, Doyle M, Beuchat L. 2007. *Listeria monocytogenes*. In: Michael P. Doyle, Larry R. Beuchat, editors. Food microbiology: fundamentals and frontiers. Washington D.C.: ASM Press. p 457-91.

Szente L, Szejtli J. 2004. Cyclodextrins as food ingredients. Trends Food Sci Technol 15(3):137-42.

Tang B, Ma L, Wang H, Zhang G. 2002. Study on the supramolecular interaction of curcumin and β-cyclodextrin by spectrophotometry and its analytical application. J Agric Food Chem 50(6):1355-61.

Thoroski J, Blank G, Biliaderis C. 1989. Eugenol induced inhibition of extracellular enzyme production by Bacillus cereus. J Food Prot 52(6):399-403.

Tommasini S, Raneri D, Ficarra R, Calabrò ML, Stancanelli R, Ficarra P. 2004. Improvement in solubility and dissolution rate of flavonoids by complexation with β-cyclodextrin. J Pharm Biomed Anal 35(2):379-87.

USDA. 2013. USDA National Nutrient Database for Standard Reference, Release 26. Last accessed on 12.05.13. http://www.ars.usda.gov/ba/bhnrc/ndl

USFDA. 2012a. Final update on multistate outbreak of listeriosis linked to whole cantaloupes. Available from: http://www.fda.gov/Food/FoodSafety/ CORENetwork/ucm272372.htm

USFDA. 2012b. Recalls, Market Withdrawls, & Safety Alerts. Last accessed 09.06.13. Available from: http://www.fda.gov/Safety/Recalls/ucm304724.htm

USFDA. 2010. Press Release: DSHS Orders Produce to Close, Recall Products Available from: http://www.fda.gov/Safety/Recalls/ArchiveRecalls /2010/ucm230709.htm

USFDA. 2001. U. S. Food and Drug Administration. Chapter 6. Microbiology challenge testing. In: *Evaluation and definition of potentially hazardous foods. A report of the Institute of Food Technology for the Food and Drug Administration of the U.S. Department of Health and Human Services*. Available from: http://www.fda.gov/Food/ScienceResearch/ResearchAreas/SafePracticesforFood Processes/ucm094141.htm.

Usta J, Kreydiyyeh S, Barnabe P, Bou-Moughlabay Y, Nakkash-Chmaisse H. 2003. Comparative study on the effect of cinnamon and clove extracts and their main components on different types of ATPases. Hum Exp Toxicol 22(7):355-62.

Valero M, Salmeron M. 2003. Antibacterial activity of 11 essential oils against Bacillus cereus in tyndallized carrot broth. Int J Food Microbiol 85(1-2):73-81.

Vasile C, Dumitriu RP, Oprea AM. 2009. Kinetics of swelling and drug release from PNIPAAm/alginate stimuli responsive hydrogels. Solid State Phenom 15417-22.

Verestiuc L, Ivanov C, Barbu E, Tsibouklis J. 2004. Dual-stimuli-responsive hydrogels based on poly (N-isopropylacrylamide)/chitosan semi-interpenetrating networks. Int J Pharm 269(1):185-94.

Wadajkar AS, Koppolu B, Rahimi M, Nguyen KT. 2009. Cytotoxic evaluation of N-isopropylacrylamide monomers and temperature-sensitive poly (N-isopropylacrylamide) nanoparticles. J Nanopart Res 11(6):1375-82.

Walsh SE, Maillard JY, Russell A, Catrenich C, Charbonneau D, Bartolo R. 2003. Activity and mechanisms of action of selected biocidal agents on Gram-positive and-negative bacteria. J Appl Microbiol 94(2):240-7.

Wang T, Li B, Si H, Lin L, Chen L. 2011. Release characteristics and antibacterial activity of solid state eugenol/β-cyclodextrin inclusion complex. J Incl Phenom Macrocycl Chem 71:207-213.

Weiss J, Takhistov P, McClements DJ. 2006. Functional materials in food nanotechnology. J Food Sci 71(9):R107-16.

Wendakoon CN, Sakaguchi M. 1995. Inhibition of amino acid decarboxylase activity of Enterobacter aerogenes by active components in spices. J Food Prot 58(3):280-3.

Wischke C, Schwendeman SP. 2008. Principles of encapsulating hydrophobic drugs in PLA/PLGA microparticles. Int J Pharm 364(2):298-327.

Yalkowsky SH, He Y. 2003. Handbook of aqueous solubility data. Boca Raton, FL: CRC Press.

Yu S, Hu J, Pan X, Yao P, Jiang M. 2006. Stable and pH-sensitive nanogels prepared by self-assembly of chitosan and ovalbumin. Langmuir 22(6):2754-9.

Zha L, Banik B, Alexis F. 2011. Stimulus responsive nanogels for drug delivery. Soft Matter 7(13):5908-16.

Zhang L, Guo R, Yang M, Jiang X, Liu B. 2007. Thermo and pH Dual-Responsive Nanoparticles for Anti-Cancer Drug Delivery. Adv Mater 19(19):2988-92.

Zhang X, Wu D, Chu CC. 2004a. Synthesis and characterization of partially biodegradable, temperature and pH sensitive Dex–MA/PNIPAAm hydrogels. Biomaterials 25(19):4719-30.

Zhang XZ, Wu DQ, Chu CC. 2004b. Synthesis, characterization and controlled drug release of thermosensitive IPN–PNIPAAm hydrogels. Biomaterials 25(17):3793-805.

Zhang Y, Jiang M, Zhao J, Ren X, Chen D, Zhang G. 2005. A novel route to thermosensitive polymeric core–shell aggregates and hollow spheres in aqueous media. Adv Funct Mater 15(4):695-9.

Zigoneanu IG, Astete CE, Sabliov CM. 2008. Nanoparticles with entrapped α-tocopherol: synthesis, characterization, and controlled release. Nanotechnology 19:105606-13.